COSMIC RAYS

An Introduction

Pierre Darriulat

Katmandou

April, 2008

CONTENT

A brief history
The main features
The sources
Acceleration in shocks

A BRIEF HISTORY

Discovery and early studies

Using cosmic rays

Larger detectors

Space astronomy

Renaissance

The discovery

At the end of the XIX^{e} century, scientists were puzzled by the spontaneous discharge of their electroscopes which suggested the presence of an ionizing radiation.
In 1909, Wulf noted that the rate of the discharge was decreasing with altitude (Eiffel tower).
Between 1911 and 1913 the Austrian physicist Viktor Hess established the existence of an unknown penetrating radiation coming from above and most probably of extraterrestrial origin with balloon measurements reaching up to five kilometers in altitude.
He shared the 1936 Nobel Prize with Carl Anderson

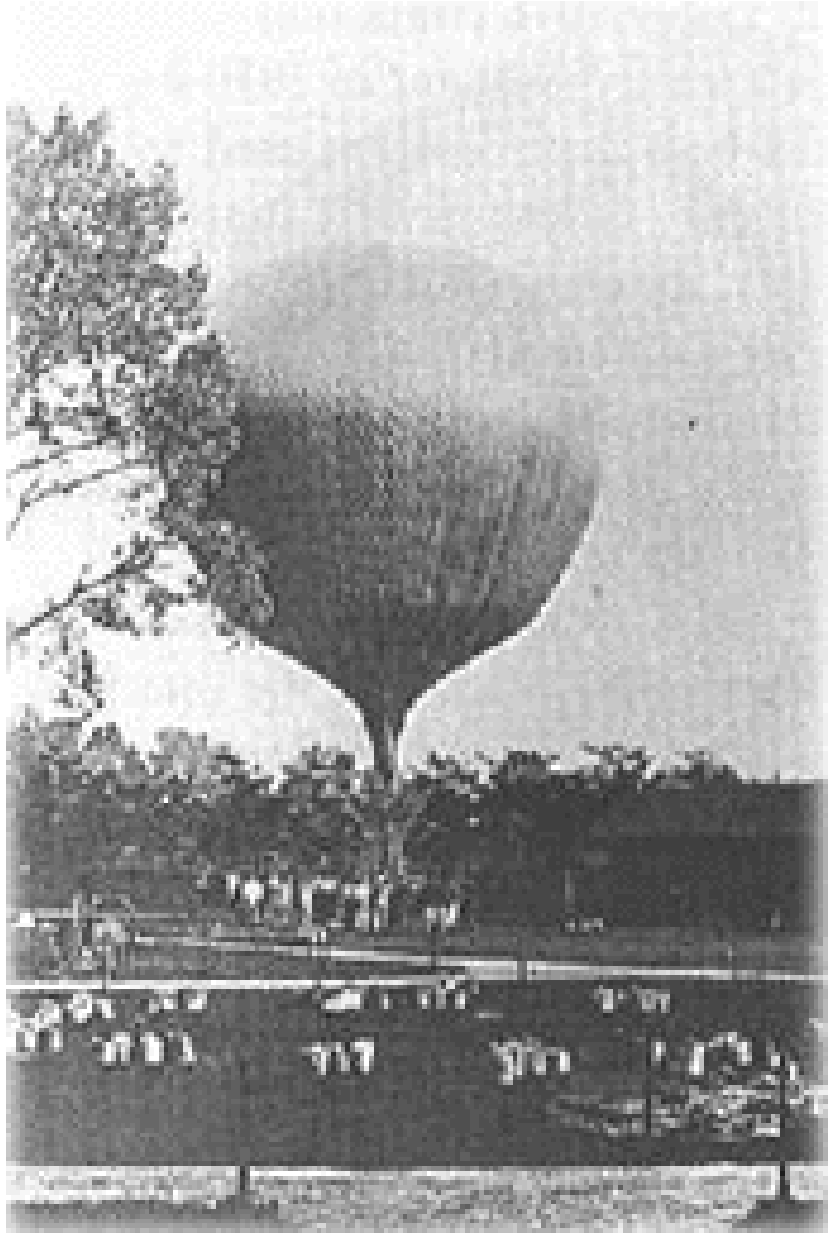

In the following years cosmic rays became the subject of intense research, in particular with Millikan (who coined the name in 1925) and Anderson at Pikes peak.

In 1927 the dependence on latitude and east-west asymmetry established unambiguously that cosmic rays were charged particles, not photons.

In 1938, Pierre Auger, using counters in coincidence, discovered extensive air showers and understood that they were produced by very high energy (up to 10^{15}eV) primaries interacting with the Earth atmosphere

Robert Millikan at Pikes Peak and Pierre Auger at the Jungfrau Joch

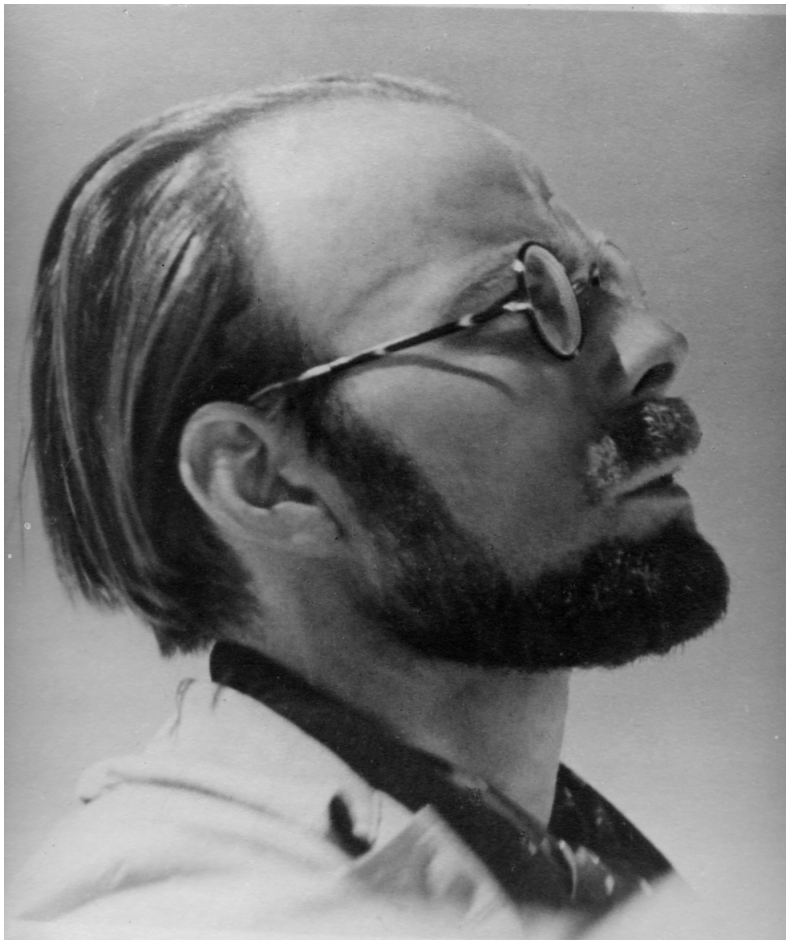

Using cosmic rays

In the thirties and fourties, when accelerators were not yet dominating the scene, cosmic rays became the laboratory for the study of particle physics

Anderson discovered the positron in 1932
and the muon in 1938

Powell and Occhialini discovered the pion in 1947

Then came strange particles, kaons, hyperons and many others

In the fifties, accelerators took over and cosmic rays got studied for their own sake

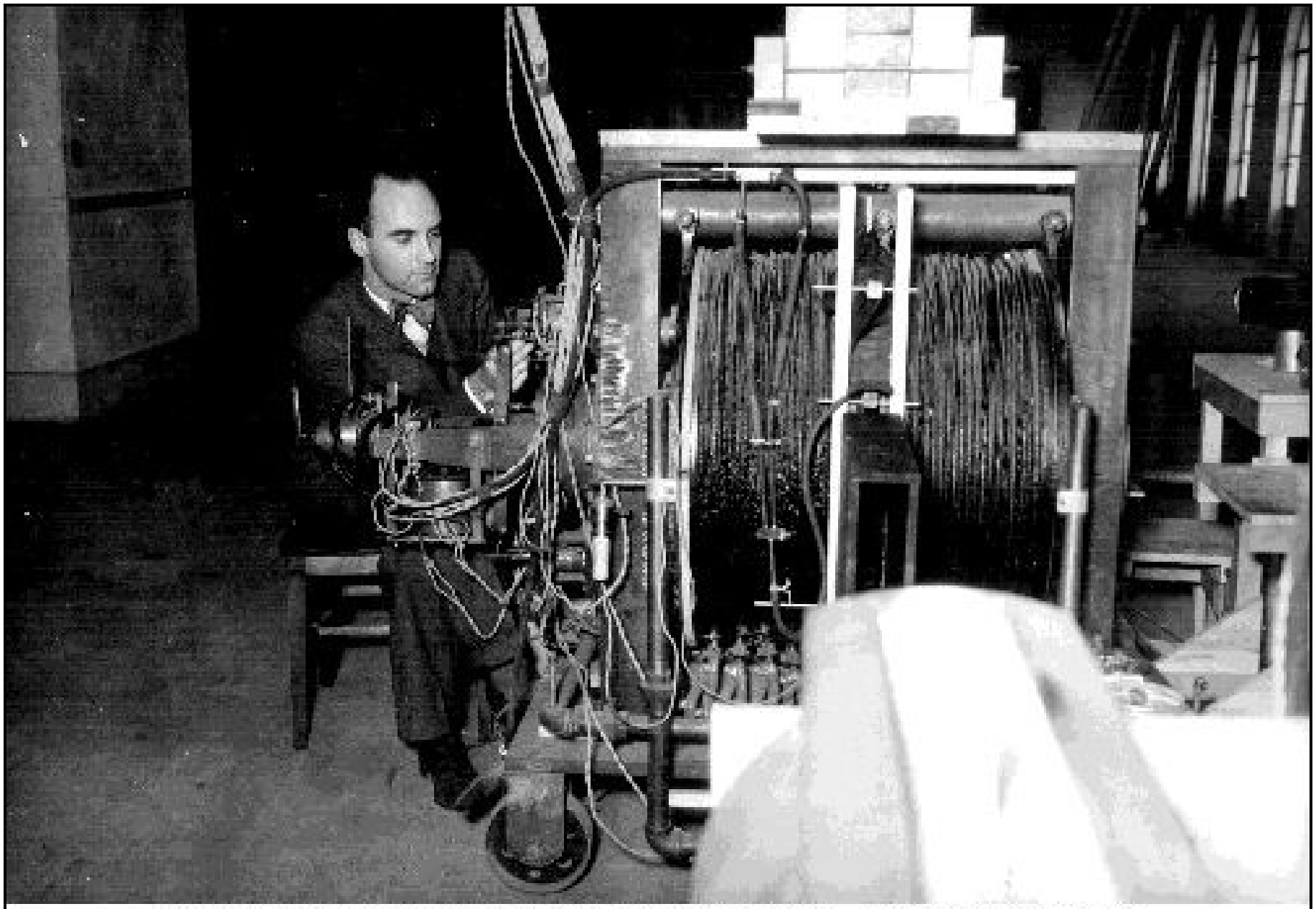

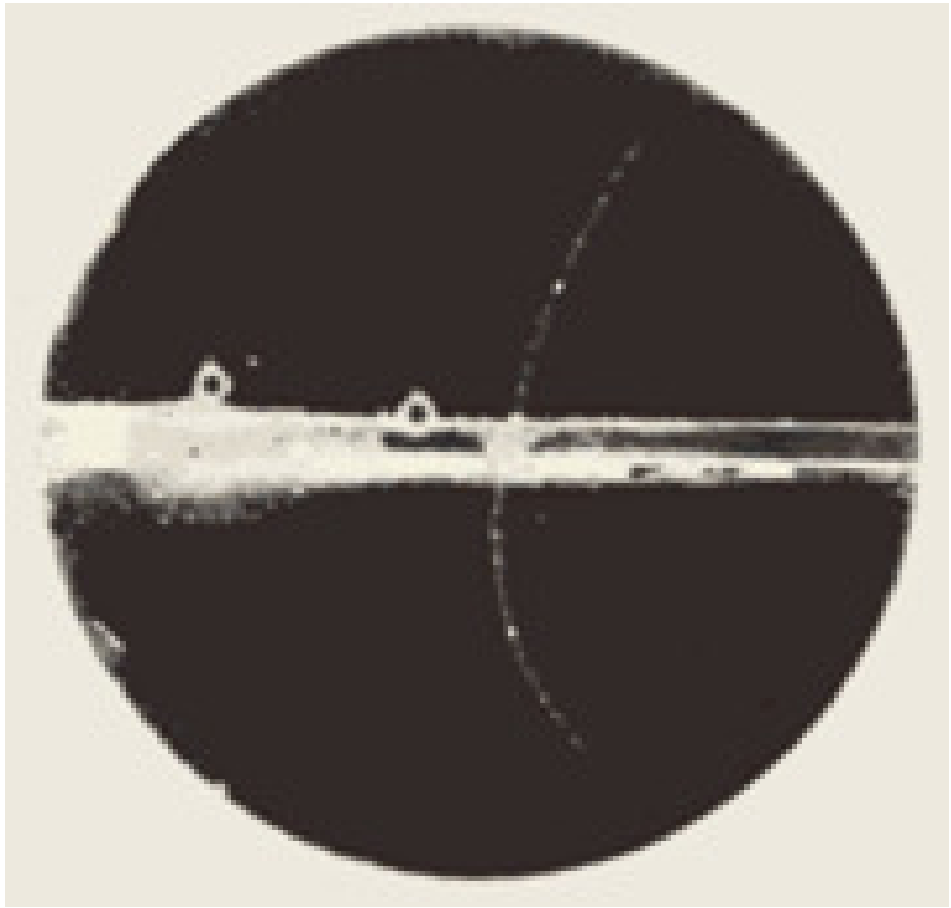

For many years following, major effort was devoted to the study of cosmic rays,

trying to understand their origin.

Ground detectors, large arrays and fluorescence telescopes, reached very high energies

(John Linsley at Volcano Ranch :

first 10^{20} eV shower in 1962)

Space astronomy has been a break through

for the study of low energy cosmic rays, in particular solar energetic particles (SEP)

John Linsley at Volcano Ranch (New Mexico) checking for rattle snakes in a stack of hay

Casa in Utah

Agasa

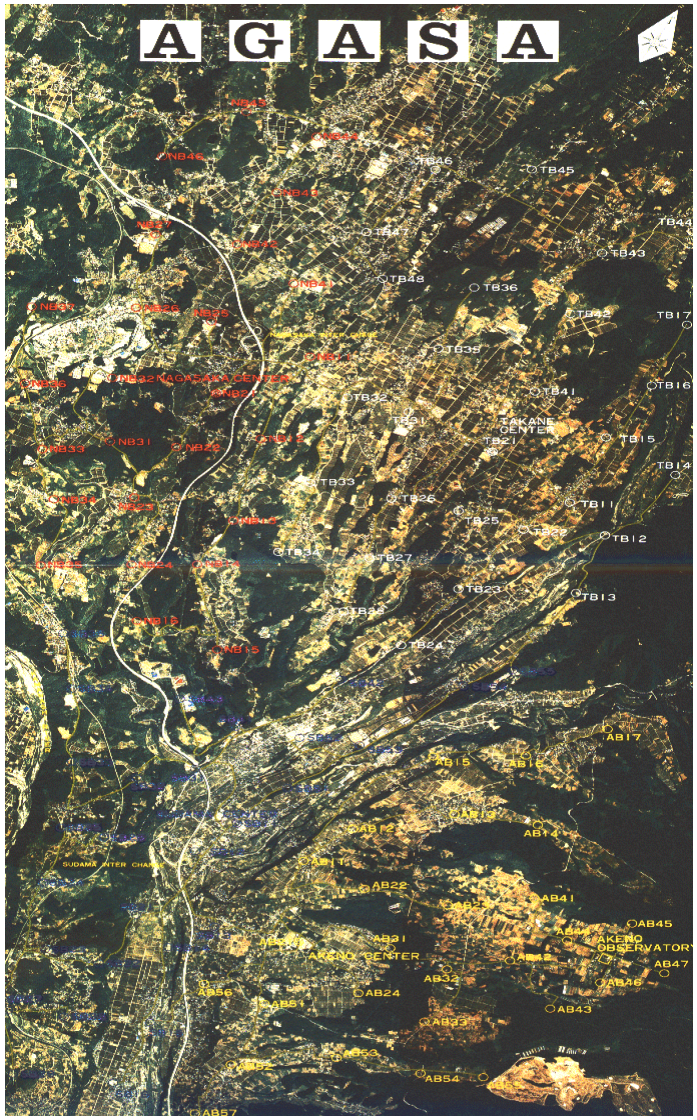
AGASA
TB46
TB45
TB44
TB43
TB48
TB36
TB42
TB17
TB41
TB16
TB21
TB15
TB14
TB11
TB12
TB13
AB15
AB16
AB17
AB14
AB22
AB41
AB45
AB47
AB43
AB54
AB57

COS-B, a pioneer in space

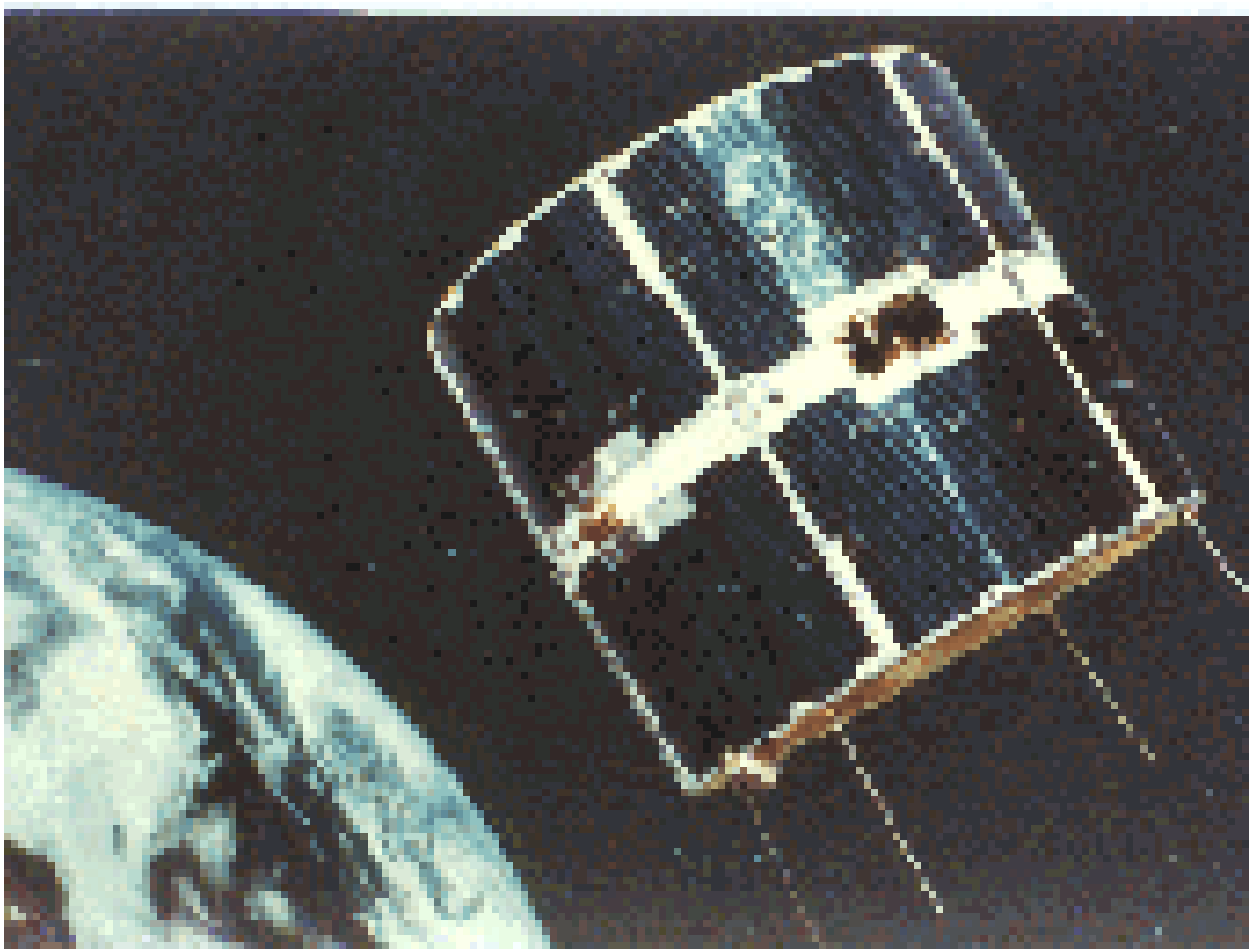

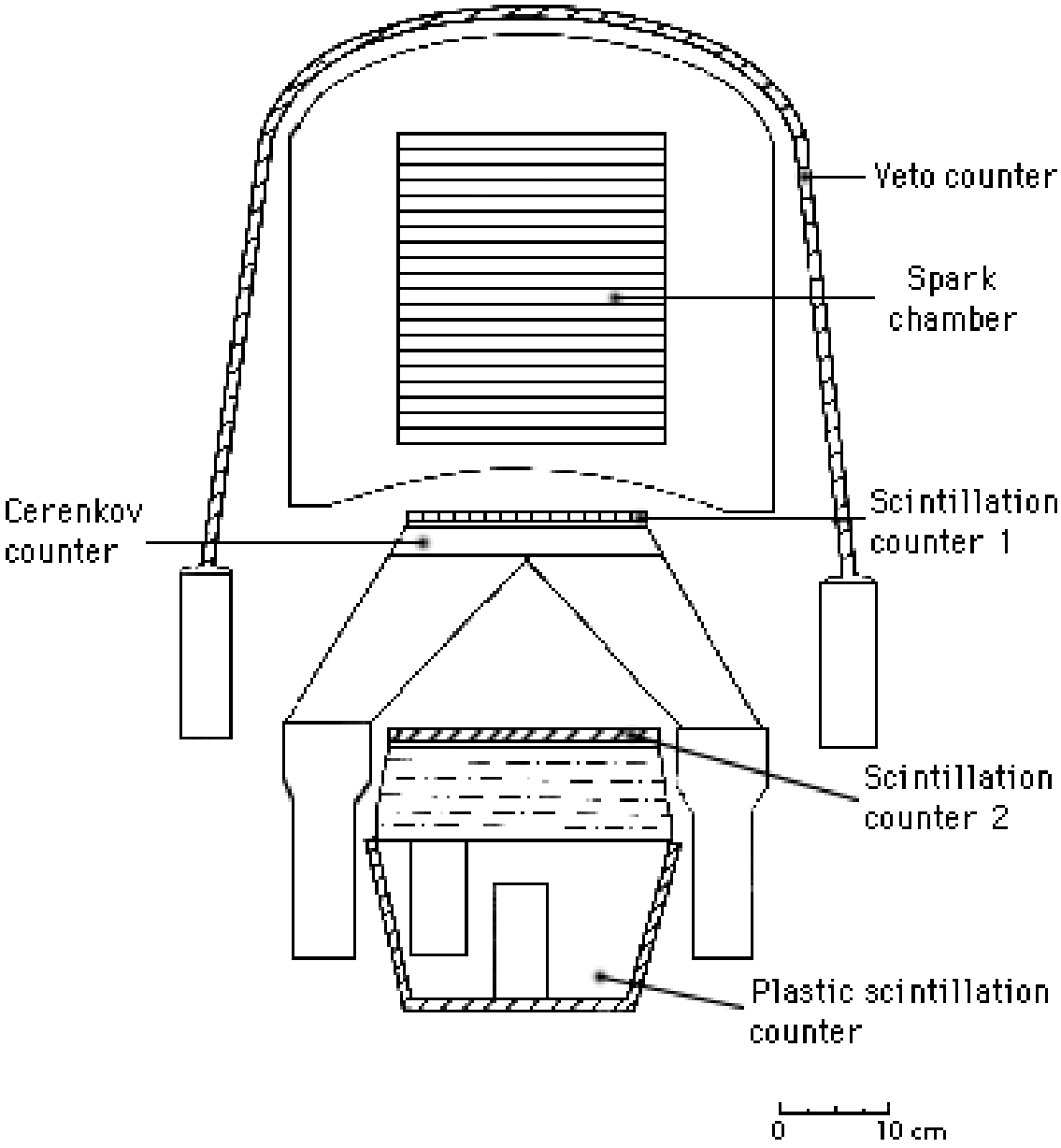
Veto counter
Spark chamber
Cerenkov counter
Scintillation counter 1
Scintillation counter 2
Plastic scintillation counter
0
10 cm

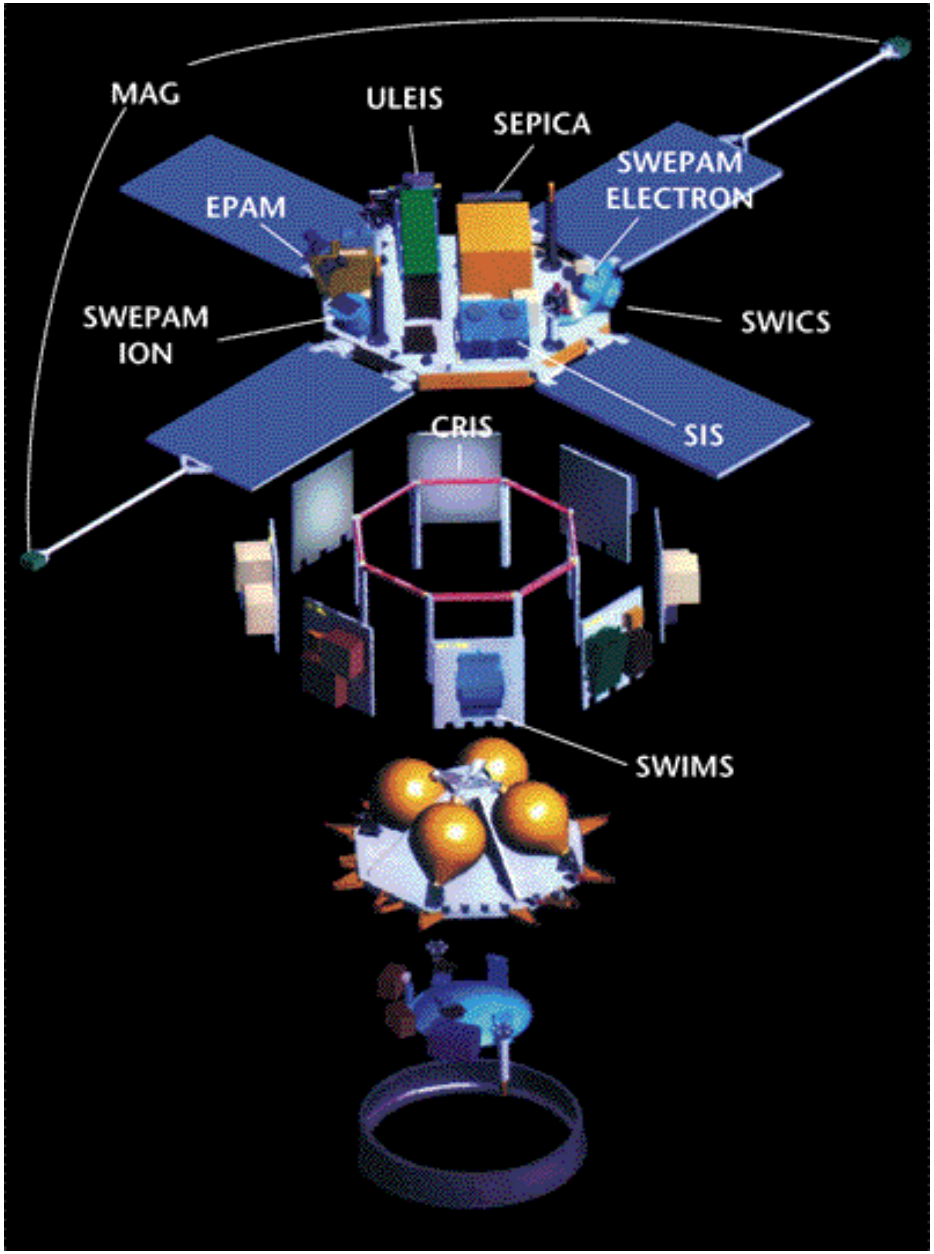

A recent example of space measurements in solar astronomy:

NASA's Advanced Composition Explorer ACE was launched from Cape Canaveral in 1997 to the Lagrange point between Sun and Earth

In the past 20 years, spectacular progress in astrophysics and long time scales implied in the construction of very high energy accelerators have caused a burst of interest in cosmic ray physics under the name of astroparticle physics.

In particular TeV gamma ray detectors have been constructed and operated. Their main asset is that they can point to the sources without suffering deflections from magnetic fields.

To study cosmic rays, a new generation of ground detectors was born.
In particular, the Pierre Auger Observatory is a huge and hybrid detector covering 1500 km^2;
Showers are detected from the fluorescence they produce in atmosphere and by their impact on a ground detector array.
Plans to use the whole Earth atmosphere as a radiator observed from space are being implemented.
Neutrino astronomy is currently being pioneered.

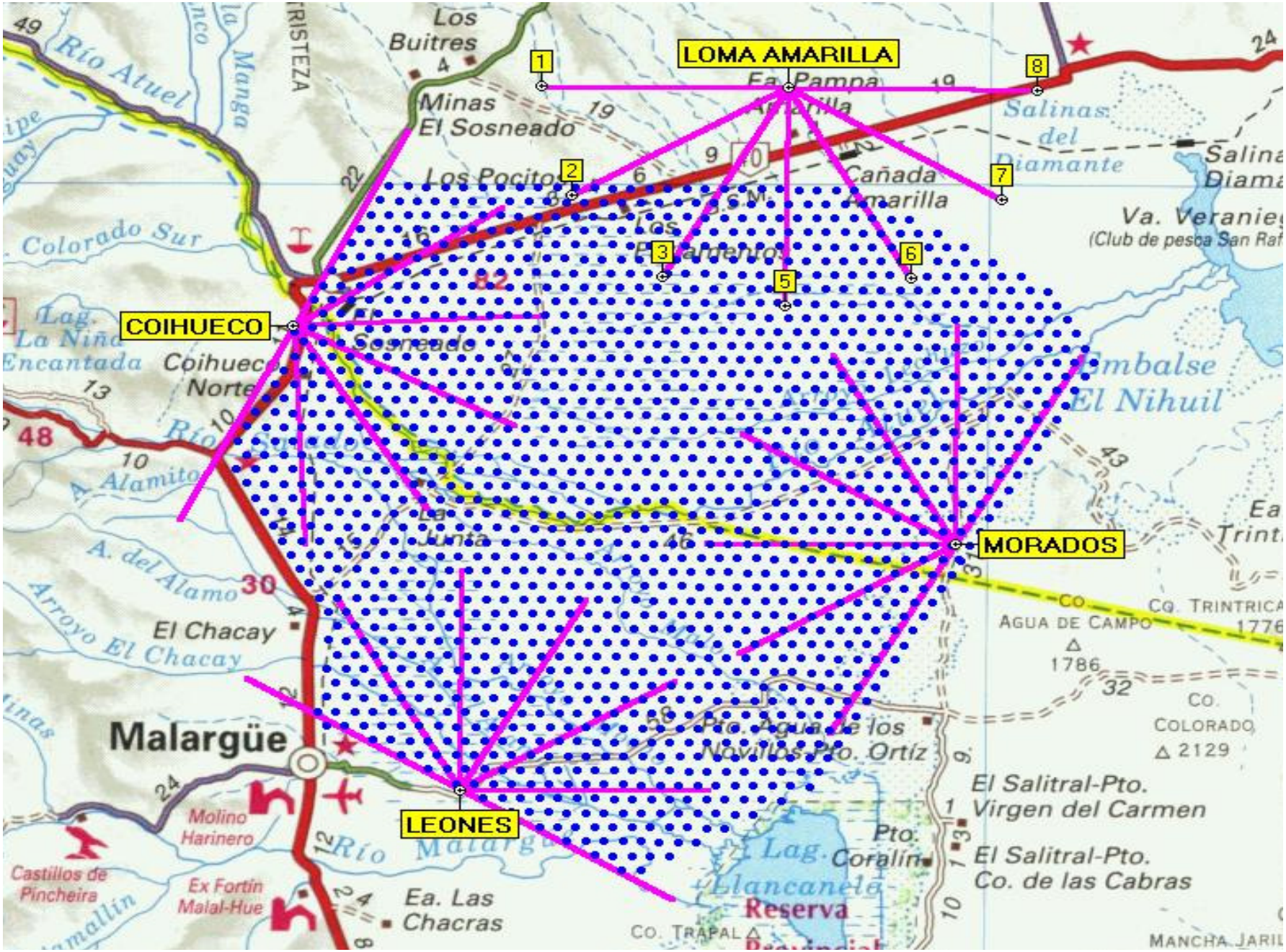
LOMA AMARILLA
COIHUECO
MORADOS
LEONES
1
2
3
5
6
7
8
Los Buitres
Minas El Sosneado
Los Pocitos
Cañada Amarilla
Los Parlamentos
Río Atuel
Río Colorado Sur
Río Salado
Río Malargüe
Lag. La Niña Encantada
Coihueco Norte
Sosneado
Embalse El Nihuil
Salinas del Diamante
Va. Veranie
(Club de pesca San Raf
El Alamito
A. del Alamo
Arroyo El Chacay
El Chacay
Malargüe
Molino Harinero
Castillos de Pincheira
Ex Fortín Malal-Hue
Ea. Las Chacras
Co. Trapal
Lag. Llancanelo
Reserva
Pto. Agua de los Novillos
Pto. Ortíz
Pto. Coralín
El Salitral-Pto. Virgen del Carmen
El Salitral-Pto. Co. de las Cabras
Co. Agua de Campo
1786
Co. Trintrica
1776
Co. Colorado
2129
Mancha Jaril
48
30
82

1600 Cherenkov counters on ground measure the shower transverse profile and 4×6 fluorescence telescopes measure the longitudinal profile with a 10% duty cycle (clear moonless nights)

In both cases timing gives the direction (1°) and intensity gives the energy (10%)

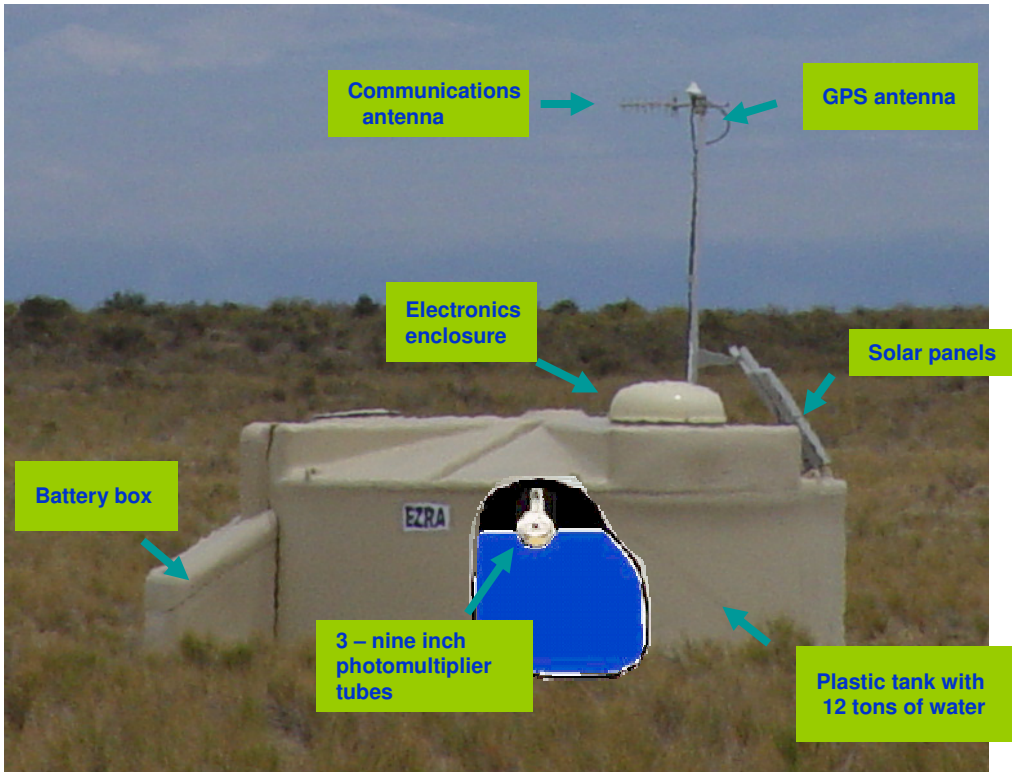

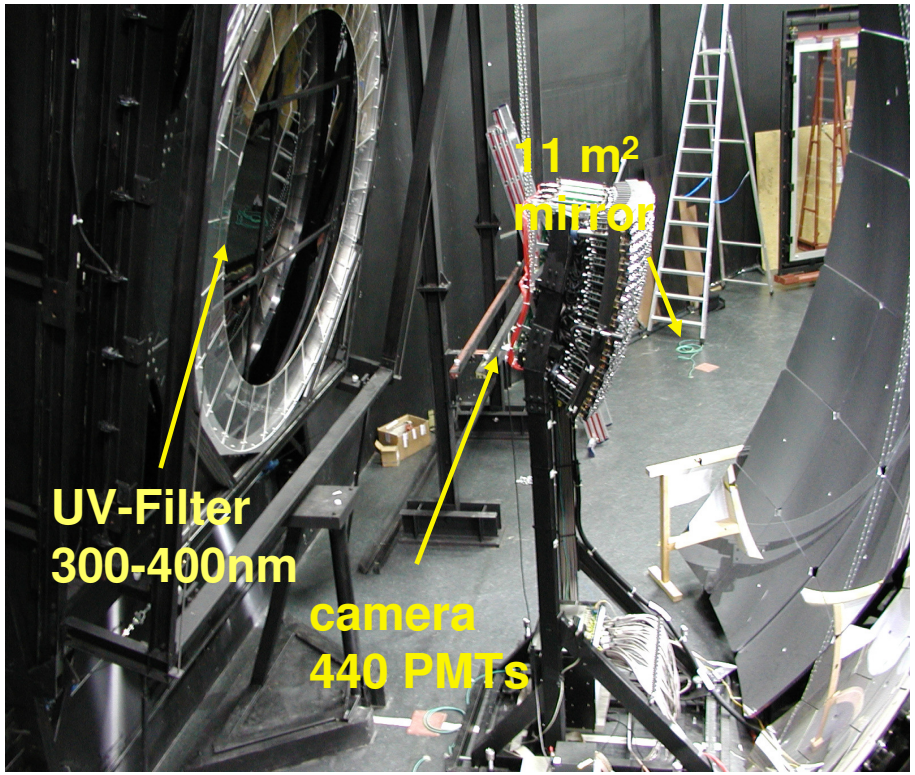

Four stations of six eyes each, each eye covering a field of view of 30°×28° with a mirror focusing on an array of 22×20 pixels (photomultiplier tubes), each having 1.5° aperture. They measure the induced fluorescence of nitrogen molecules (near UV).

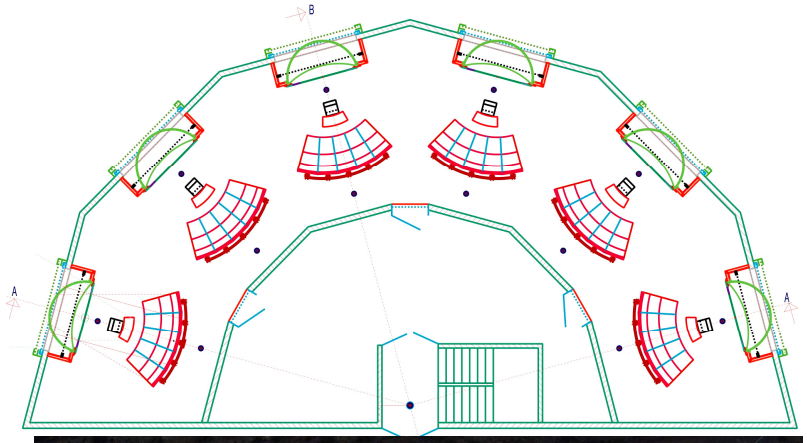

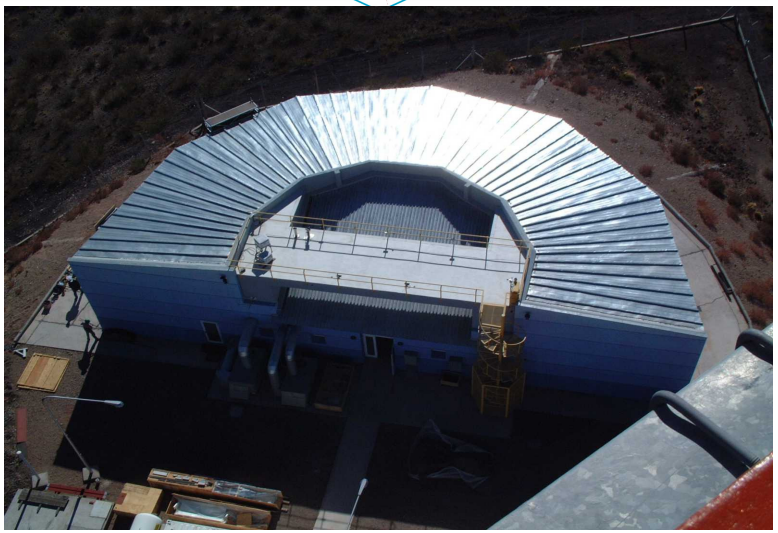

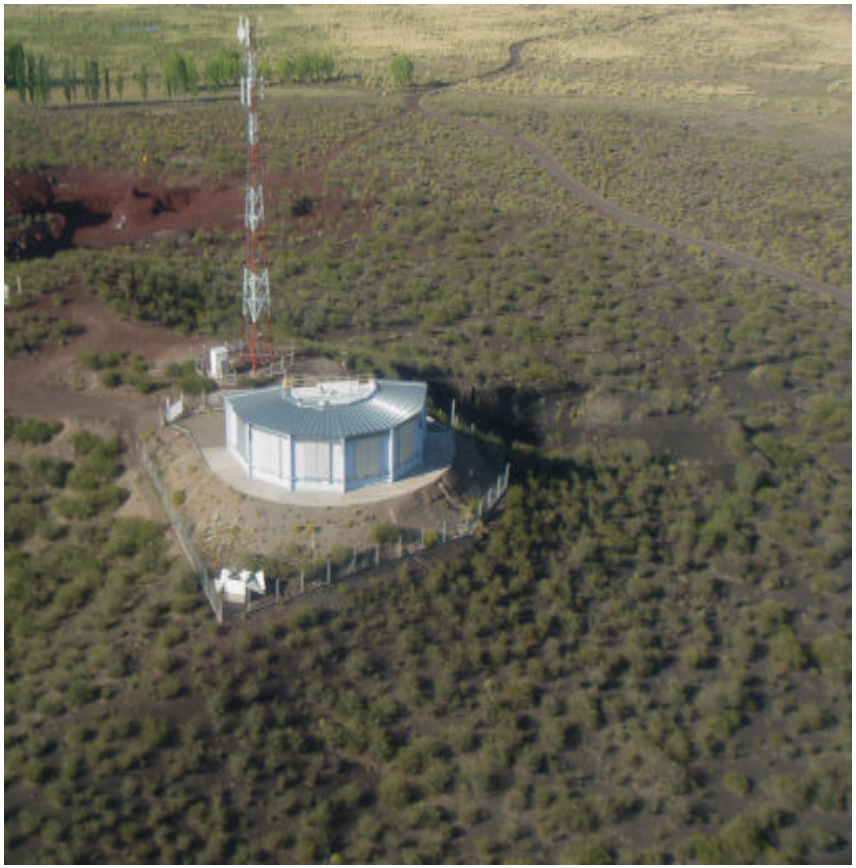

The first four-fold event
May 2007, ~10^{19} eV

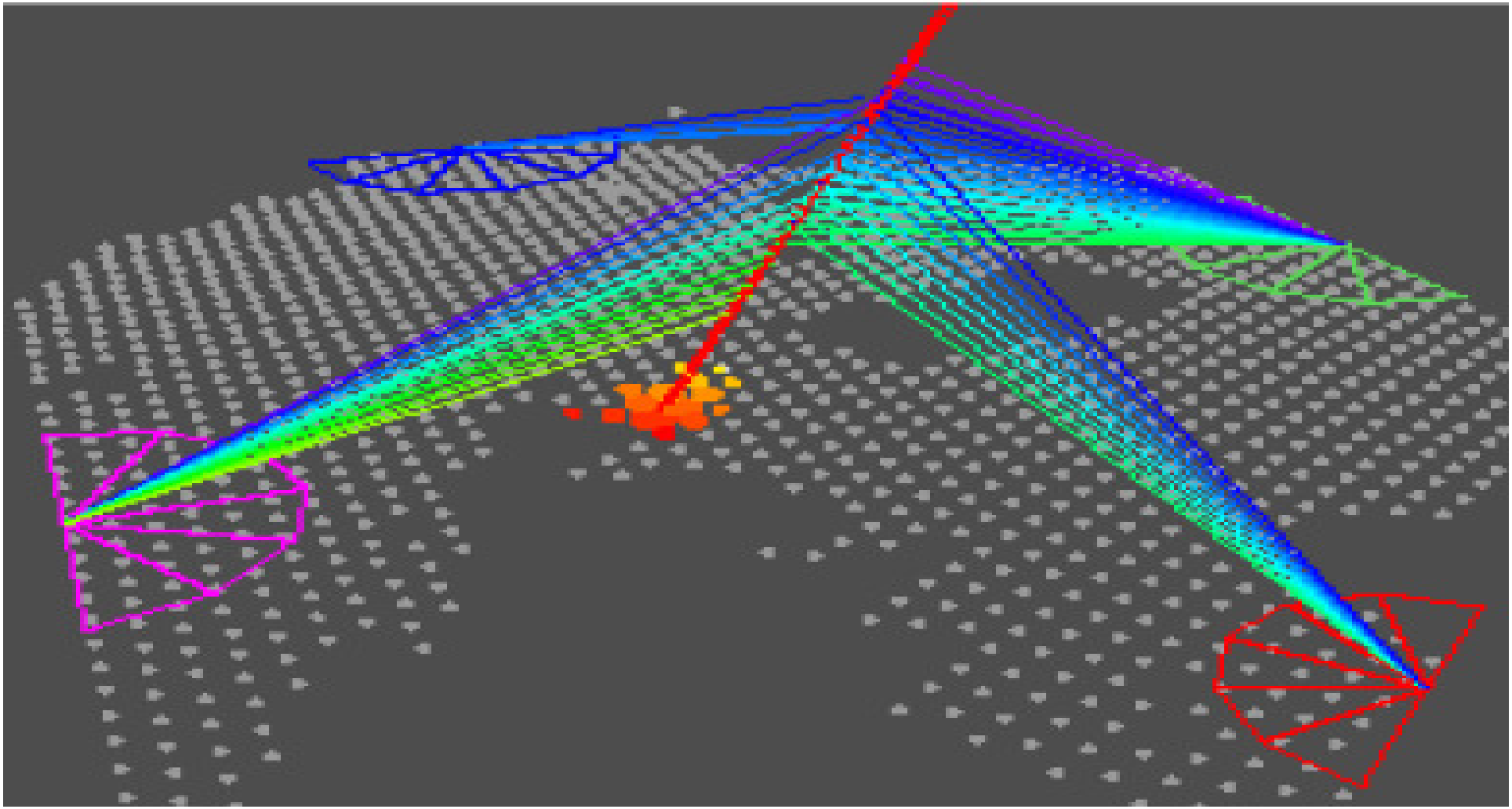

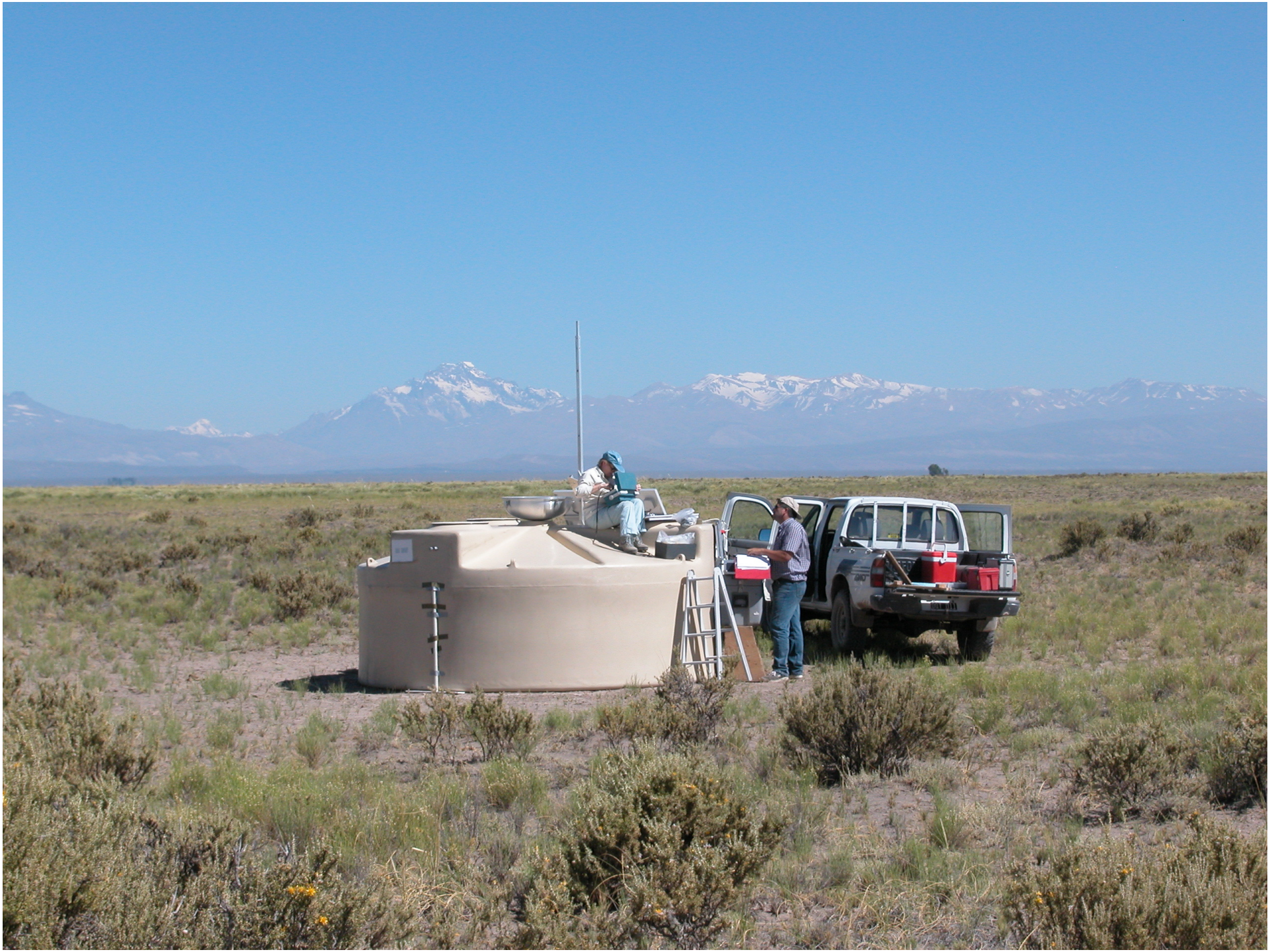

Data are transferred by radio to an acquisition centre which filters them and sends them to the laboratories associated with this research.

While the ground array is not yet fully complete, the Observatory already reported two important results:

It has given evidence for the interaction of ultra high energy cosmic rays (UHECR) with the cosmic microwave background (CMB).

It has shown that at least part, if not all, UHECRs originate in regions which are rich in AGNs.

Looking into the future:

The EUSO project

EUSO concept: a space TPC

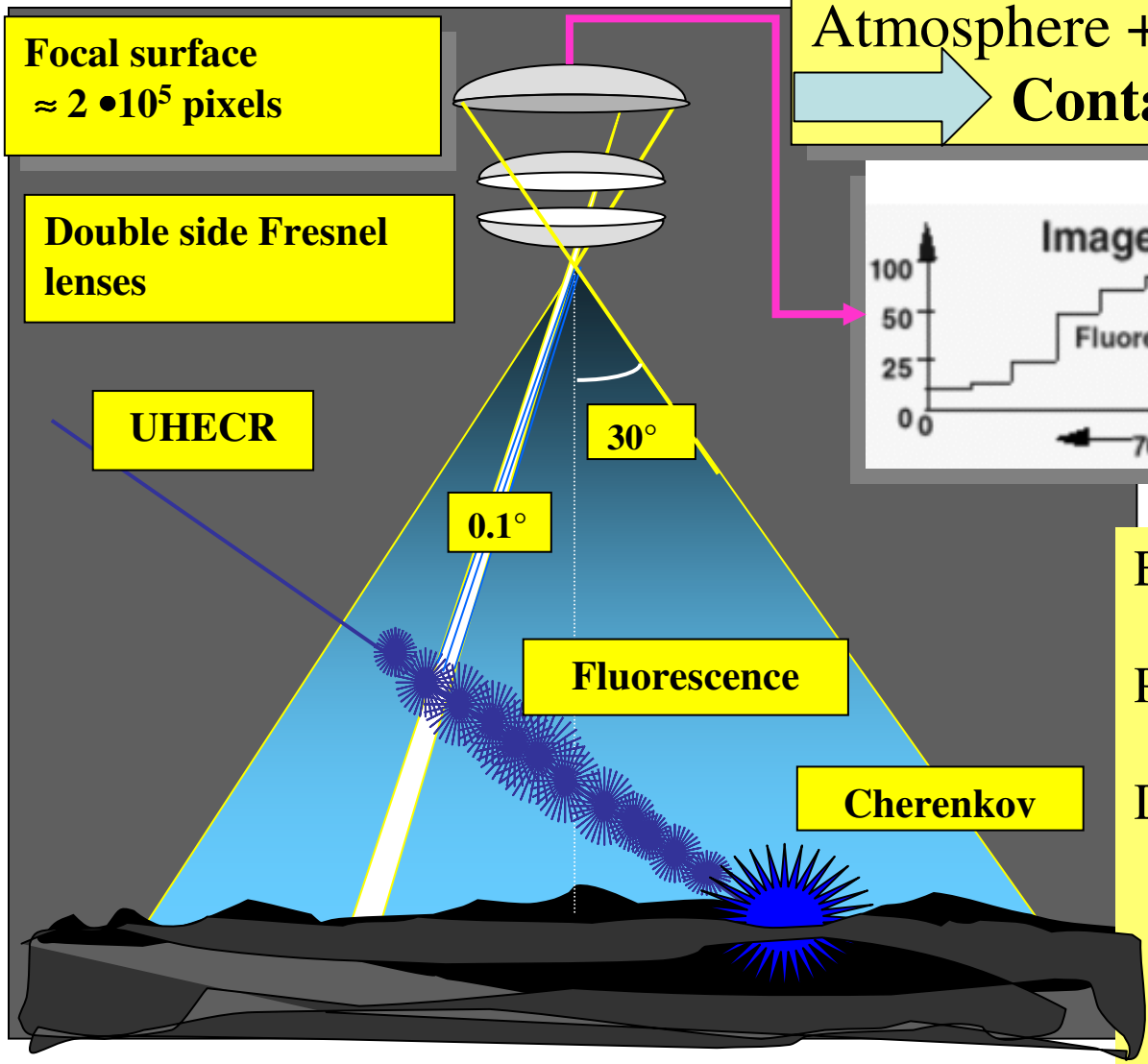

Atmosphere + EUSO = Calorimeter

Contained EAS

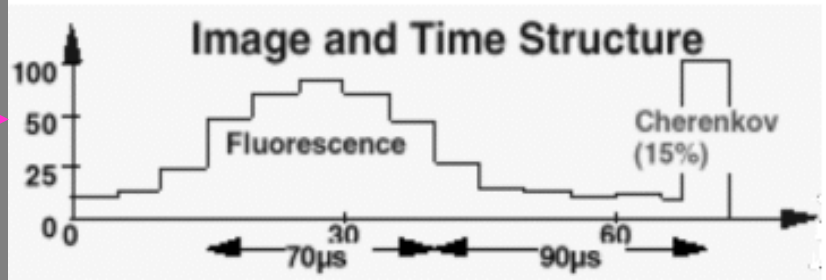

Energy

Fluorescence + Cerenkov

Position

X,Y,Z (t): 0.3 - 1 km

Direction

Multi-hits tracks

.σ_θ ~ 0.3°(h) - 3°(v)

EUSO Collaboration

A compact instrument for the observation of EECRs and Neutrinos

Europe
ESA

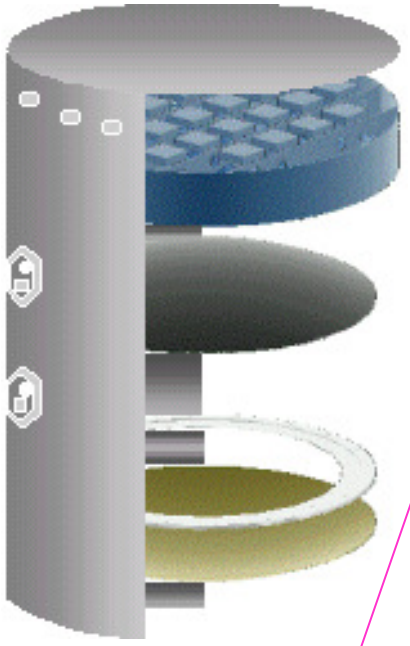

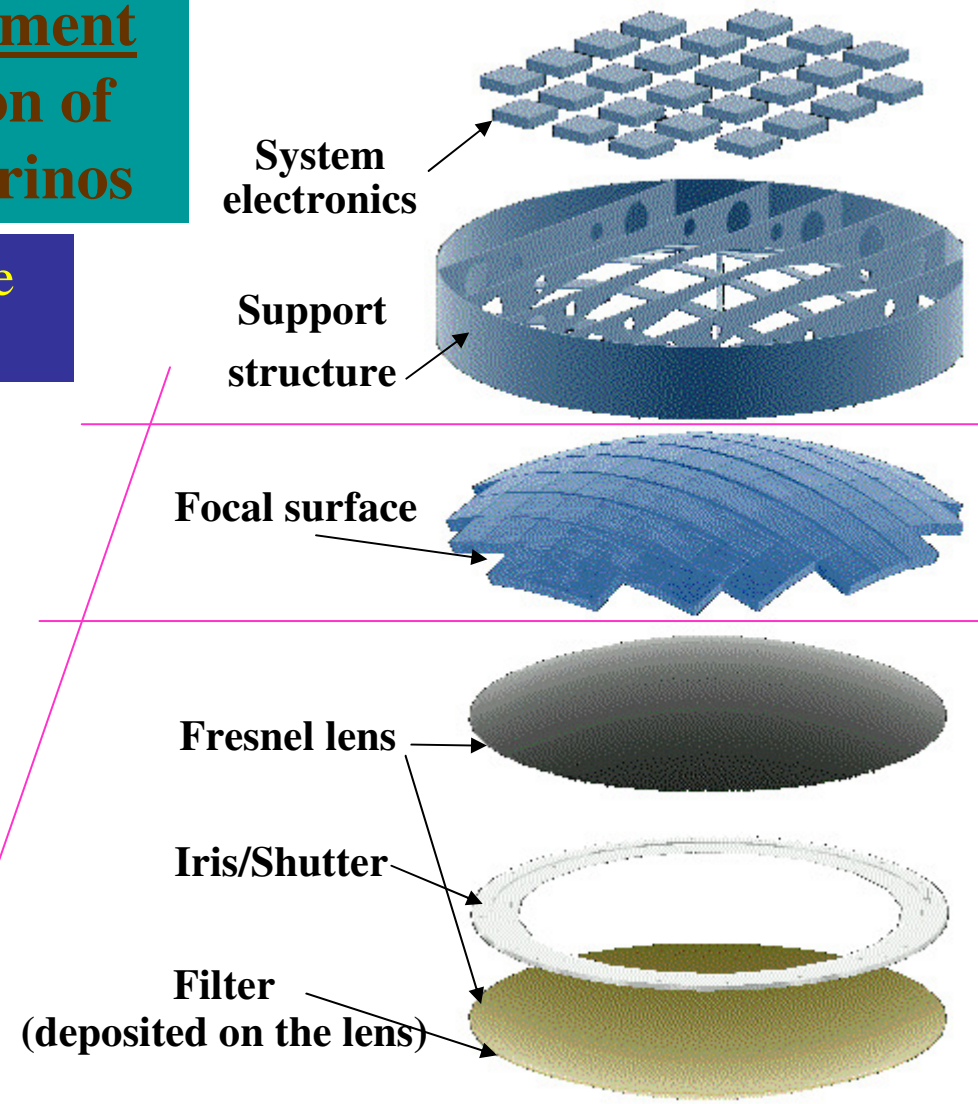

France
(IN2P3/CNES)
Italy:
(INFN/ASI)
Portugal:
(ICCT/FCT)
D/UK/CH

Japon
RIKEN
NASDA

USA
OWL
NASA

THE MAIN FEATURES

Introduction

Showers

Knee, ankle, GZK

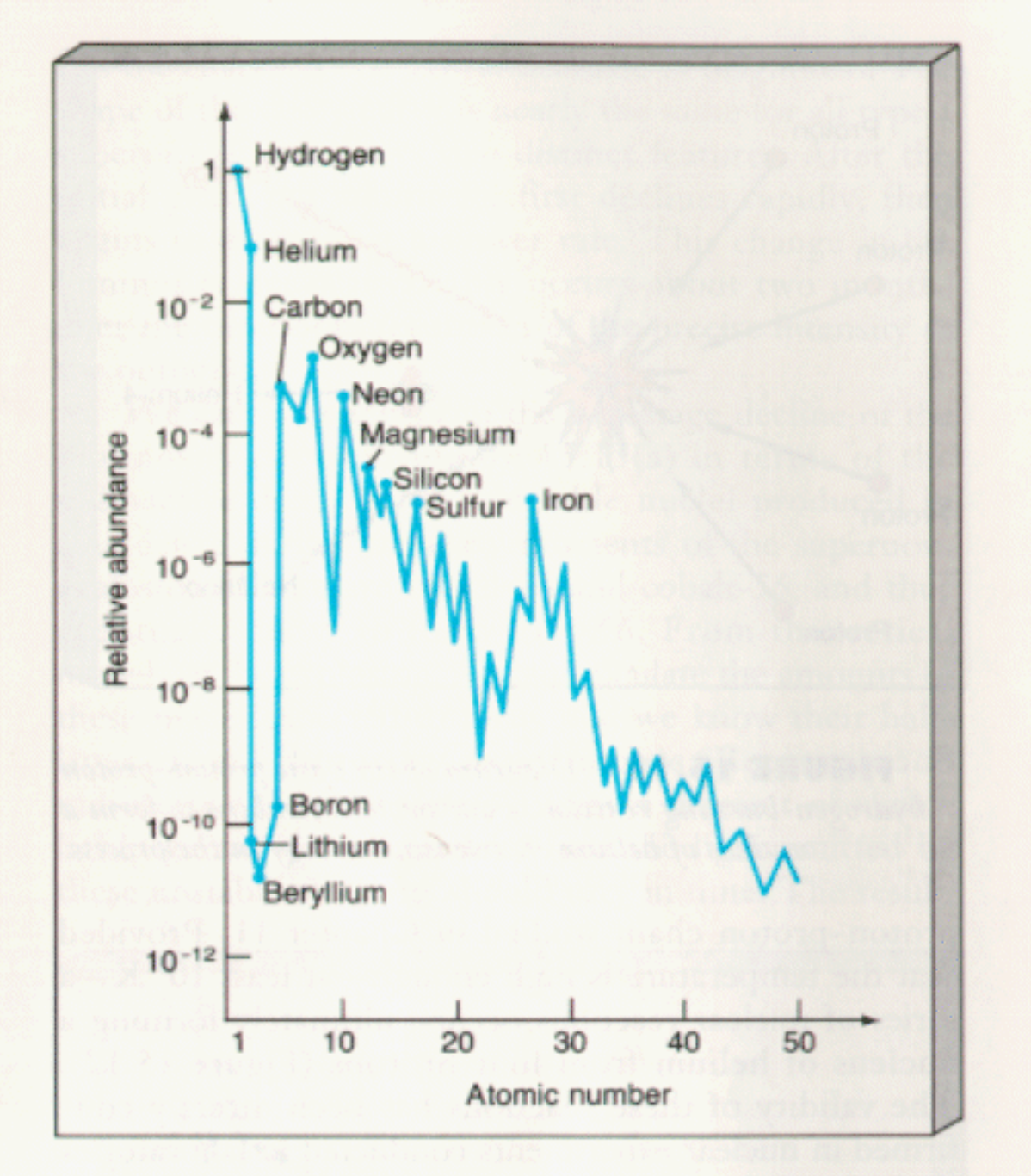

Elemental abundances

While hydrogen and helium are essentially primordial the heavier elements have been produced in stars and supernova explosions Even-even nuclei are naturally favored and the iron region which corresponds to the strongest nuclear binding is enhanced

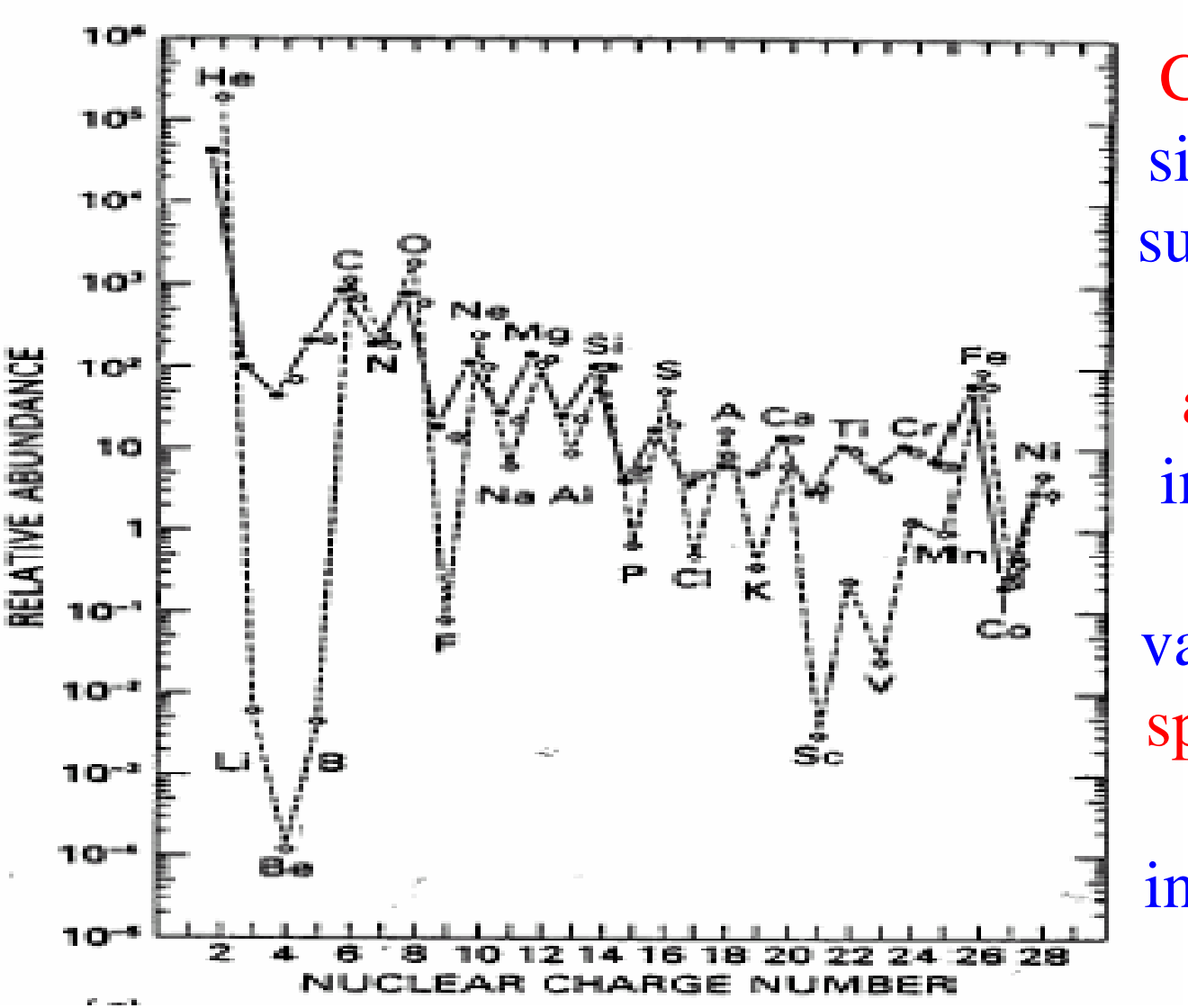

Cosmic rays show similar abundances suggesting that they have been accelerated from interstellar matter. However, the valleys are filled by spallation reactions on matter in the interstellar medium (~7 gcm^{-2})

- Cosmic rays are ionized nuclei that travel in space up to extremely high energies,

  $\sim 10^{20}$ eV=16 Joules!

- There are very few of them but they carry as much energy as the CMB or the visible light or the magnetic fields ~1eV/cm^3

- They have a power law spectrum over 32 decades (12 decades in energy),

  $\sim E^{-2.7}$.

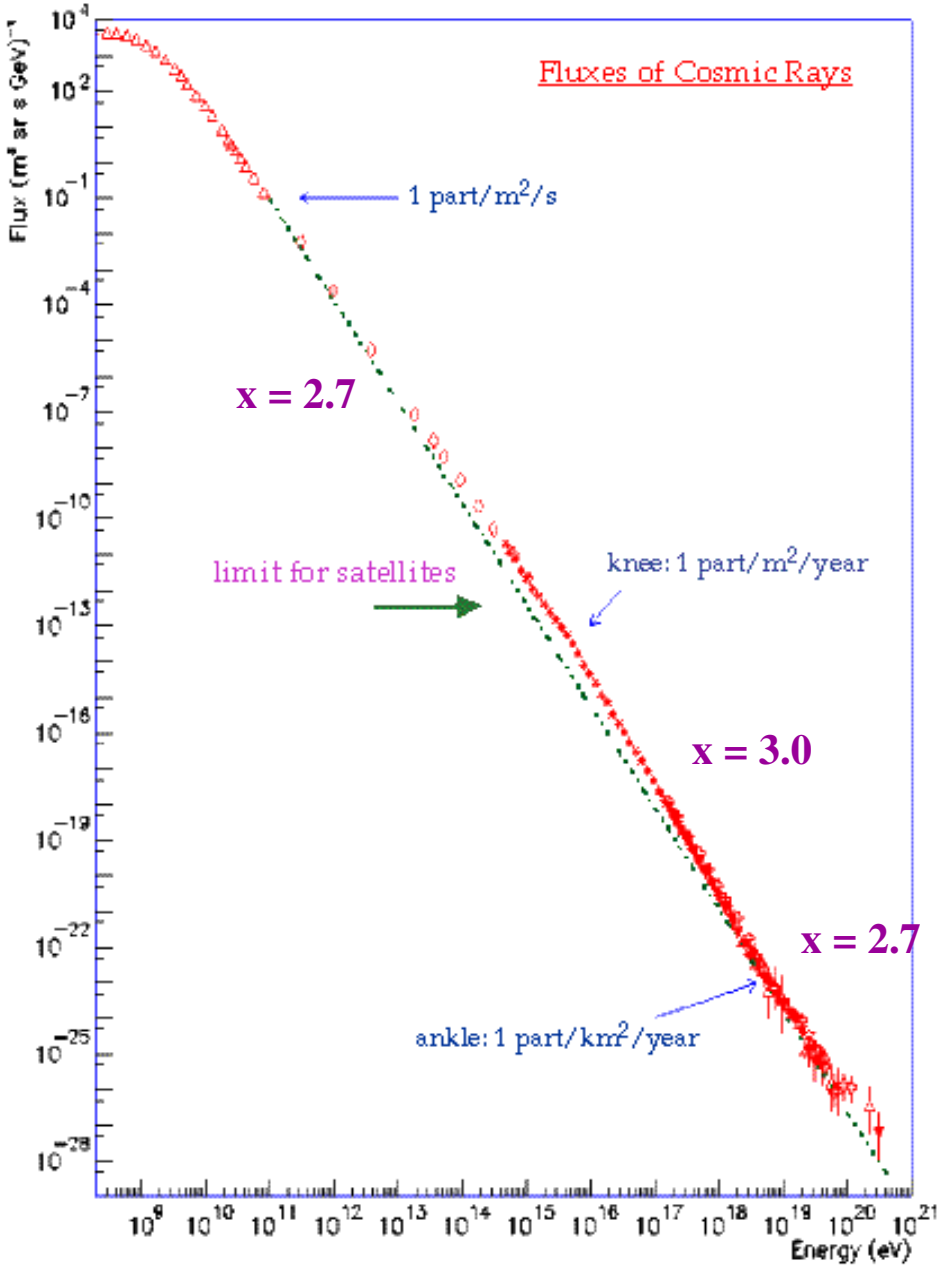

Energetics of cosmic rays

Energy density

$r_E \sim 10^{-12}$ erg/cm^3

Galactic escape time

~ 3 10^6 y

Power

~ 10^{-26}erg/cm^{3}s

SN power

10^{51}erg/SN

~3 SN per century

in the disk

~ 10^{-25} erg/cm^{3}s

~10% efficiency

Spectral Energy Distribution
(linear inset → most E < 100 GeV)

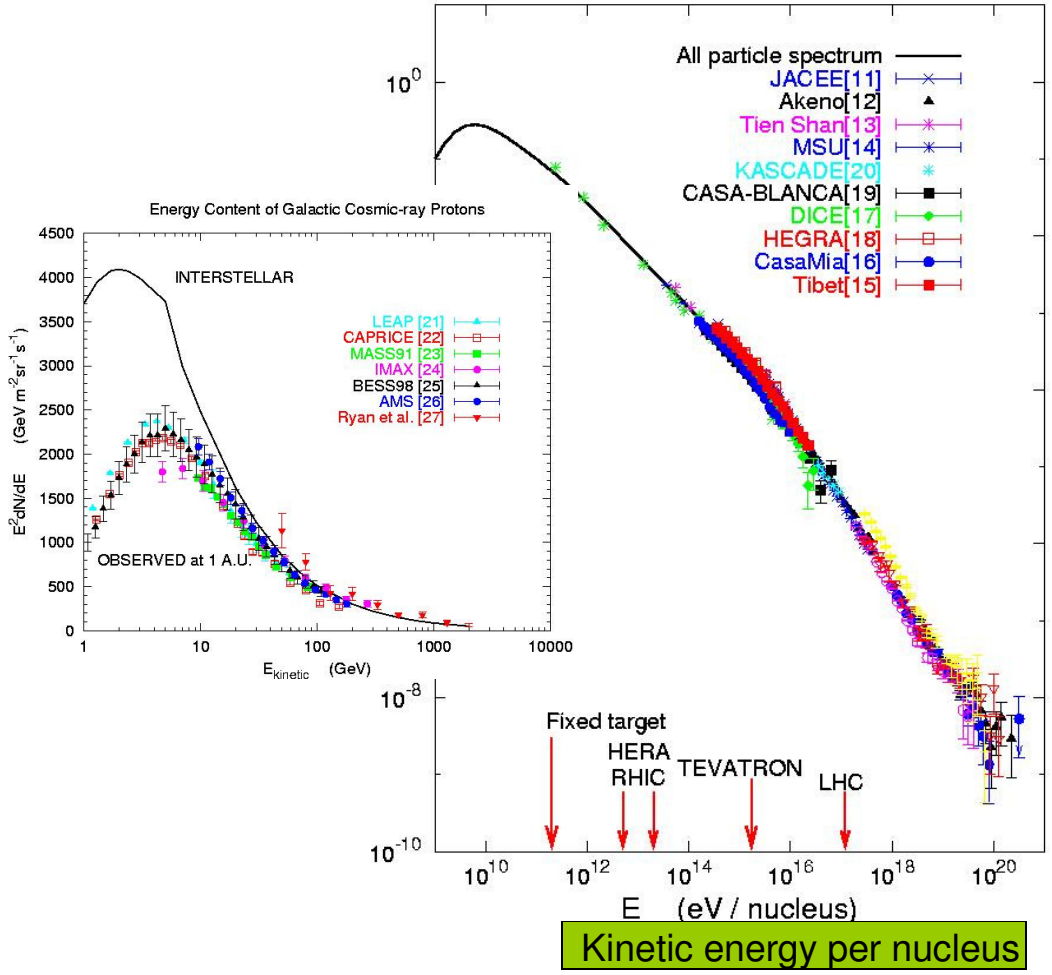

Kinetic energy per nucleus

Energy of extragalactic component

Energy density

ρ_{CR}

$>2\ 10^{-19}$erg/cm^3

Estimate

requires

low energy

extrapolation

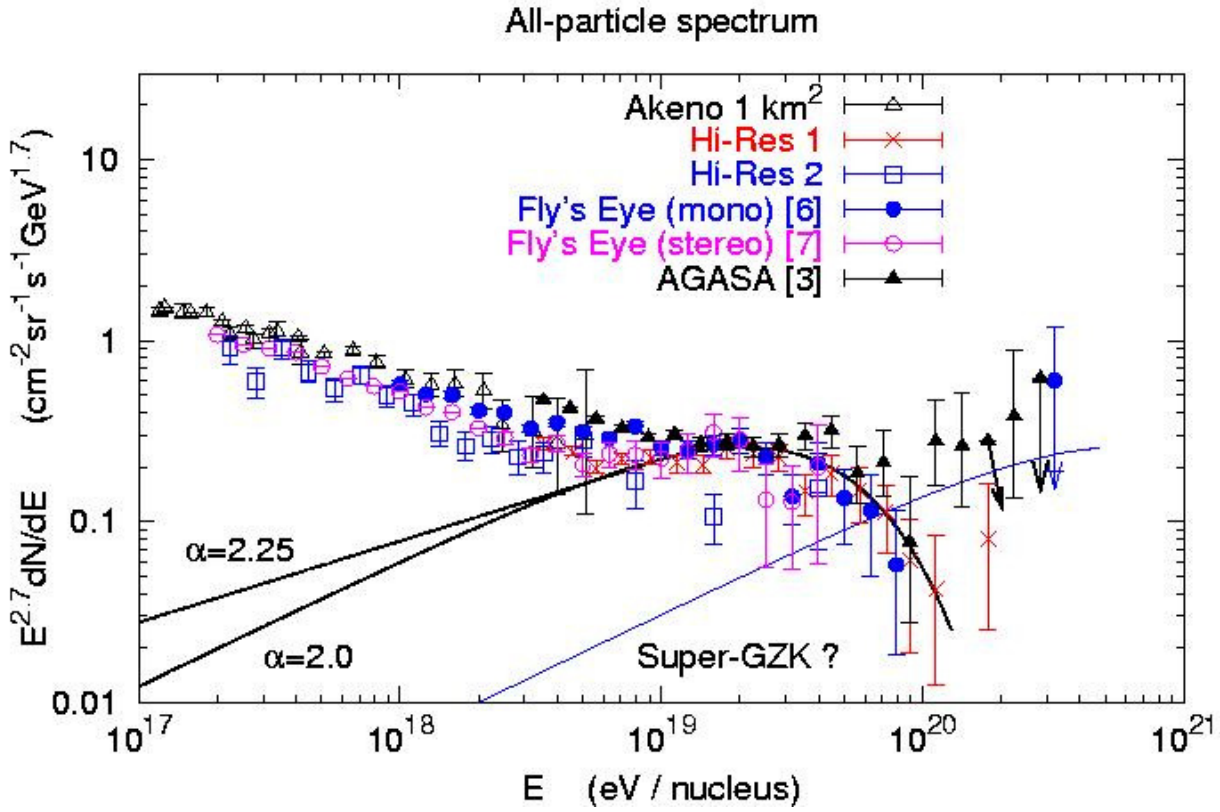

Power needed $>\rho_{CR}/10^{10}$ y ~ 1.3 10^{37} erg/Mpc^3/s

10^{-7} AGN/Mpc^3 need $>10^{44}$ erg/s/AGN

1000 GRB/y Need $>3\ 10^{52}$erg/GRB

Electron and photon showers

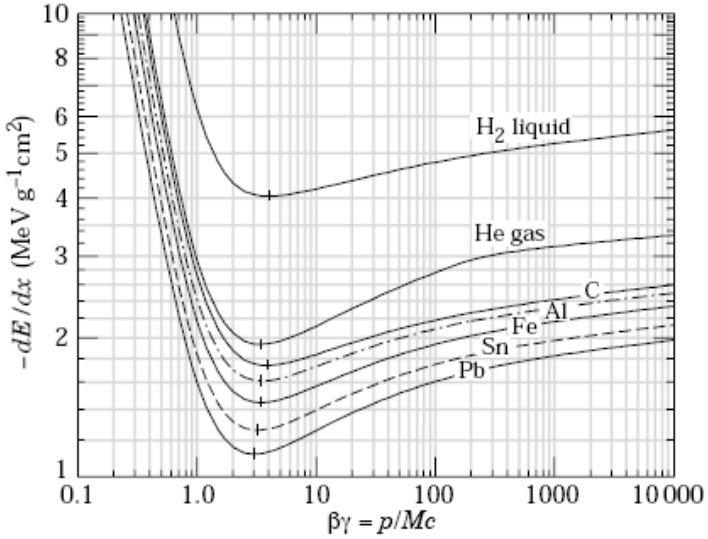

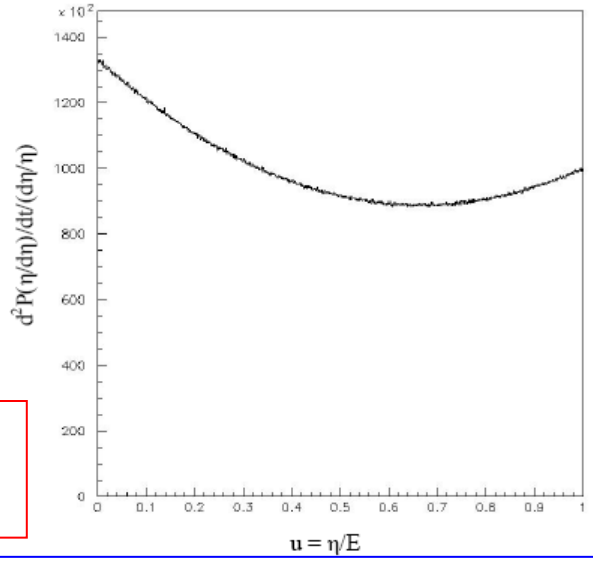

Equal at critical energy 80 MeV

Ionization losses: Bethe Bloch ~2 MeV/g/cm^2 at minimum.

Exponential radiation losses: Bremsstrahlung, radiation length in air 37g/cm^2

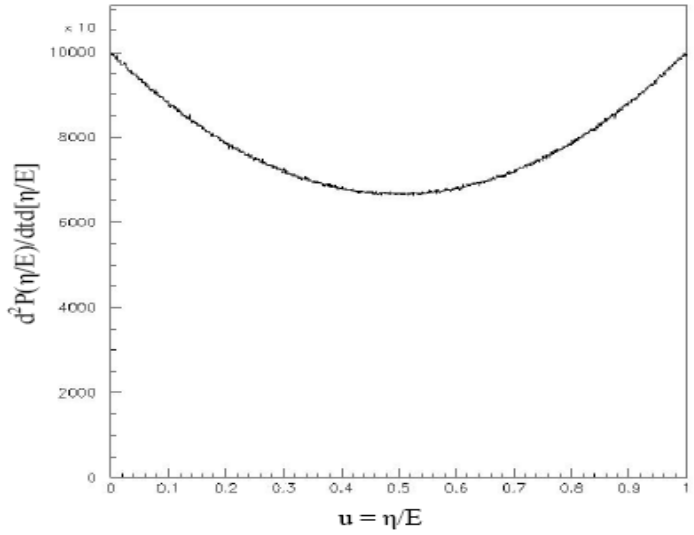

Pair creation probability:
7/9 per radiation length
Transverse extension:
Moliere radius is
21 MeV/ critical energy
=¼ rad. l. = 100 m

Hadronic showers

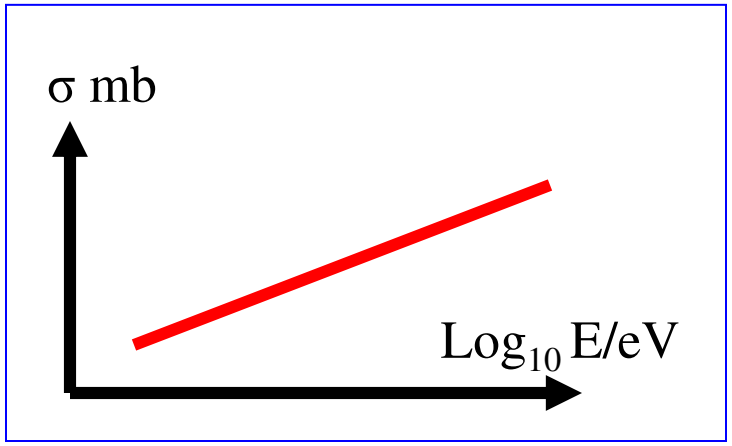

Total cross section
Int. length~70g/cm^2

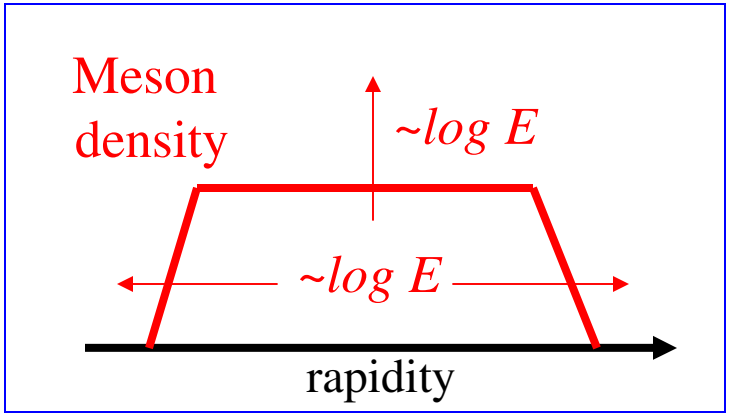

Leading proton (1– η)×energy
η = inelasticity ~ 0.9
Rapidity~*ln tan* $\theta/2$

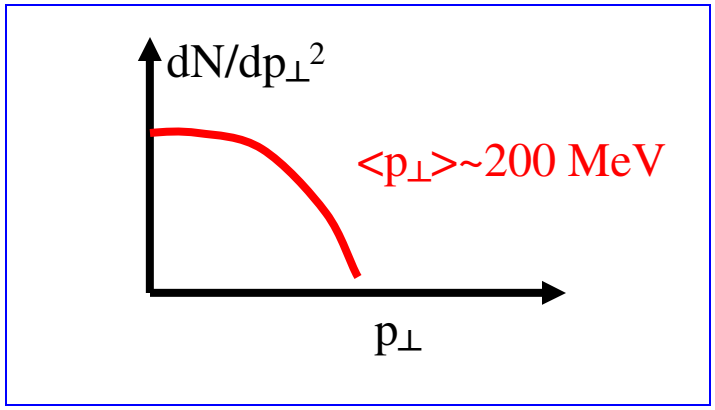

Transverse momentum

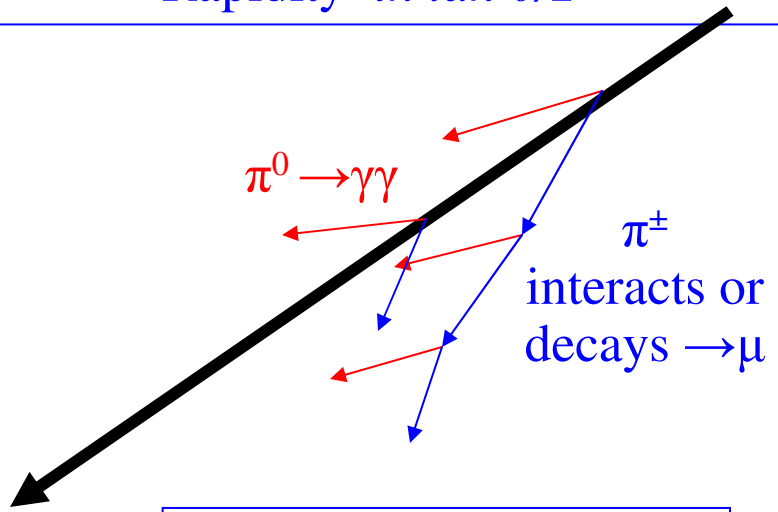

Electron-photon dominated

Shower development

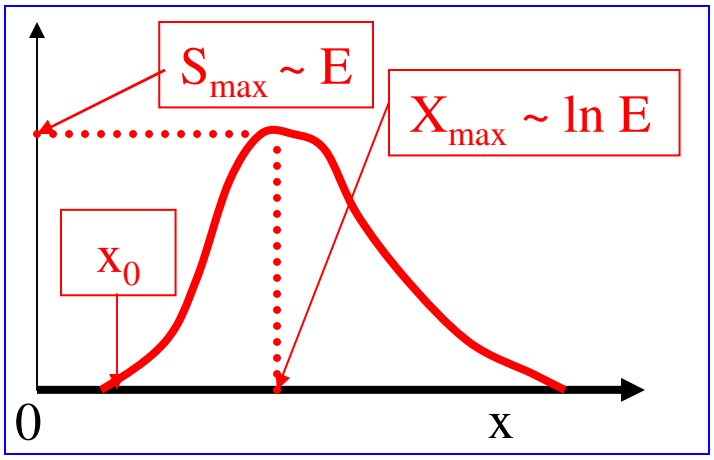

Gaisser Hillas profile

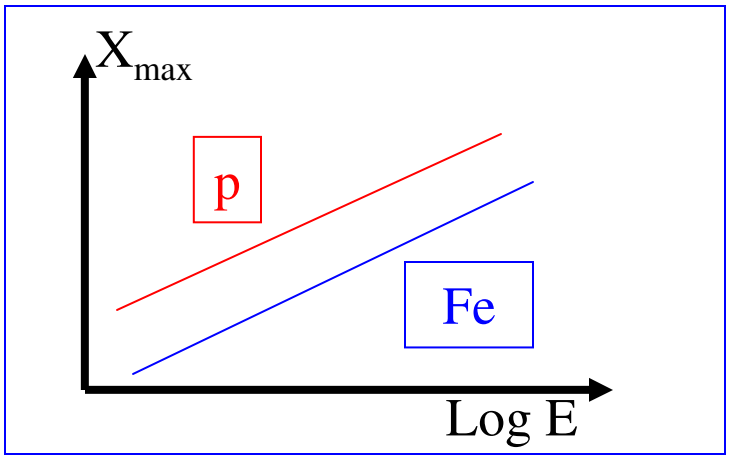

Elongation rate

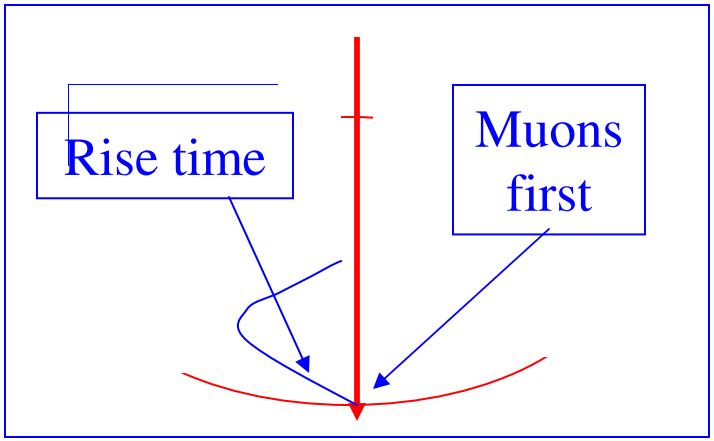

Shower front and rise time

High energy showers are electron/photon dominated because π^0s decay immediately ($\gamma\gamma$) while $\pi^{\pm}$ may either interact again or decay ($\mu\nu$).
A nucleus of energy E and atomic number A behaves as A nucleons of energy E/A
Heavier nucleus implies smaller x_0

A developing shower

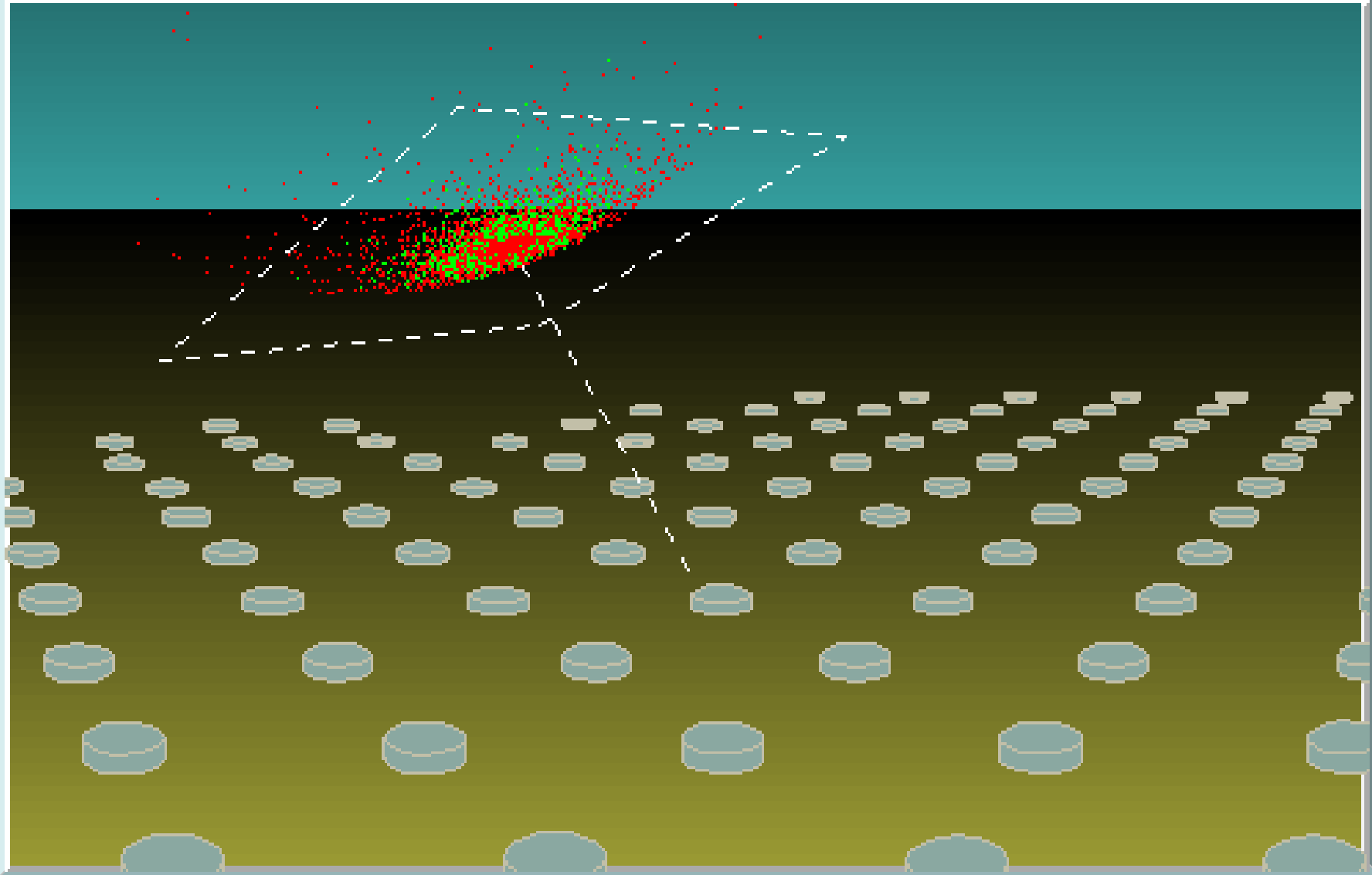

Measuring the shower energy

Ground array : Transverse

Well-defined acceptance

Indirect measurement:

needs simulation and/or

hybrid calibration

Fluorescence : Longitudinal

Track-length integral gives

calorimetric measure of energy

X_{max} sensitive to primary mass:

$X_{max} \sim L \ln(E_0/A)$

Delicate systematics

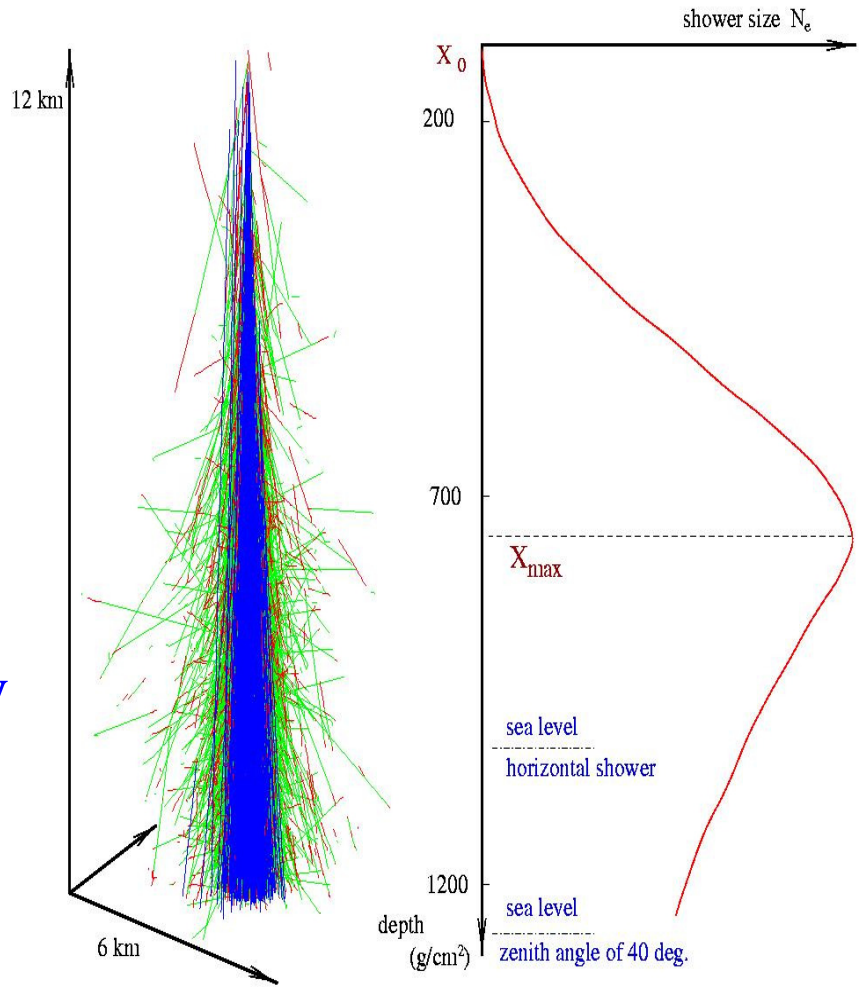

Fluorescence Detectors: SHOWER RECONSTRUCTION

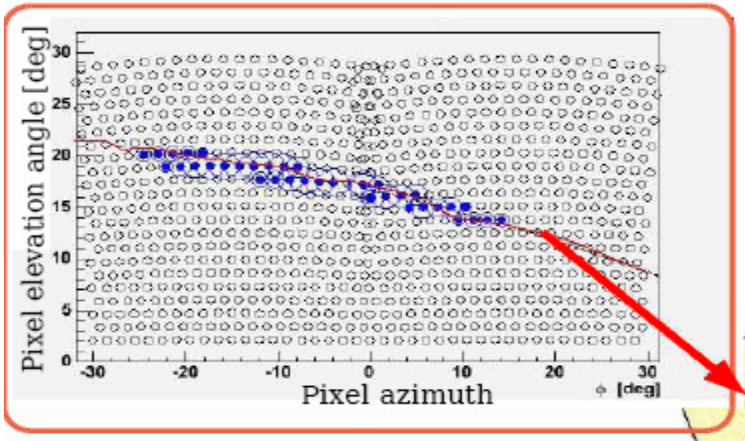

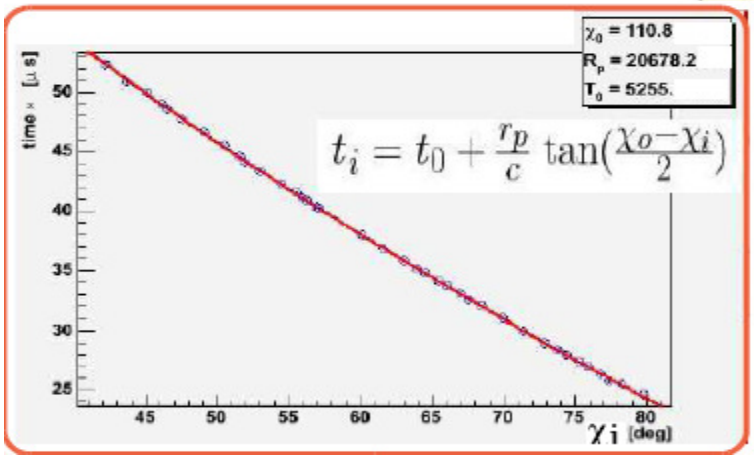

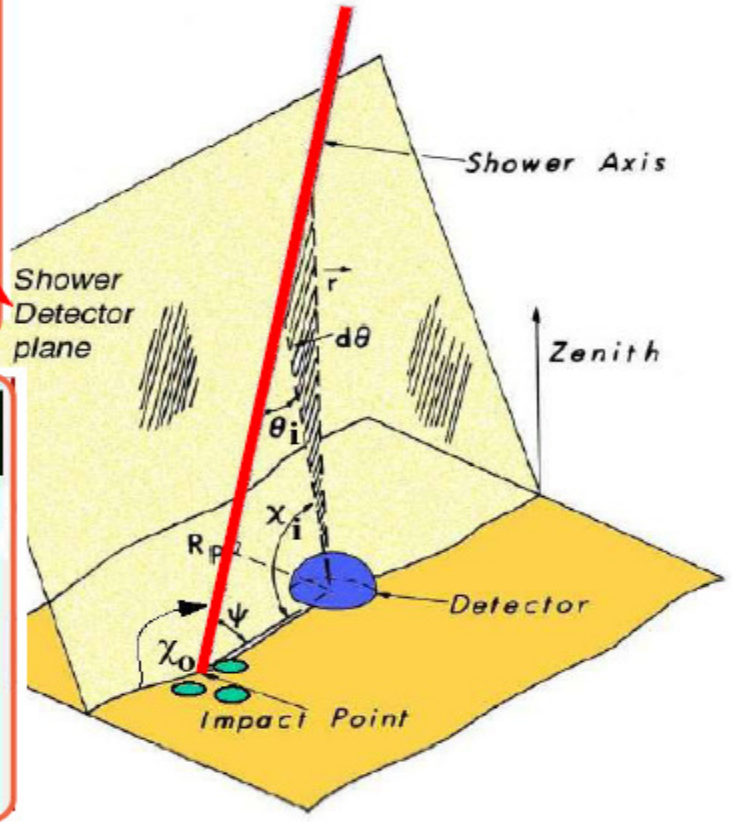

The pixel pattern defines the shower detector plane (accurately), the time distribution along the track locates the shower within this plane (not accurately)

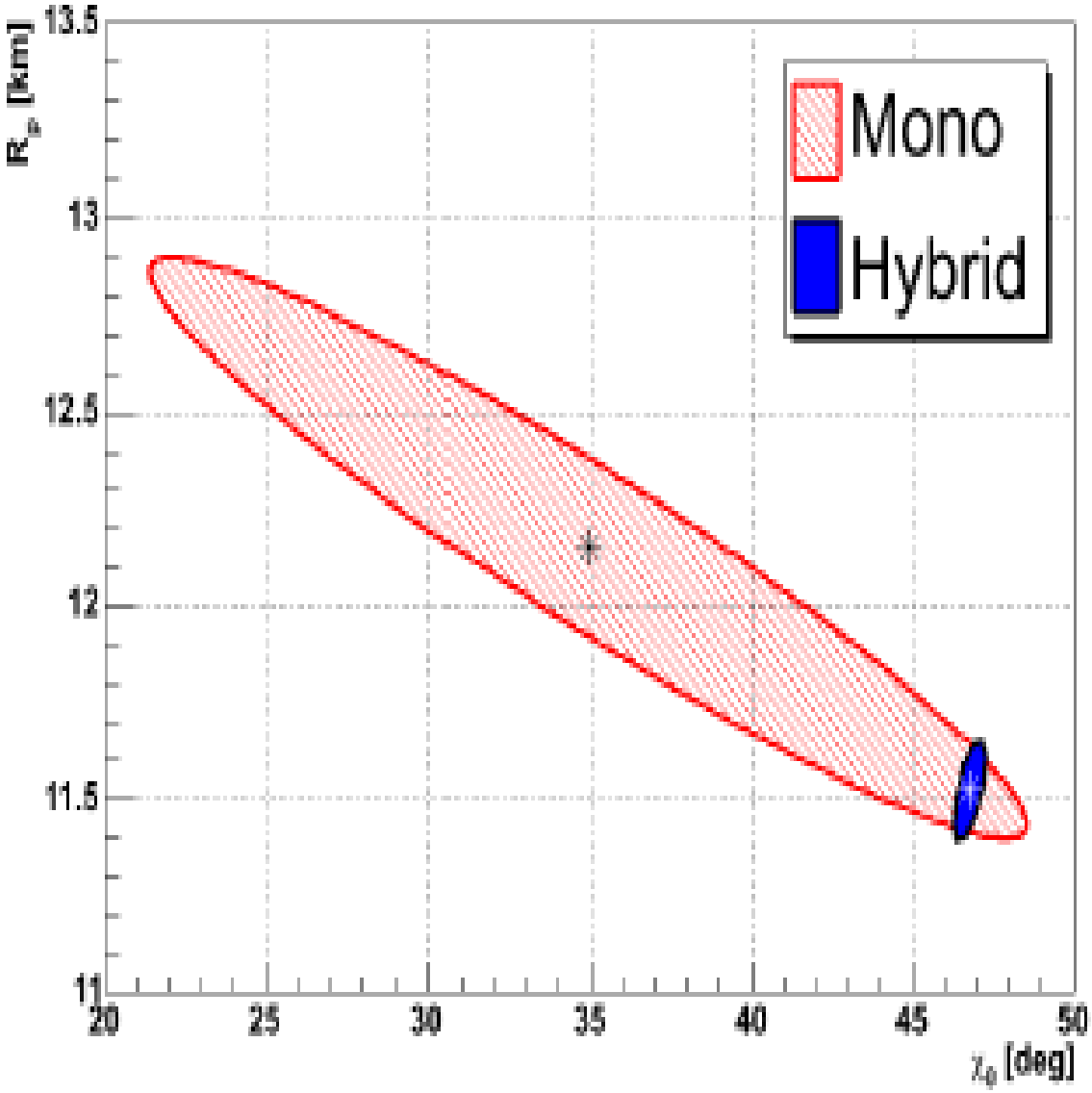

Fluorescence:

A single eye alone is insufficient for an accurate location of the shower in the plane. Binocular detection or hybrid detection (FD and SD) are necessary. Both are available in Auger.

SHOWER RECONSTRUCTION

4 unknowns: event time t_0,

shower front curvature C,

shower axis direction cosines $\mathbf{u}$

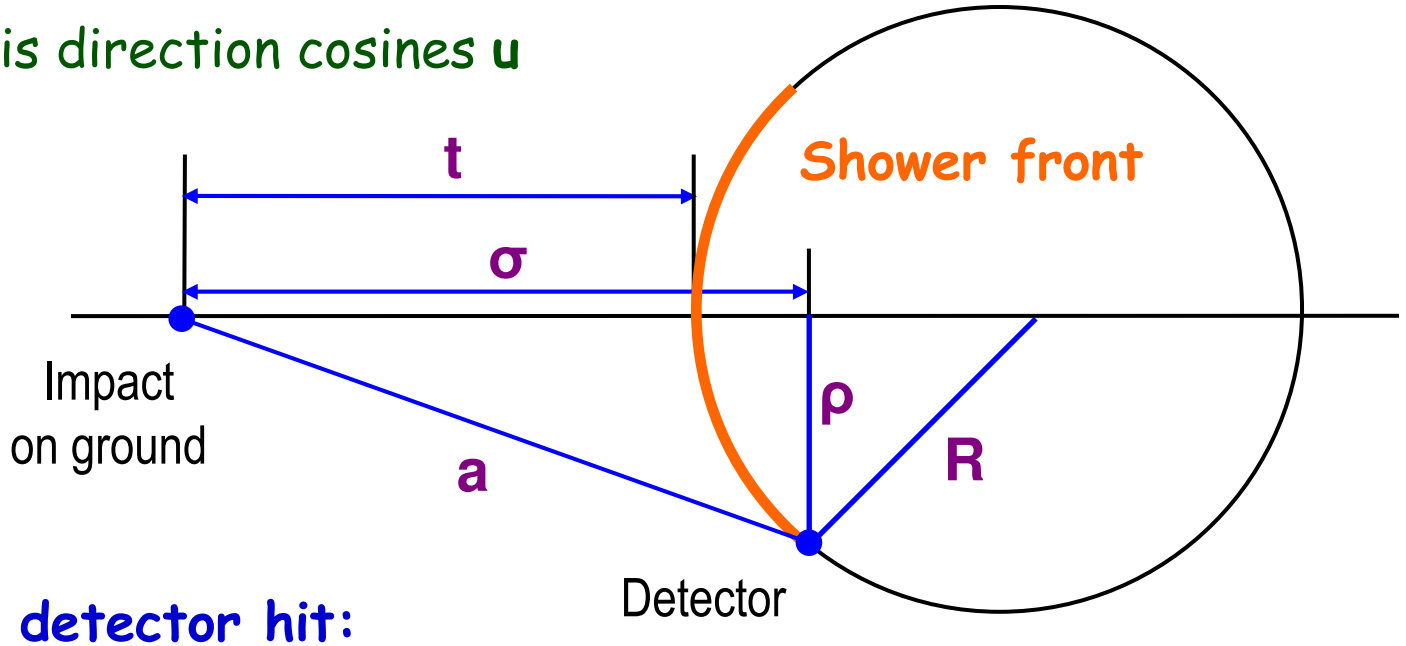

For each detector hit:

$$\sigma = \mathbf{u}.\mathbf{a}$$

$$t = t_0 + \sigma - C[t^2 + \mathbf{a}^2 - 2\sigma t]$$

The figure is drawn in the shower detector plane when the shower front hits the detector

ENERGY MEASUREMENT IN THE GROUND ARRAY

The energy measurement obtained from the surface detector relies on the dependence of the measured signals on the distance to the shower axis (so-called lateral distribution function, LDF).

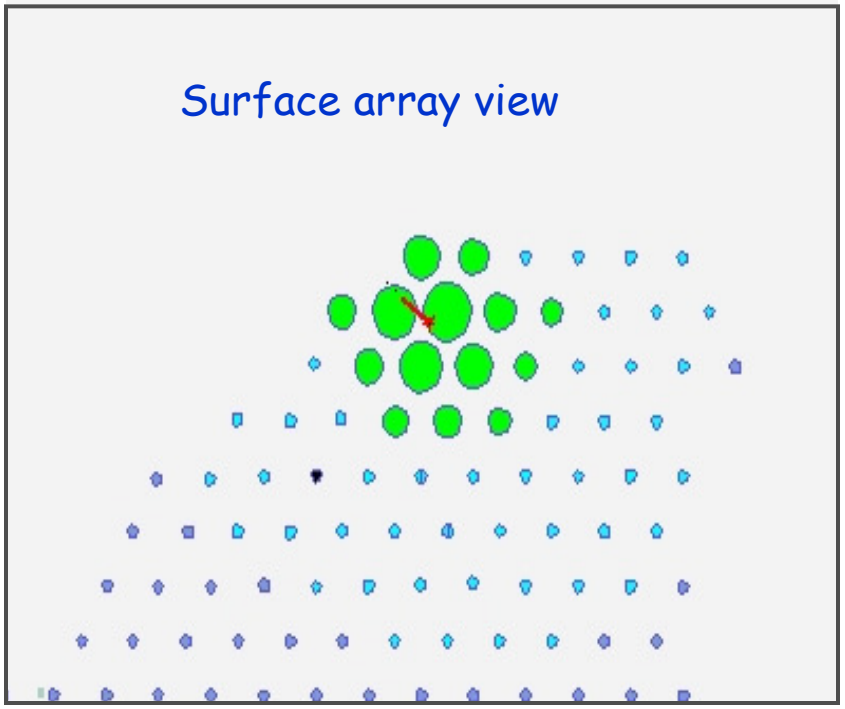

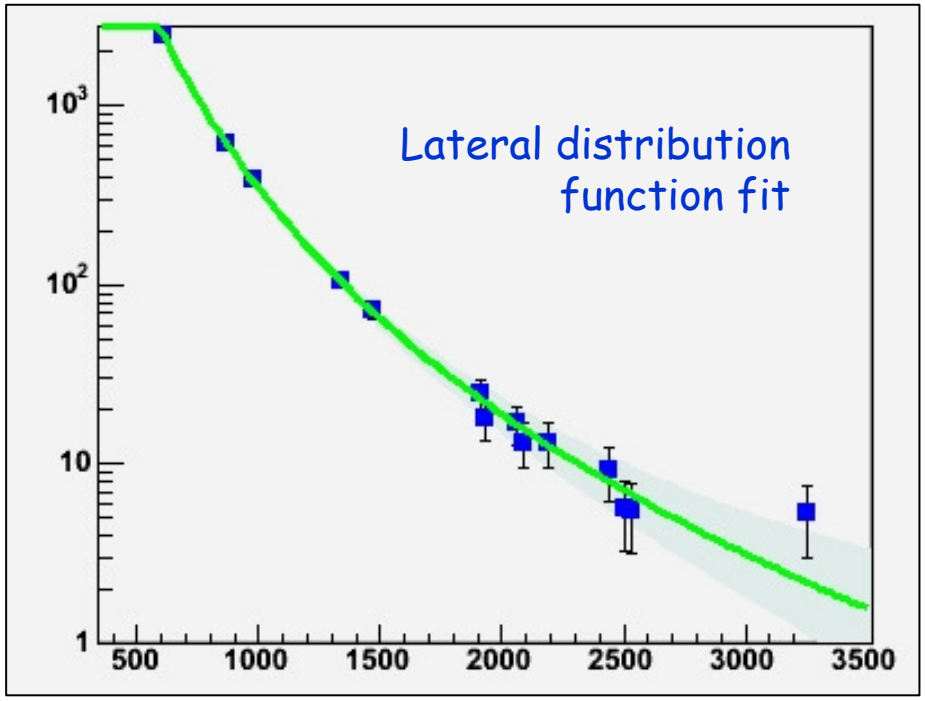

Calibration using hybrid events

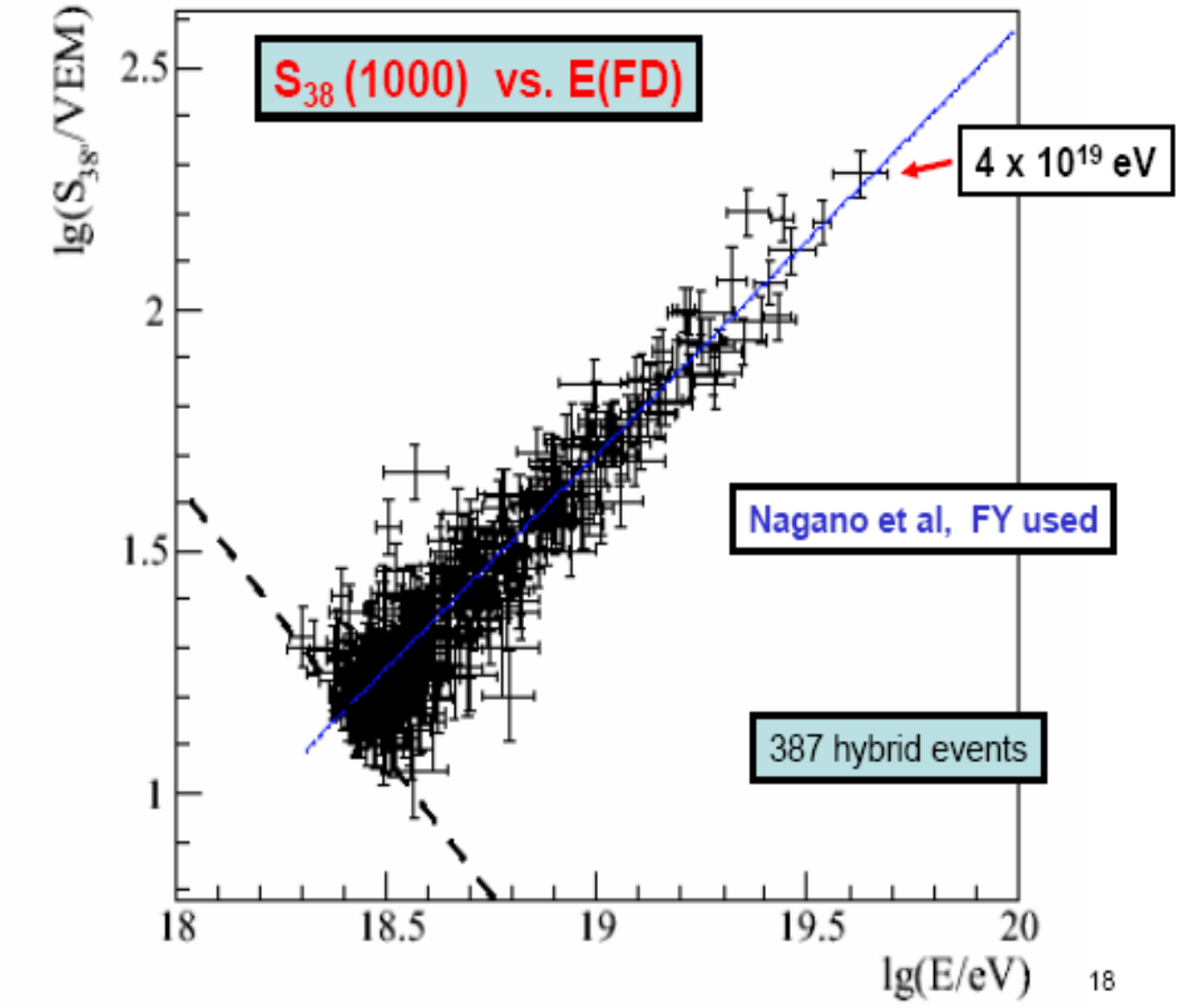

X_{max} vs energy

Protons penetrate deeper into atmosphere,

heavy nuclei develop higher up

Shower to shower fluctuations should give additional information

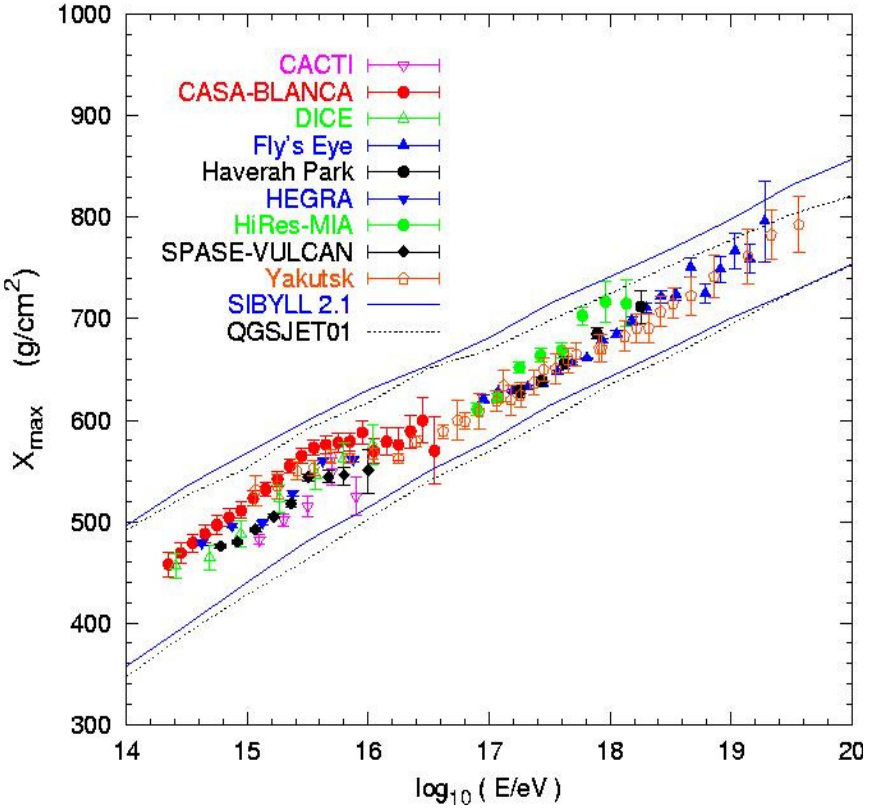

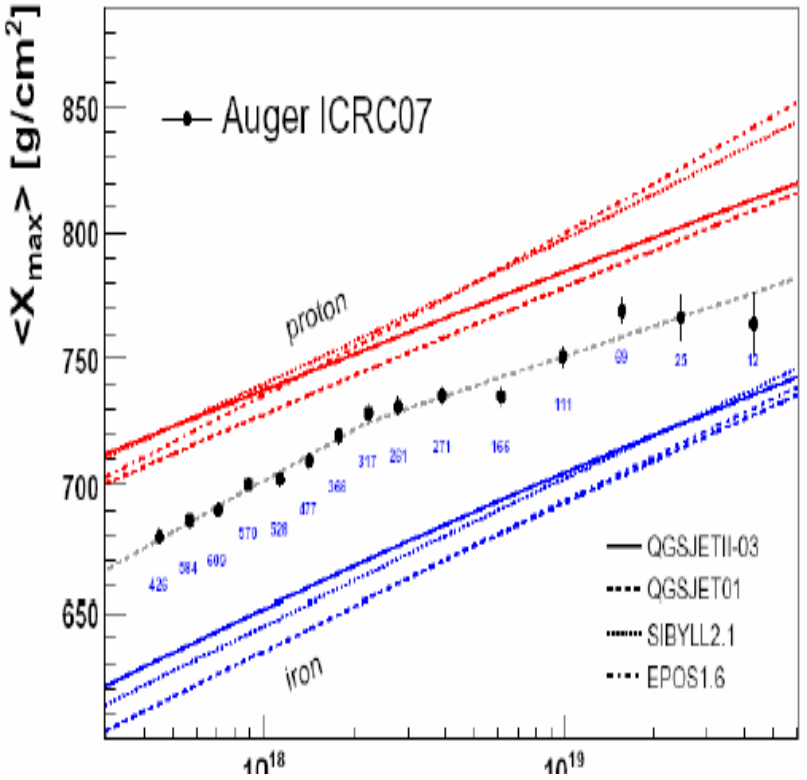

Knee of spectrum

Differential spectral index changes at ~ 3 10^{15}eV

a = 2.7 → a = 3.0

Continues to 3 x 10^{18} eV

Expect exp{-E / Z E_{max}} cutoff for each Z

Fine-tuning problem: to match smoothly a new source with a steeper spectrum

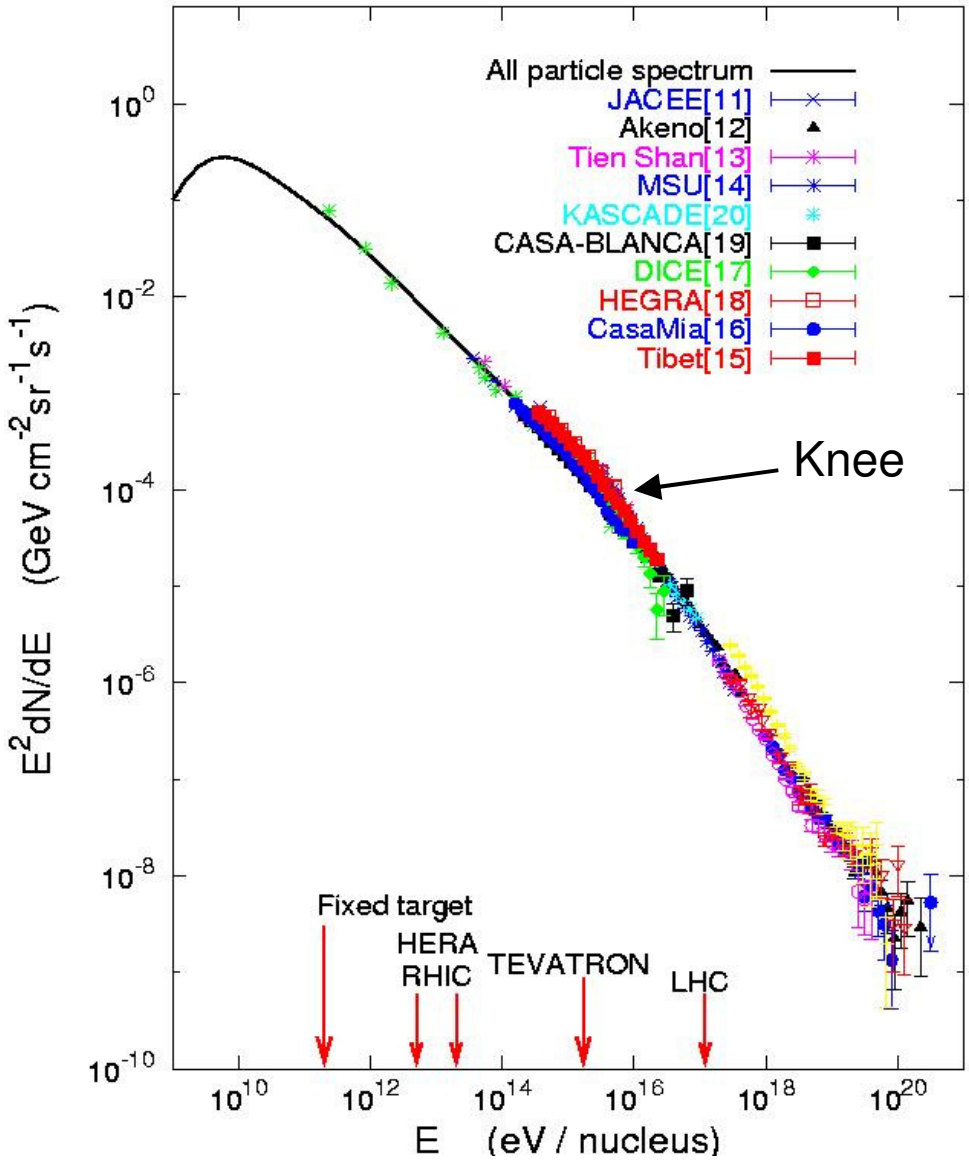

Energy spectrum of CRs

Dip scenario

Dip
$p + \gamma \rightarrow p + e^+ + e^-$

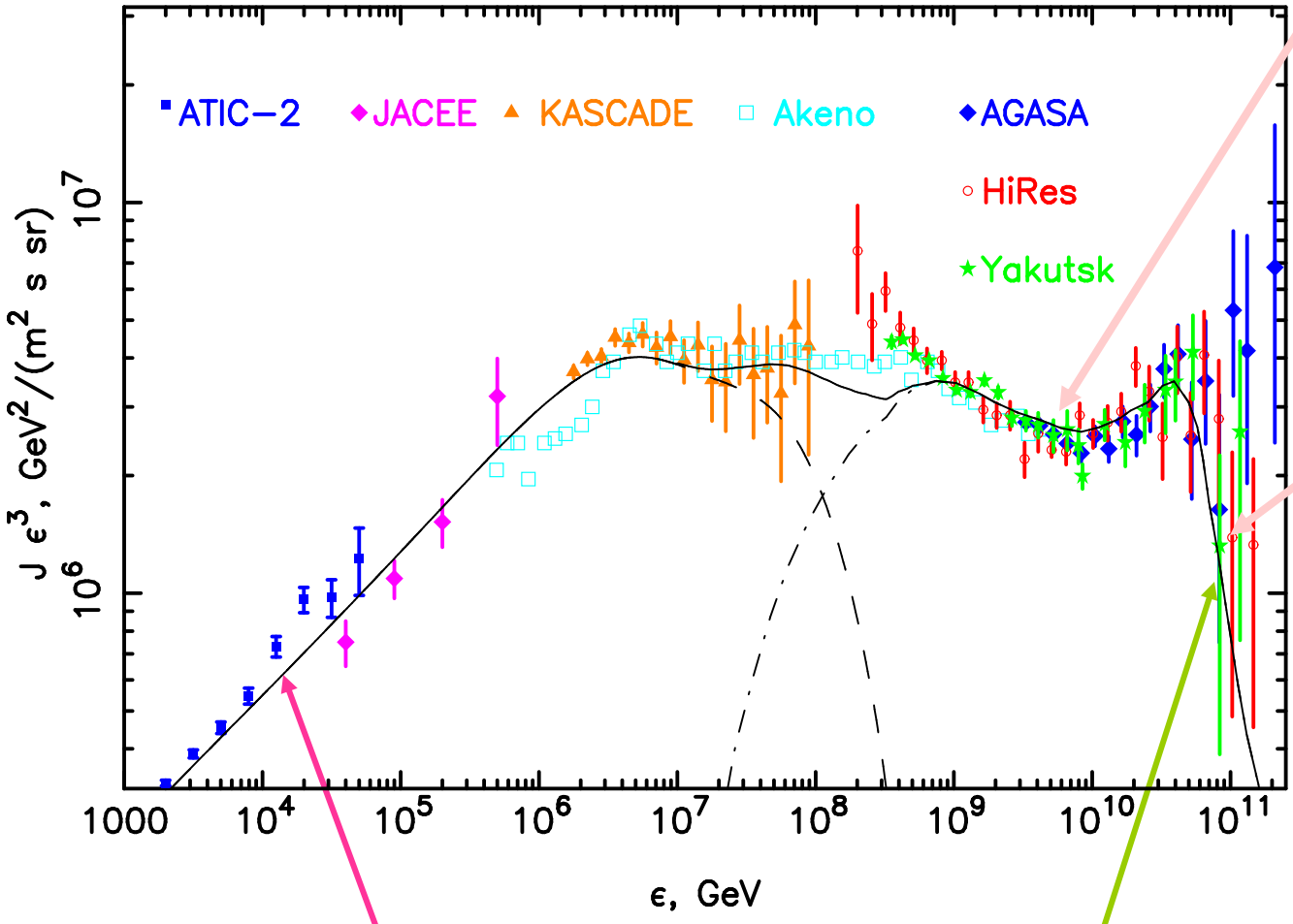

GZK cutoff
$p + \gamma \rightarrow N + \pi$

Experiment:
Akeno-AGASA
(Takeda et al. 2003)
HiRes
(Abbasi et al. 2005)
Yakutsk
(Egorova et al. 2004)

CR spectrum, produced in SNRs

CR spectrum from $J_{EG} \sim \varepsilon^{-2.7}$ extragalactic sources (*Berezinsky et al.2006*)

Interaction with the CMB

The photoproduction of pions is expected to occur above a threshold of some

10^{20}eV

$$p+\gamma \rightarrow p+\pi$$

$$M^2(p+\pi)=M_p^{\,2}+2(E_p+P_p)E_\gamma$$

$$\approx M_p^{\,2}+2\,M_pM_\pi$$

$$M_pM_\pi \approx 2E_pE_\gamma \qquad E_\gamma = 2.7K = 3.10^{-4}eV$$

$$E_p = \tfrac{1}{2}\, 0.14\, 10^{18}\, 10^4/3 = 2\, 10^{20}\, eV$$

Greisen Zatsepin Kuzmin (GZK)

With a typical interaction length in the few 10 Mpc scale: cosmic rays coming from larger distances will not make it to the Earth without interacting, and therefore loosing energy: their flux will be significantly damped

Earlier data : AGASA vs HiRes

Exposures (10^3 km^2 yr sr)
AGASA: 1.3
HiRes (mono): 2.2
Number of events >10^{20}
AGASA: 10 (+2?)
HiRes (mono): 2?
Both detectors have (different) energy-dependent acceptances

HiRes stereo data
Favored GZK cutoff

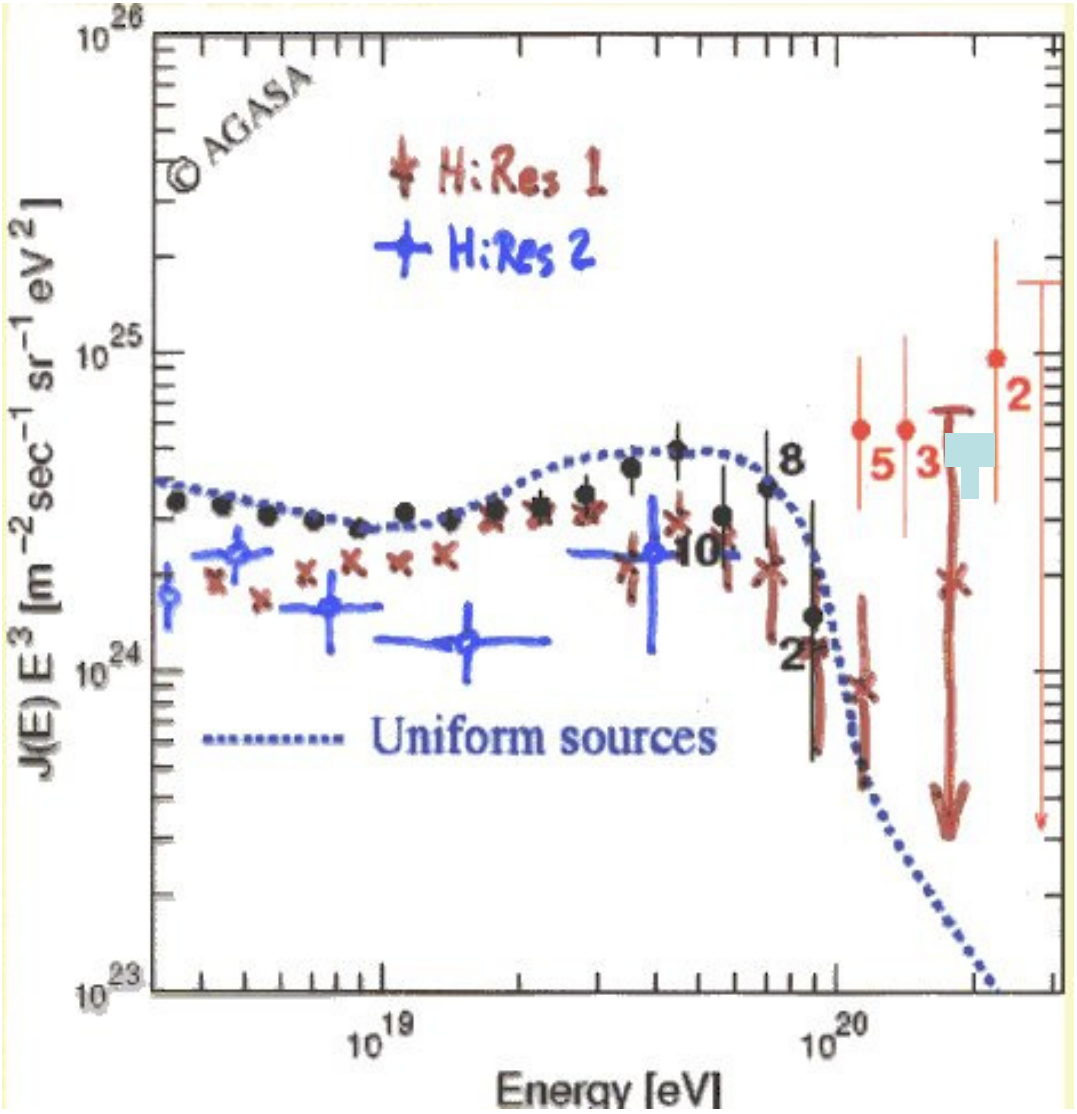

While earlier results were inconclusive the Auger results have now sufficient statistics to establish unambiguously the existence of the GZK cutoff

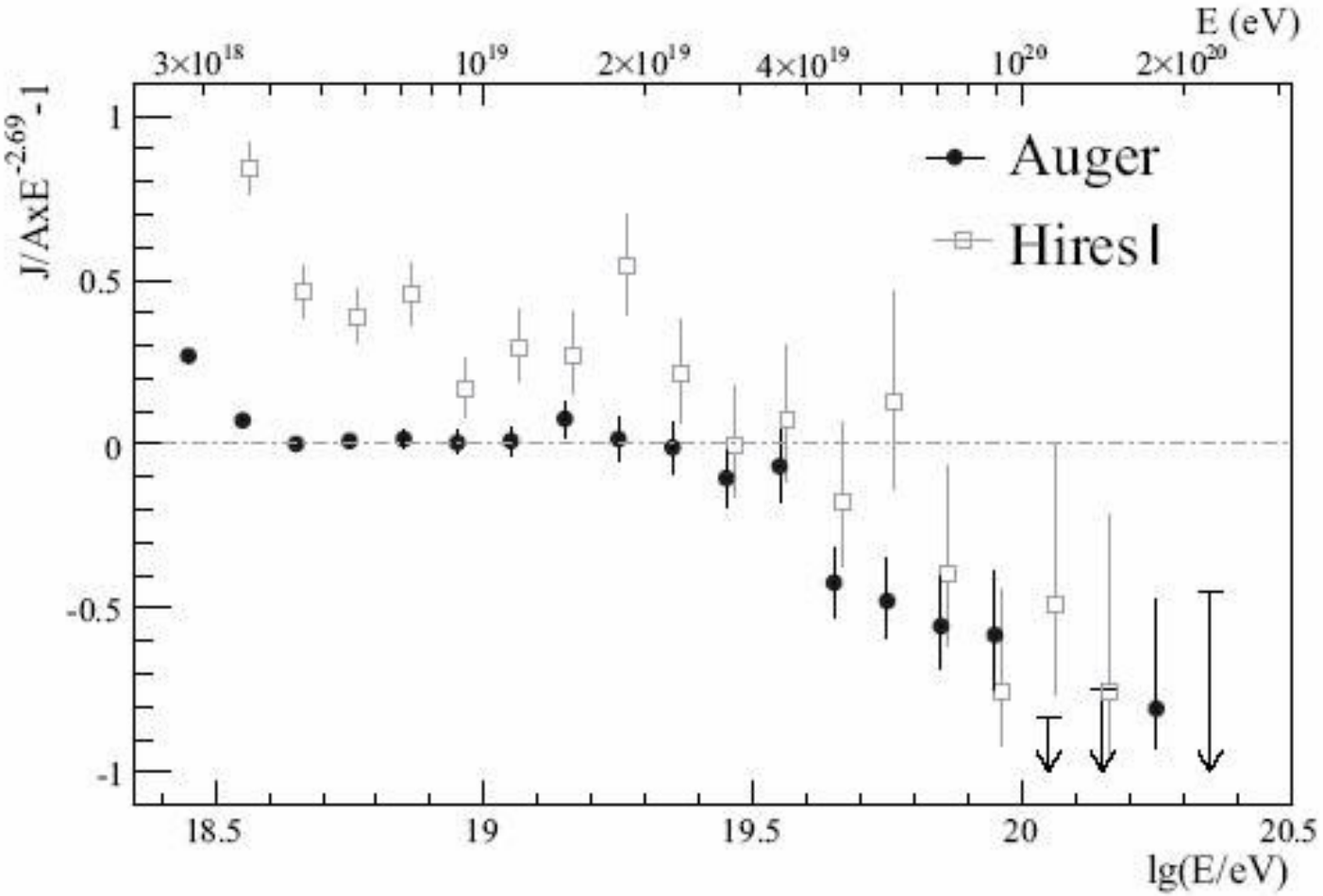

As a consequence, only nearby (<100 Mpc) sources can contribute to the UHECR spectrum

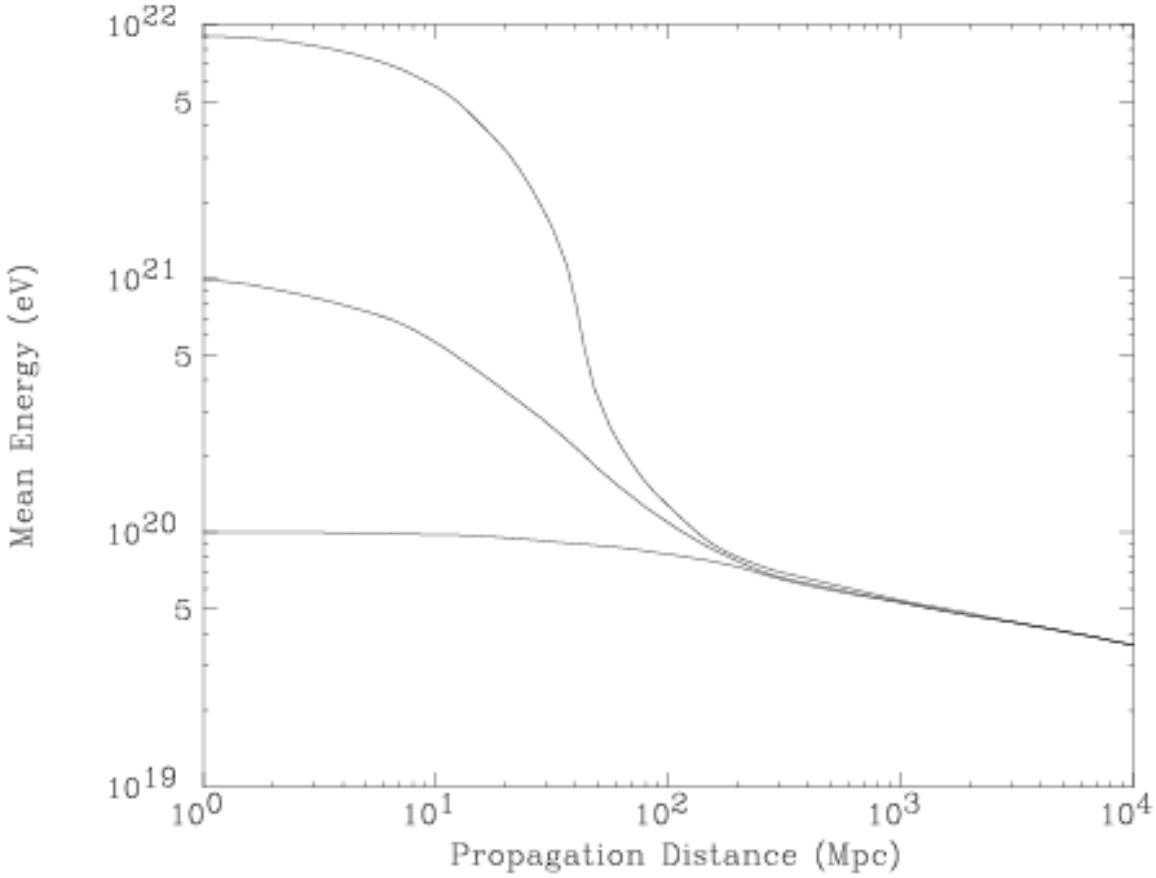

Mean energy of protons as a function of propagation distance through the CMB. Curves are for energy at the source of 10^{22} eV, 10^{21} eV, and 10^{20} eV. (from J W Cronin)

Georgi Zatsepin (Pamir, 1946)

THE SOURCES

Solar energetic particles
(SEP)
Gamma ray astronomy and
Supernova remnants
(SNR)
Ultra high energy cosmic rays
(UHECR)

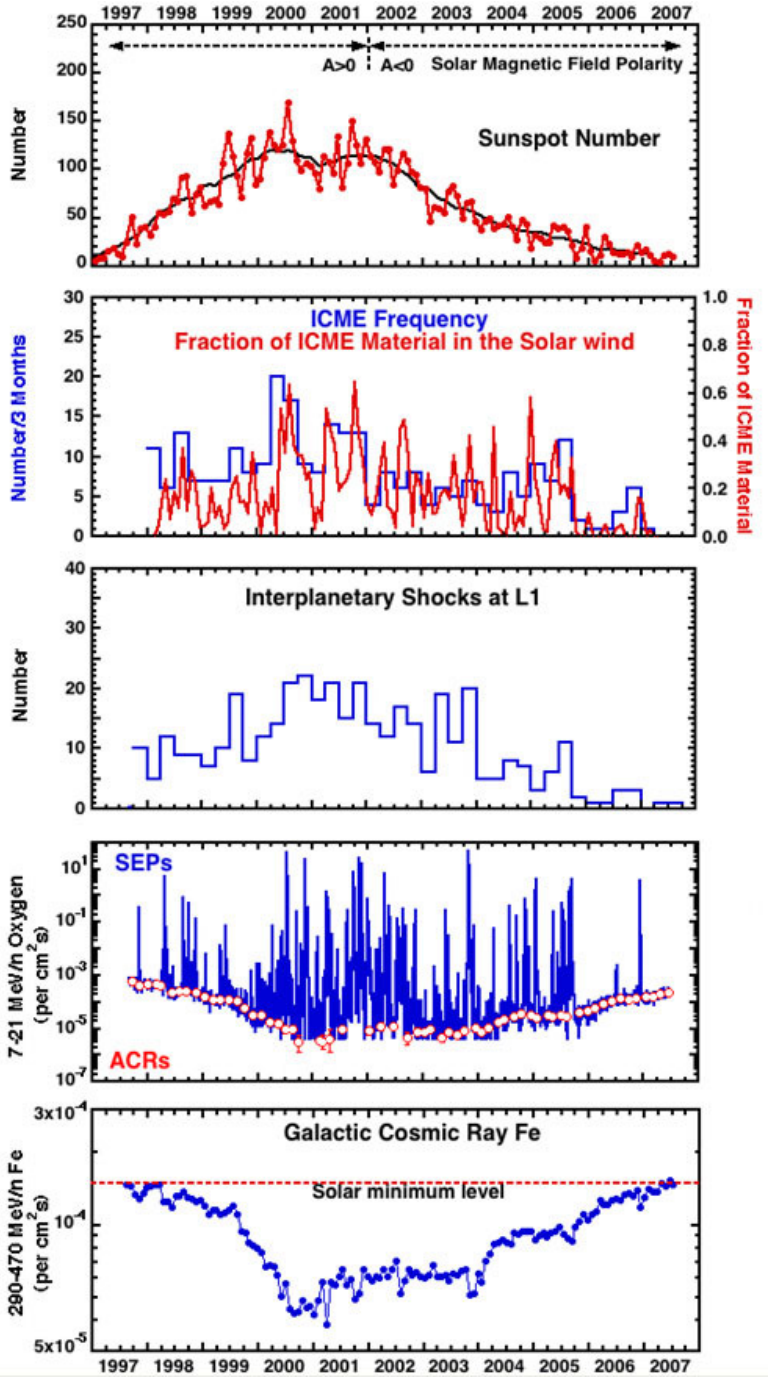

SUN

Particles coming from the Sun reach 100 MeV and are mostly associated with solar activity and flares (magnetic field lines recombination and field inversion with a 11 yr cycle). Coronal Mass Ejections and interplanetary shocks (most are caused by CME) are similarly correlated. On the contrary, galactic cosmic rays are anticorrelated with the solar activity increasing the magnetic field which acts as a shield.

SUN:ACE Energetic particle fluences

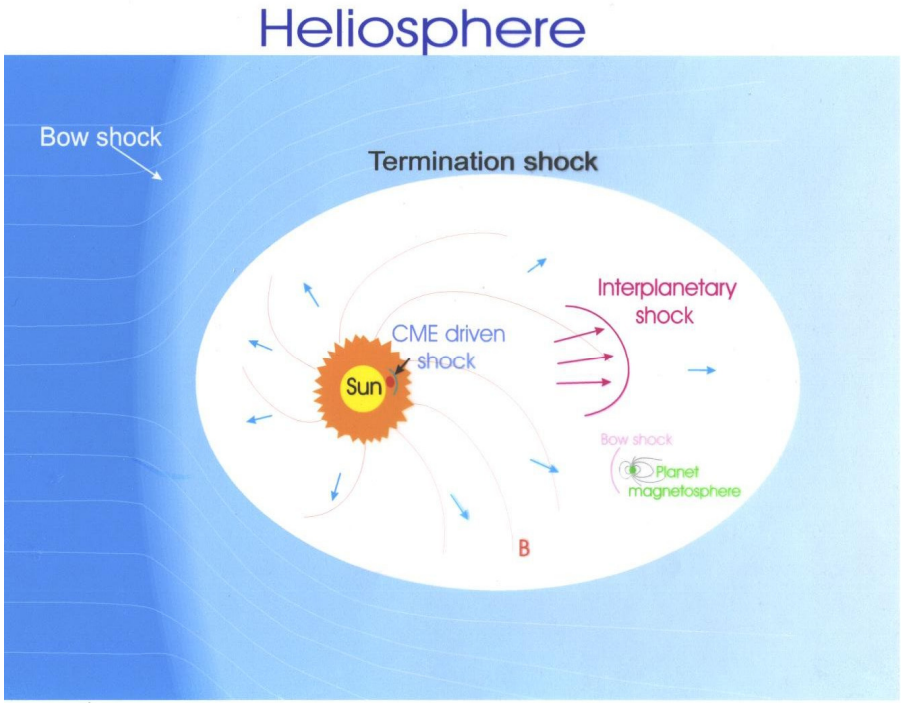

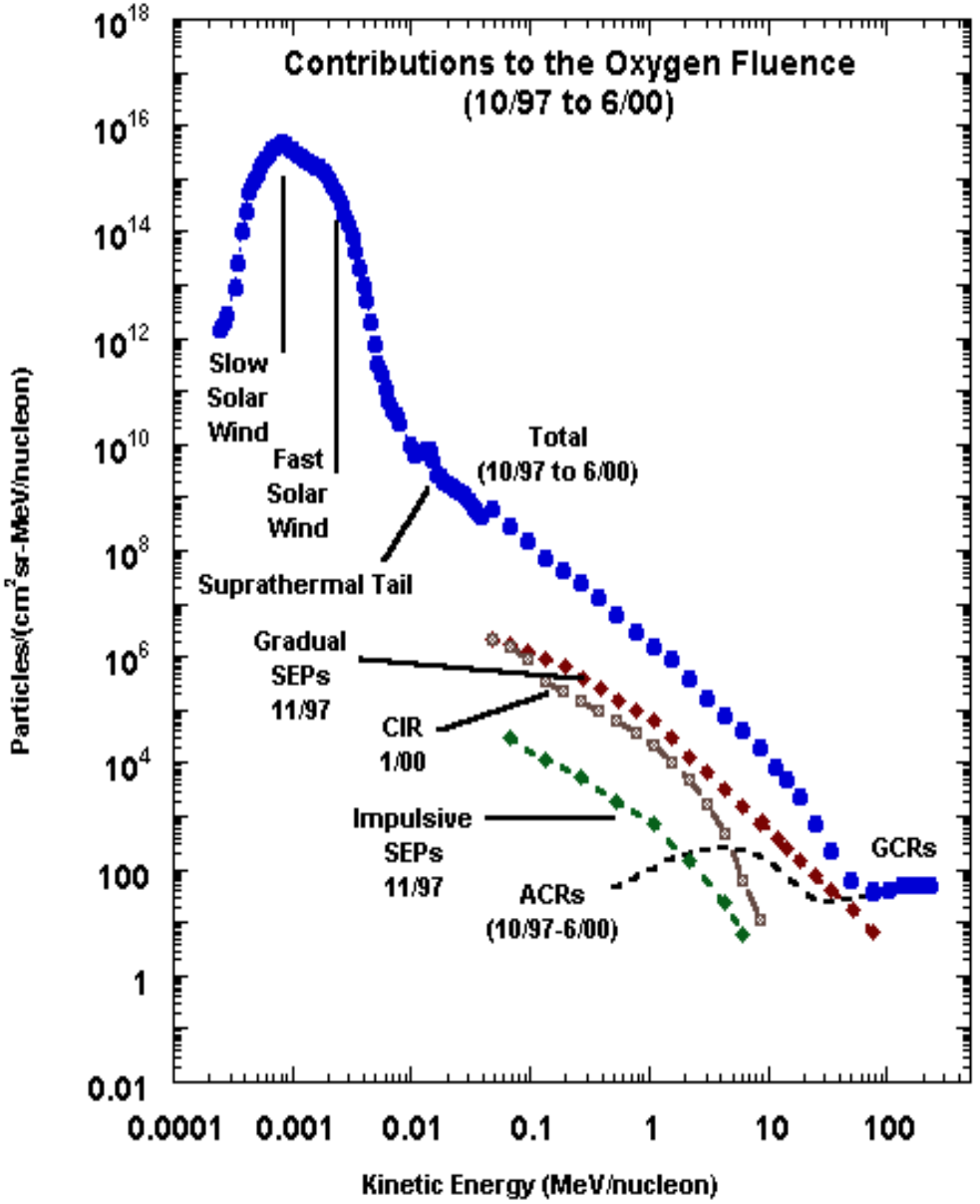

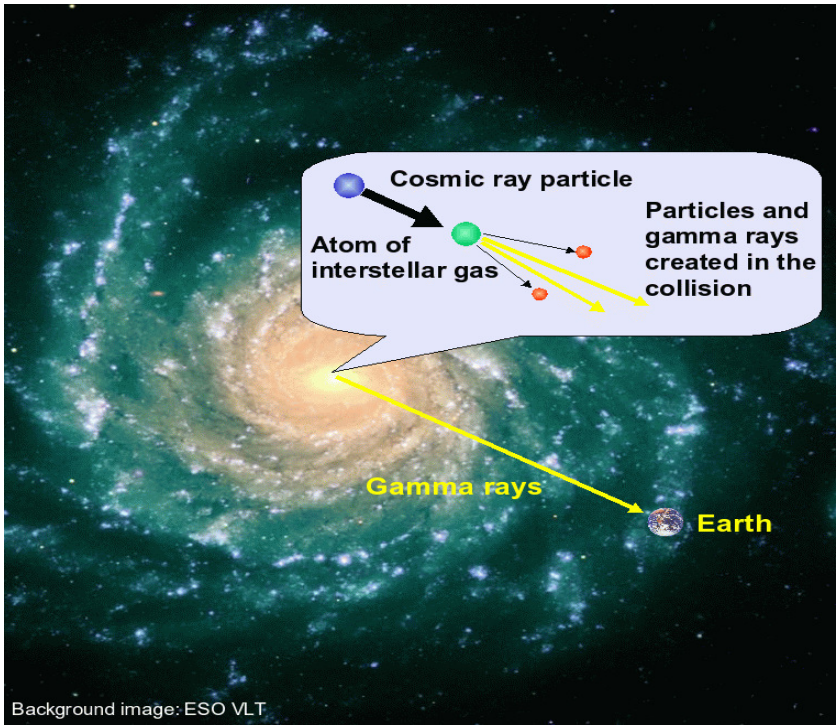

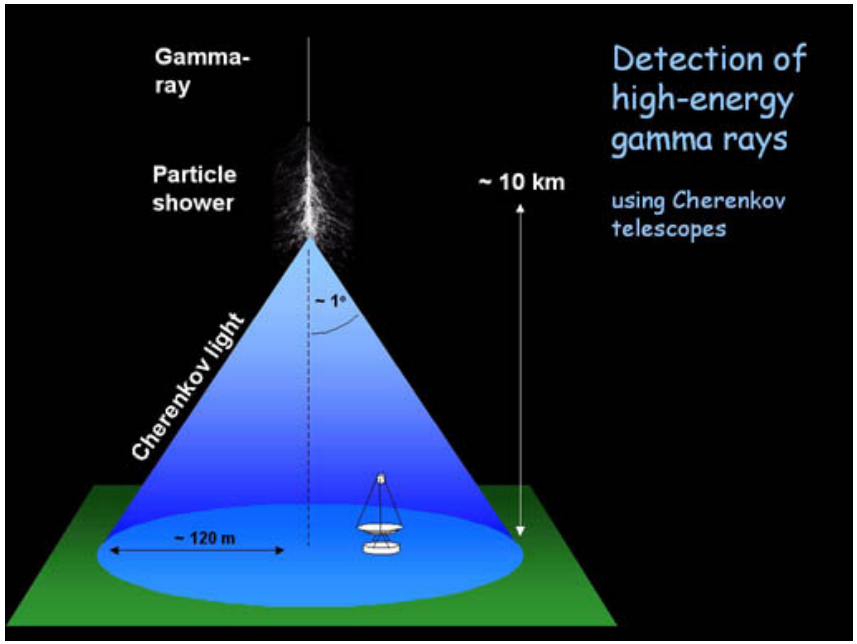

Gamma ray astronomy as a tracer of cosmic ray sources

Contrary to cosmic rays, gamma rays travel straight in the universe and point back to the sources.

They are good at detecting the high energy decay photons coming from neutral pions produced in the interaction of very high energy cosmic rays with interstellar matter.

The High Energy Stereoscopic System (HESS, Namibia): four telescopes at the corners of a 120×120 m^2 square, operating above 100 GeV. Its field of view is 5^o and its resolution a few arc minutes. It takes only 30 seconds to take a picture of the Crab.

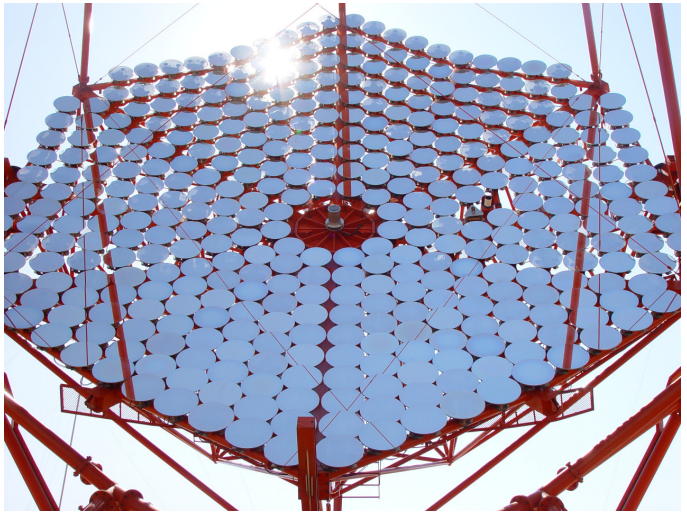

Gamma ray astronomy has established that most galactic cosmic rays originate from Supernova remnants (SNRs) by comparing their X-ray and γ-ray images

Main sources of photons are bremsstrahlung (synchrotron radiation) at low energies and at high energies π^0 decays (hadrons) or inverse Compton on CMB (electrons)

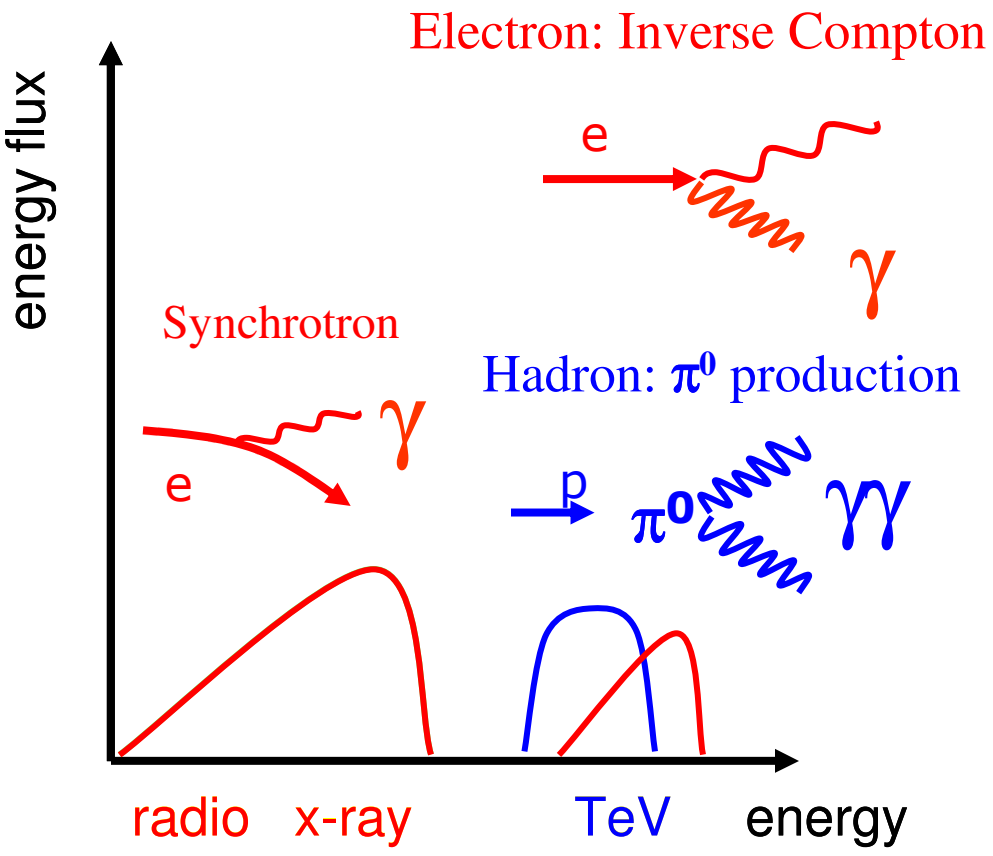

HESS TeV Observations have revealed numerous shell-type SNRs

Largest TeV source known : RX J0852.0-4622

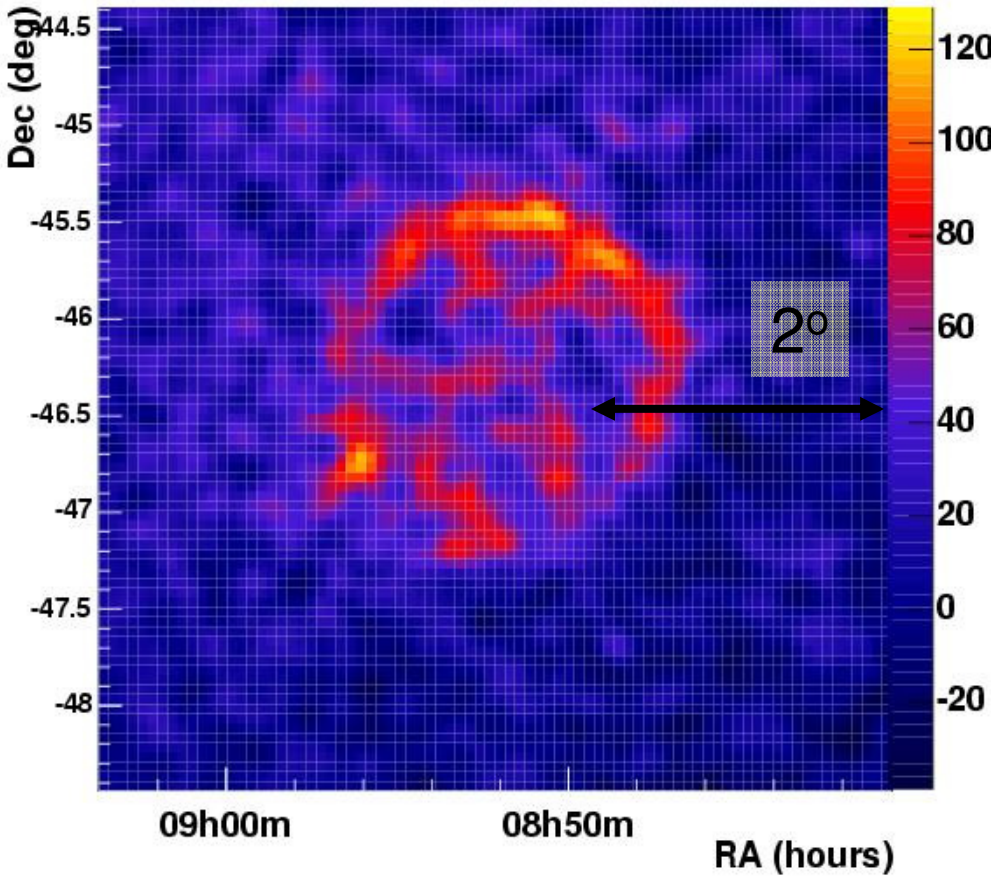

G347.3-0.5

ROSAT PSPC

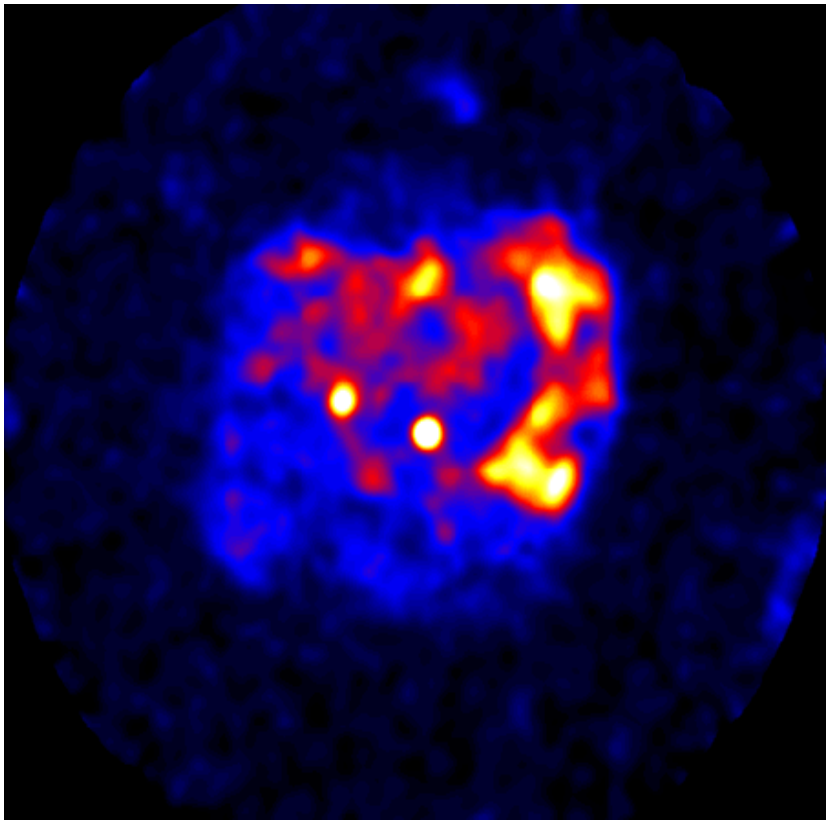

HESS

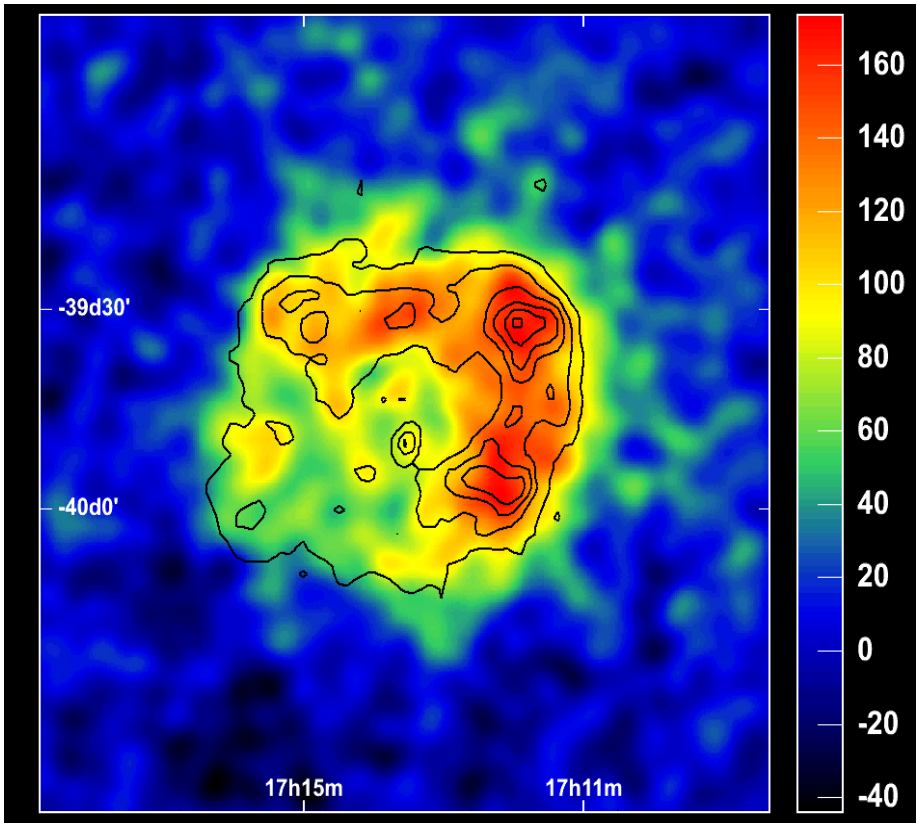

RX J1713

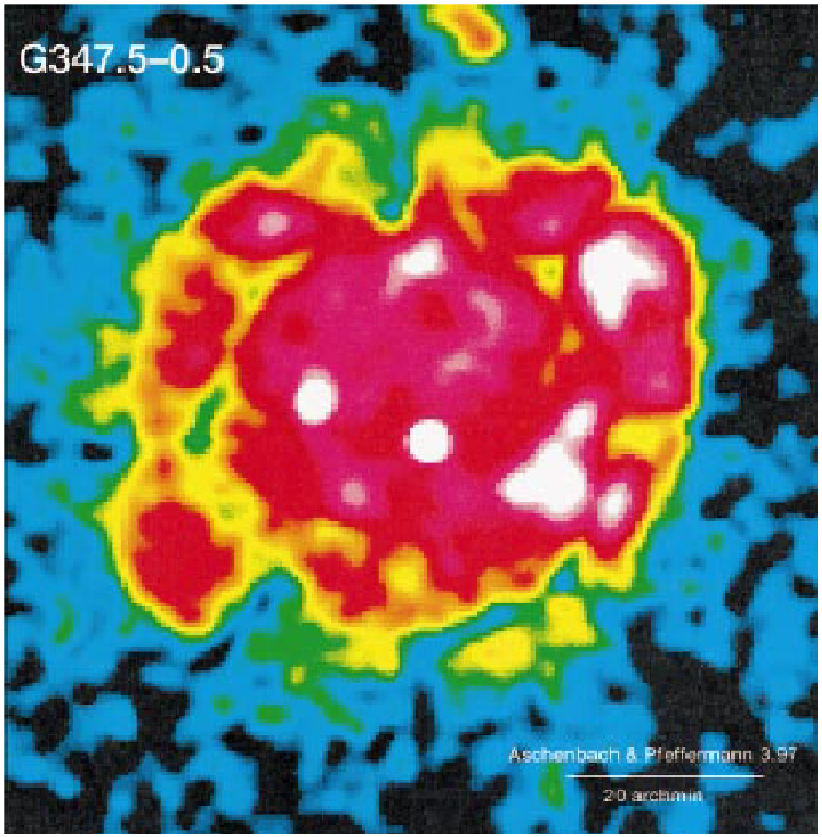

ROSAT 1996
Mostly non-thermal X-rays
D ~ 1 kpc

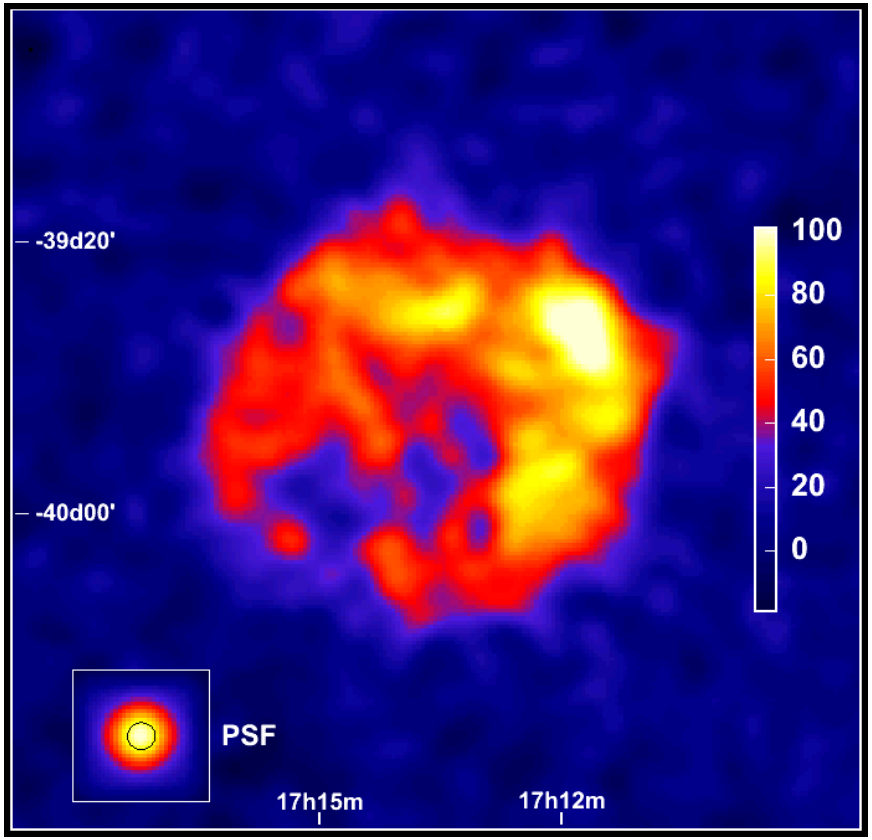

H.E.S.S. 2004
4-telescope 33 h live-time
Shell resolved

X-Ray observations locate the shock accurately

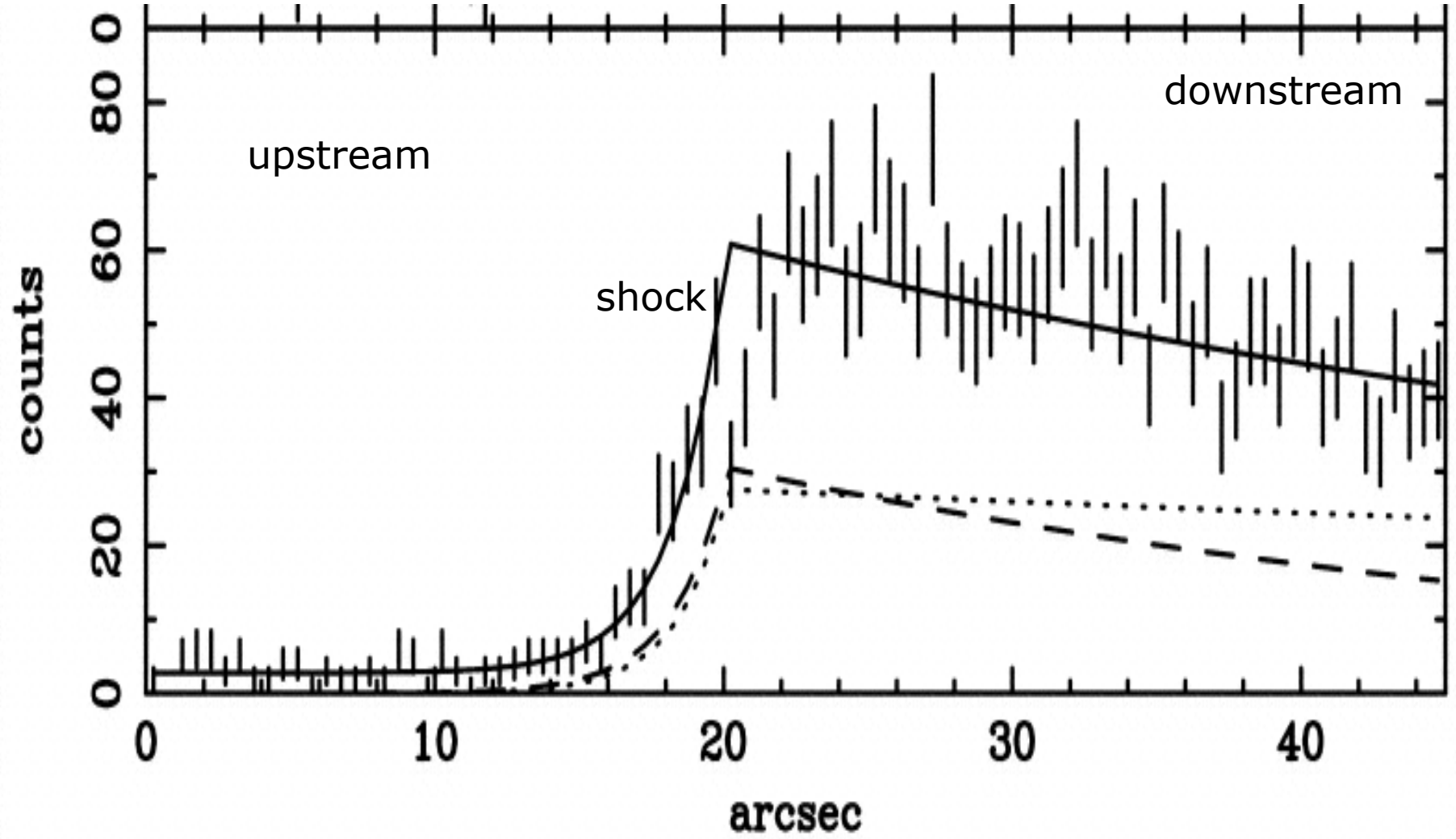

80% correlation between TeV γ-rays and X-rays (HESS and ASCA)

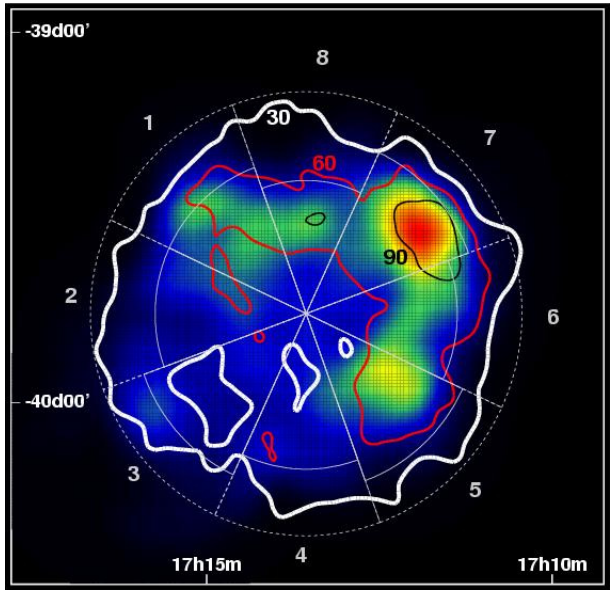

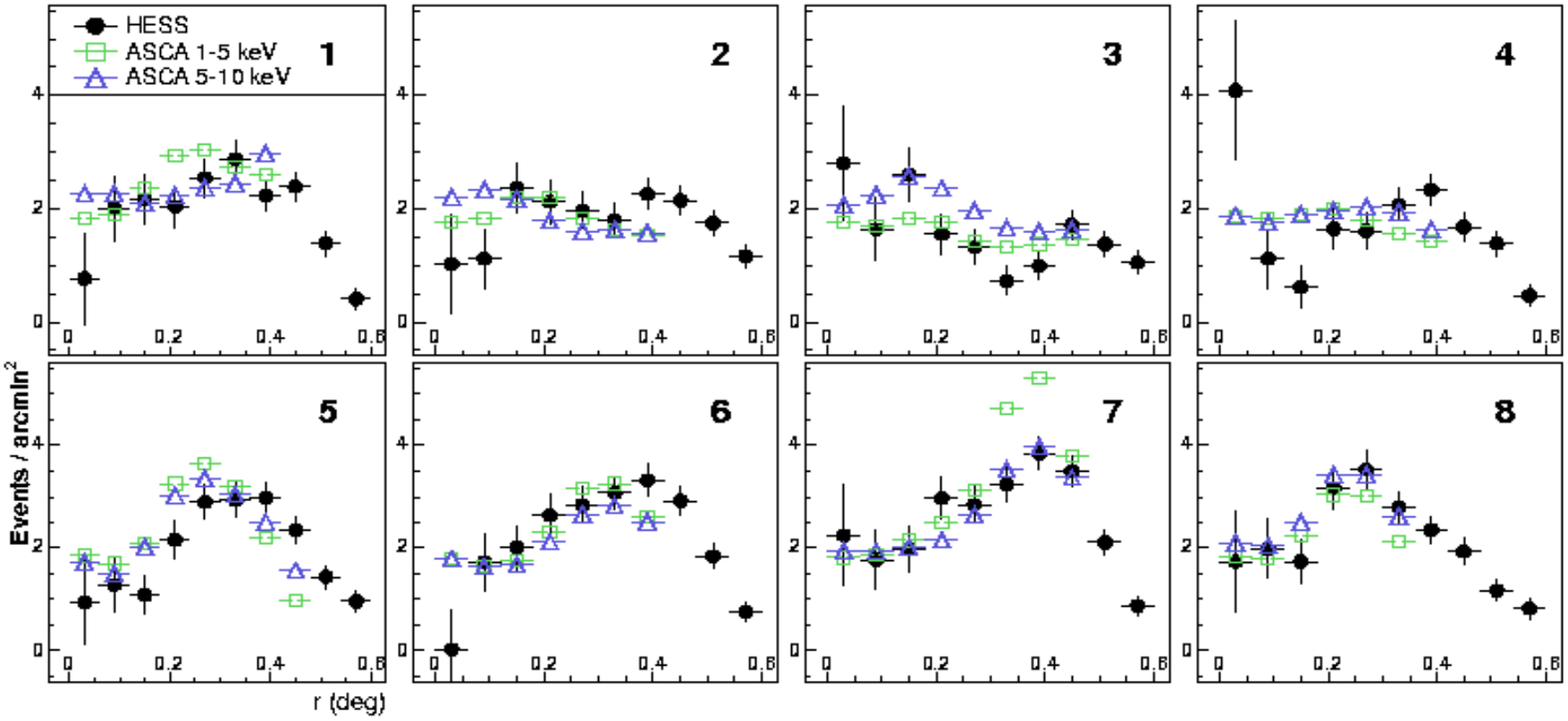

UHECR

Auger data show a clear correlation
of UHECR (>6 10^{19} eV)
with nearby (<75 Mpc) galaxies.
There is an even better correlation
with nearby AGNs.
Correlation disappears when including lower
energy cosmic rays (pointing accuracy) or
farther away galaxies (GZK).

Our environment (100 Mpc radius) is extremely inhomogeneous

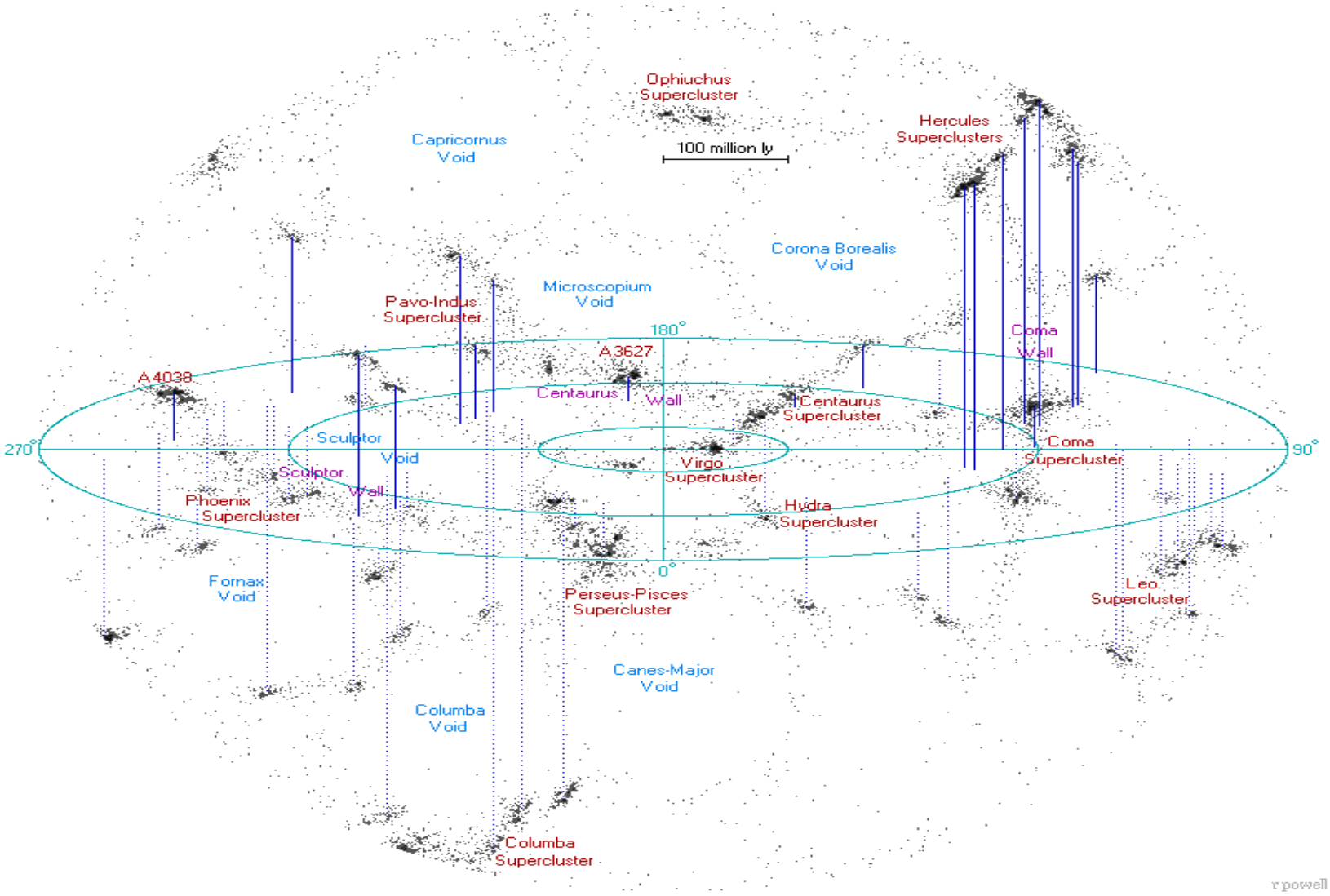

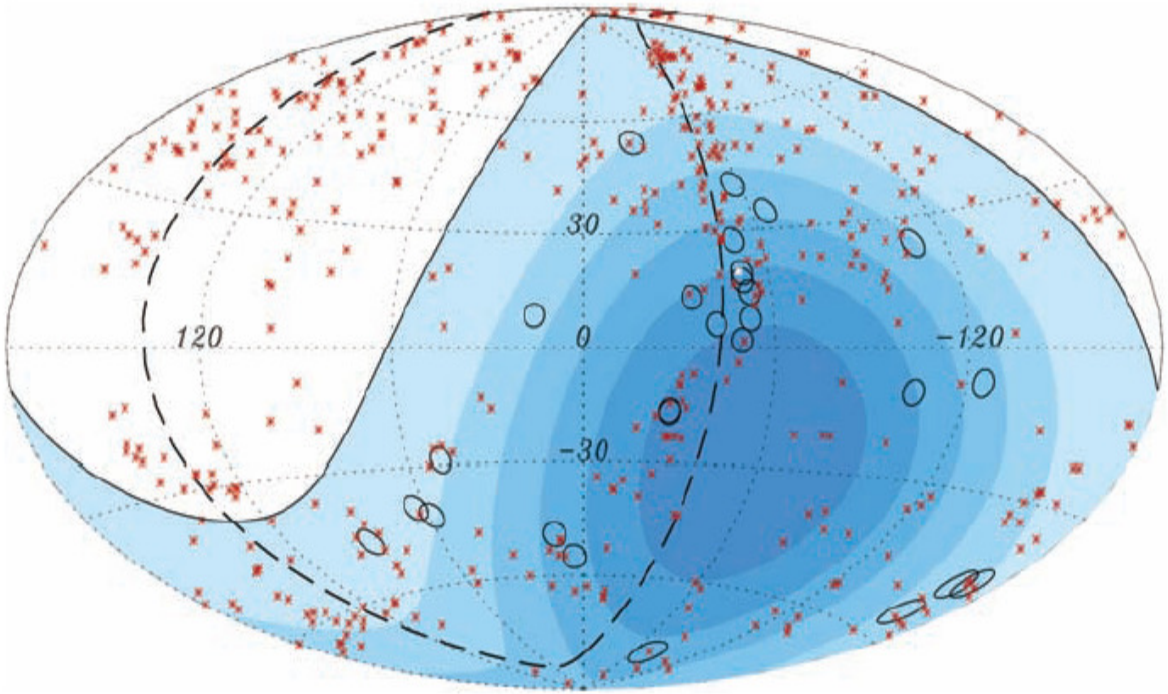

Circles of 3.1^{o} on 27 UHECR detected by Auger
Red crosses are 472 AGN (318 in field of view)
having z<0.018 (D<75Mpc)
Solid line shows field of view (zenith angle < 60^{o})
Color tells exposure
Dashed line is super galactic plane

The UHECR detected by the PAO are able to point to sources in the sky (typically within 1°).
It was not a priori so obvious because of uncertainties in magnetic fields met by UHECR during their journey to the Earth (typically 3μG in the disk mean 6 10^{17} eV).

A new page of astronomy has been opened,

until now only photons could be used.

It remains to be understood why such and such a galaxy, AGN or else, is a source

while such and such another is not.

Neutrinos are next to come

Not many celestial objects have large enough Magnetic field × volume

to be candidates for UHECR acceleration

(Hillas plot)

Apart from magnetars which would suffer of excessive synchrotron losses,

the only possible candidates are

GRBs or active galaxies

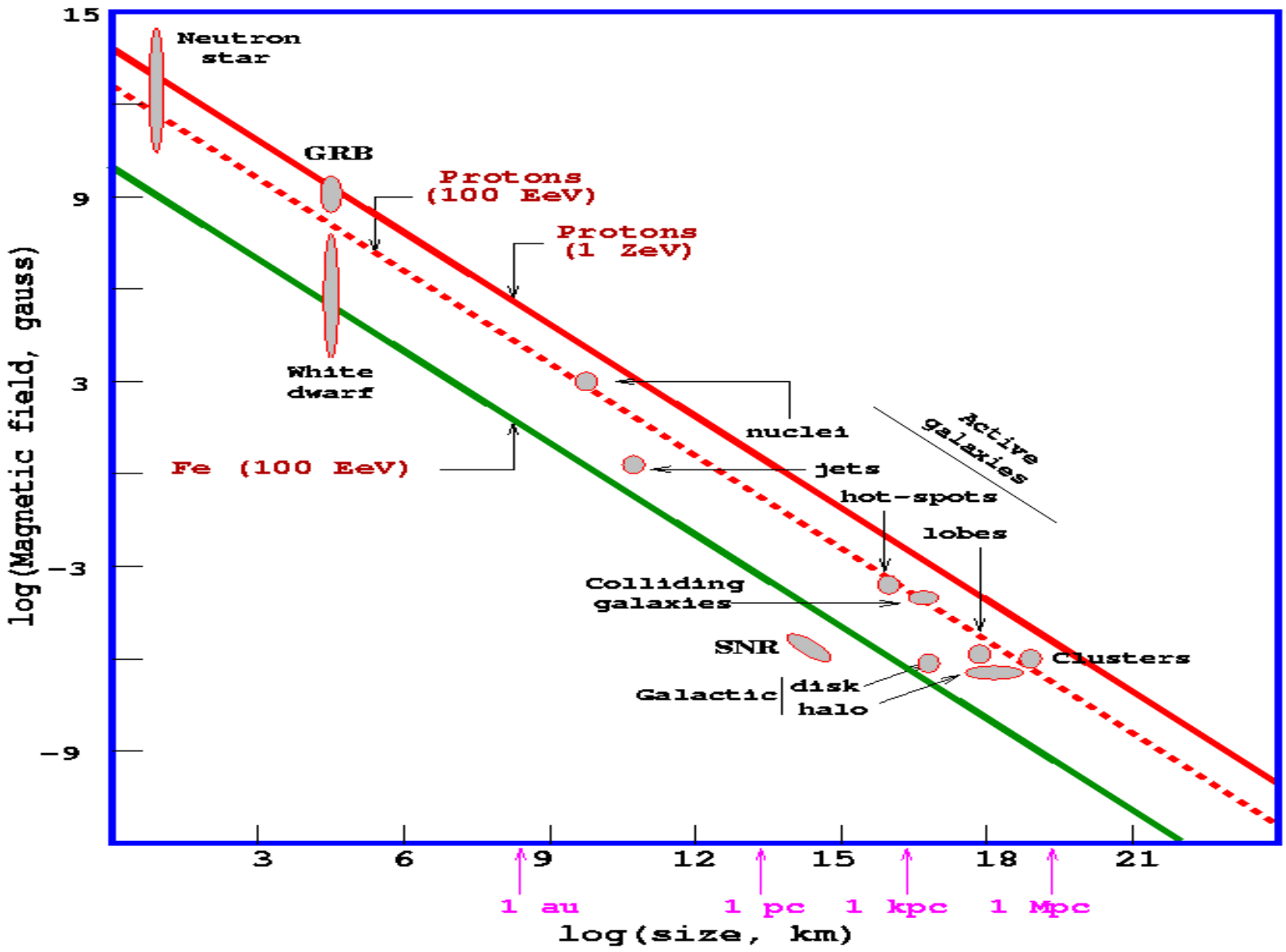

$E_{max} \sim ZBL$ (Fermi)

$E_{max} \sim ZBL\Gamma$ (Ultra-relativistic shocks-GRB)

SUMMARY OF THE FIRST LECTURE

Cosmic rays are accelerated atomic nuclei with elemental abundances as prevails in the Universe (apart from spallation reactions) but uncertainties subsist at UH energies; CR have a power law spectrum with index ~2.7 cutoff at ~10^{20}eV by interactions with the CMB; they contribute ~1eVcm^{-3} to the energy density of the Universe, as much as visible light, CMB or magnetic fields; they play an important role in the ISM dynamic. The Sun, wind and shocks, contributes to low energies. Most cosmic rays are of galactic origin and accelerated in the shells of young SNRs. Most UHECR have their sources in AGN rich regions. Recent progress in γ ray and UHECR astronomies have made cosmic ray physics a field of astrophysics in its own right

ACCELERATION IN SHOCKS

Introduction

ISM and magnetic fields

Generalities on SNRs

Generalities on shocks

Magnetic field amplification

Larger scale shocks

Diffusive shock acceleration: an introduction

As in a cyclotron the particle is accelerated locally on traversing the shock (equivalent of the gap between the dees) and is guided by magnetic fields on either side in such a way as to come back to the shock (equivalent of the dipole guide field).

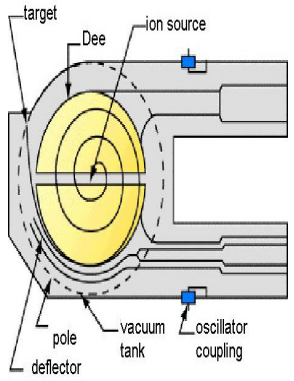

However both the acceleration
and guiding processes
are very different from the cyclotron case.
Guiding is provided by stochastic collisionless
scattering on magnetic turbulences.
Acceleration is best described in the shock
frame where both upstream and downstream
media move toward eachother
with large relative velocity β.

Hence the energy $E+\Delta E$ of the cosmic ray (mass M) after having traversed the shock is given as a function of its energy E before having traversed the shock as

$$E+\Delta E = \gamma\beta E+\gamma p$$

with $\gamma^2 = \gamma^2\beta^2+1$ and $E^2+p^2 = M^2$

$$\beta<<1 \rightarrow \gamma\sim 1$$

For relativistic cosmic rays, p = E and

$$\Delta E = \beta E+O(\beta^2)$$

$\Delta E/E=\beta$ implies

$E_n= E_0(1+\beta)^n$ after n shock traversals

One speaks of

first order Fermi acceleration

A stochastic succession of such processes nearly cancels: second order Fermi acceleration has negligible effects

Inter Stellar Medium (ISM)

Not static but alive, continuously recycled through star collapses, made of three basic constituants:
matter, magnetic fields and cosmic rays
Amounts to 10-15% of the MW disk mass, half of it in clouds occupying 1-2% of the ISM volume, mostly very cold dark molecular peaking at R=5±2 kpc
and cold diffuse atomic extending from 0 up to 20 kpc
Elemental abundances close to solar system, 91% H
About 0.5-1% in mass in the form of dust
OB associations and SNs affect ISM through winds, radiation, heating, ionization, explosions

ISM density is so small that collisions can be neglected: momenta (not energy!) change exclusively via the action of magnetic fields

Component	T(K)	Observed	N(cm^{-3})
Molecular	10-20	2.6mm CO	10^2-10^6
Cold atomic	50-100	21cm H_I	20-50
Warm atomic	6 000-10 000	21cm H_I	0.2-0.5
Warm ionized	~8 000	Dispersion pulsar signals	0.2-0.5
Hot ionized	~10^6	UV abs lines X soft emission	A few 10^{-3}

Reflexion from a moving magnetic wall

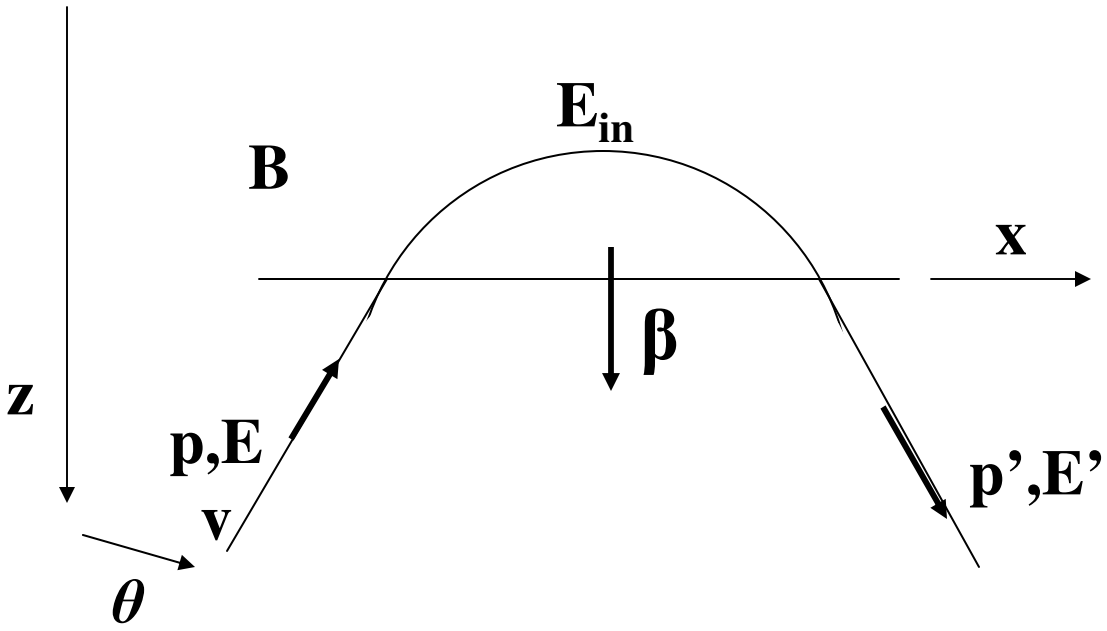

$$\Delta E/E \sim -2\beta v\cos\theta$$

$$V<0 \rightarrow \Delta E>0$$

$$E_{in} = \gamma E - \gamma\beta p_z$$

$$p_{zin} = \gamma\beta E - \gamma p_z$$

$$E' = \gamma E_{in} + \gamma\beta p_{zin}$$

$$P'_z = \gamma\beta E_{in} + \gamma p_{zin}$$

$$E' = \gamma^2(1+\beta^2)E - 2\gamma^2\beta p_z$$

$$p_z = p\cos\theta = vE\cos\theta$$

$$E' = \gamma^2(1+\beta^2 - 2\beta v\cos\theta)E$$

$$\Delta E/E \sim -2\beta v\cos\theta$$

for $|v| >> \beta$

The induced electric field is $-\beta B$ along x
Integrating over the arc gives the same result
A similar result would apply for a magnetic bottle, indeed for any moving magnetic field

Typical ISM magnetic fields are at μG scale

Star light polarisation due to spinning dust grains aligned on B: local field parallel to galactic plane and tangential

Zeeman splitting (21cm H_I line) shows ISM field in the few μG region with little dependence on density

Faraday rotation of the plane of linear polarization of pulsars gives the B component along the line of sight in the warm ionized medium: uniform and random components, μG scale

Synchrotron radiation of all sky radio continuum due to cosmic rays suggests again a few μGscale.

GENERALITIES ON SNRs

Supernovae and SNRs

Type Ia: a white dwarf, member of a binary, accreting from its companion until reaching Chandrasekhar mass of 1.4 solar masses: the core is fully burned, the SNR shell is empty

Type II: a massive star collapsing into a neutron star that remains in the center, possibly detected as a pulsar (Crab) the wind of which gives energy to the remnant (plerion)

Shell SNRs and plerions

Cassiopeia A (Chandra)

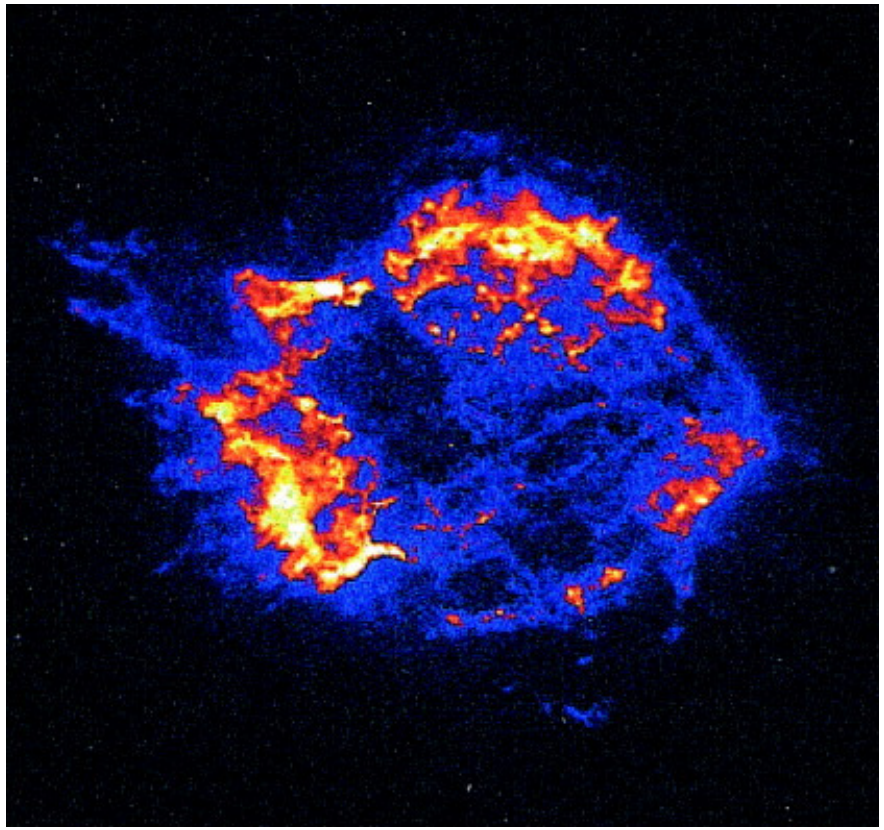

Crab Nebula (Chandra)

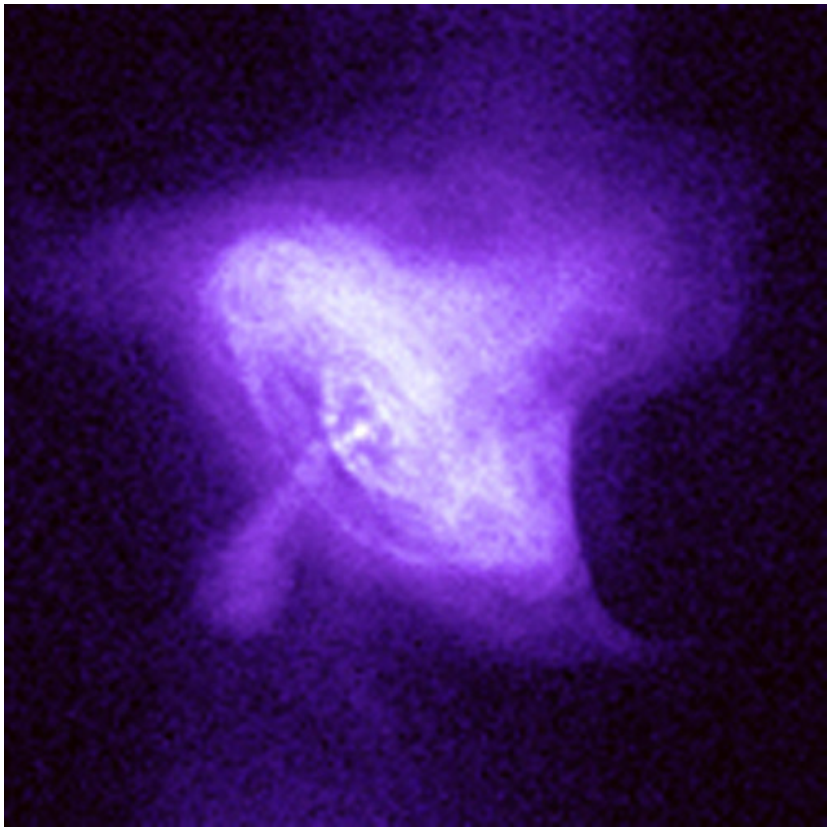

X ray images allow for very high resolutions

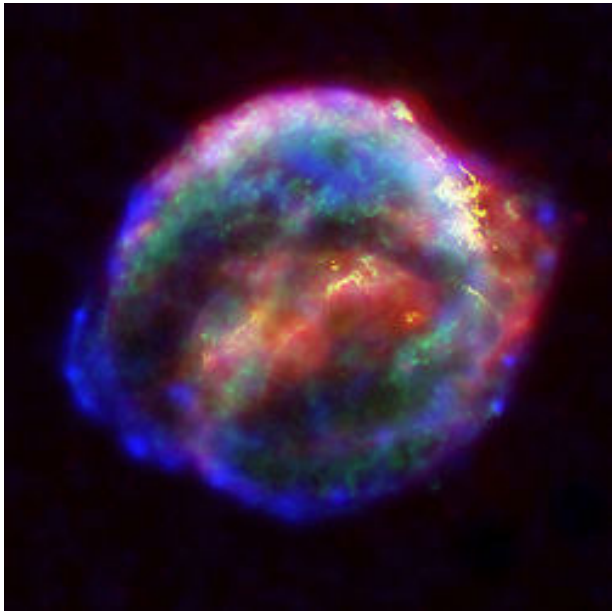

Kepler
SNR 1604

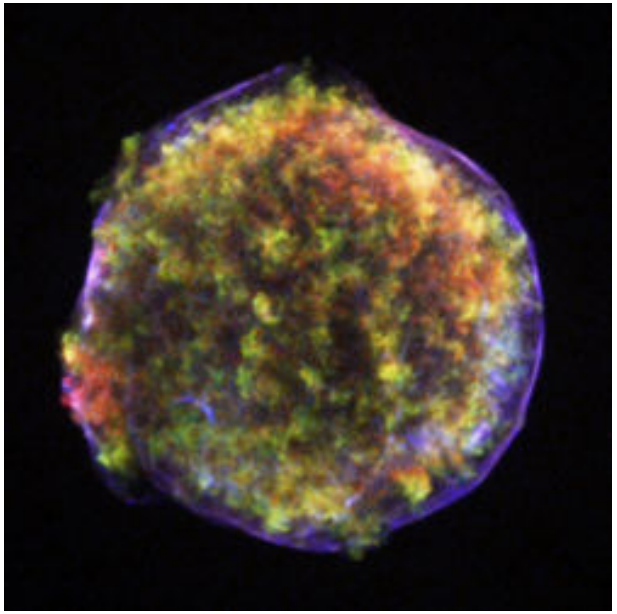

Tycho
SNR 1572

N 49

X-ray emission: abundances

Dominated by thermal emission at ~1keV

Optically thin plasma means strong atomic lines (C to Fe), stronger in young SNRs (enriched ejecta)

Type Ia progenitors yield more Si/S/Ar/Fe than Type II

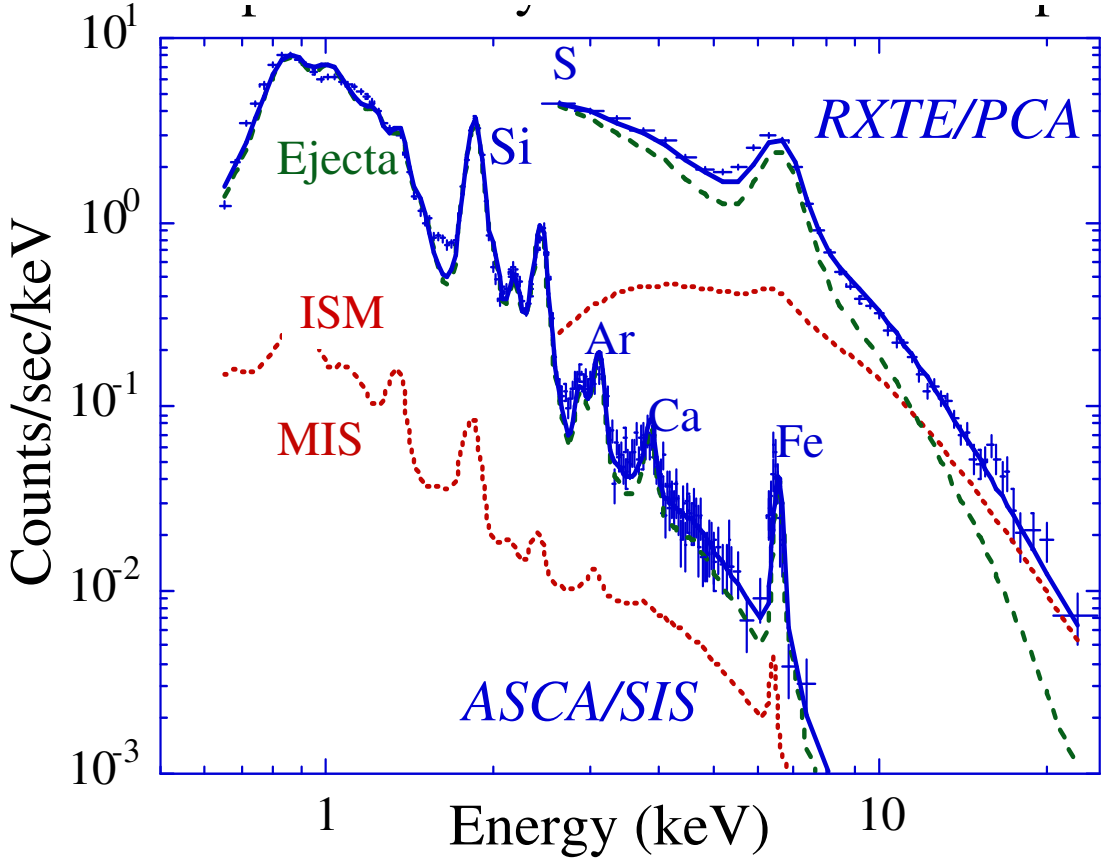

Kepler (X-ray)

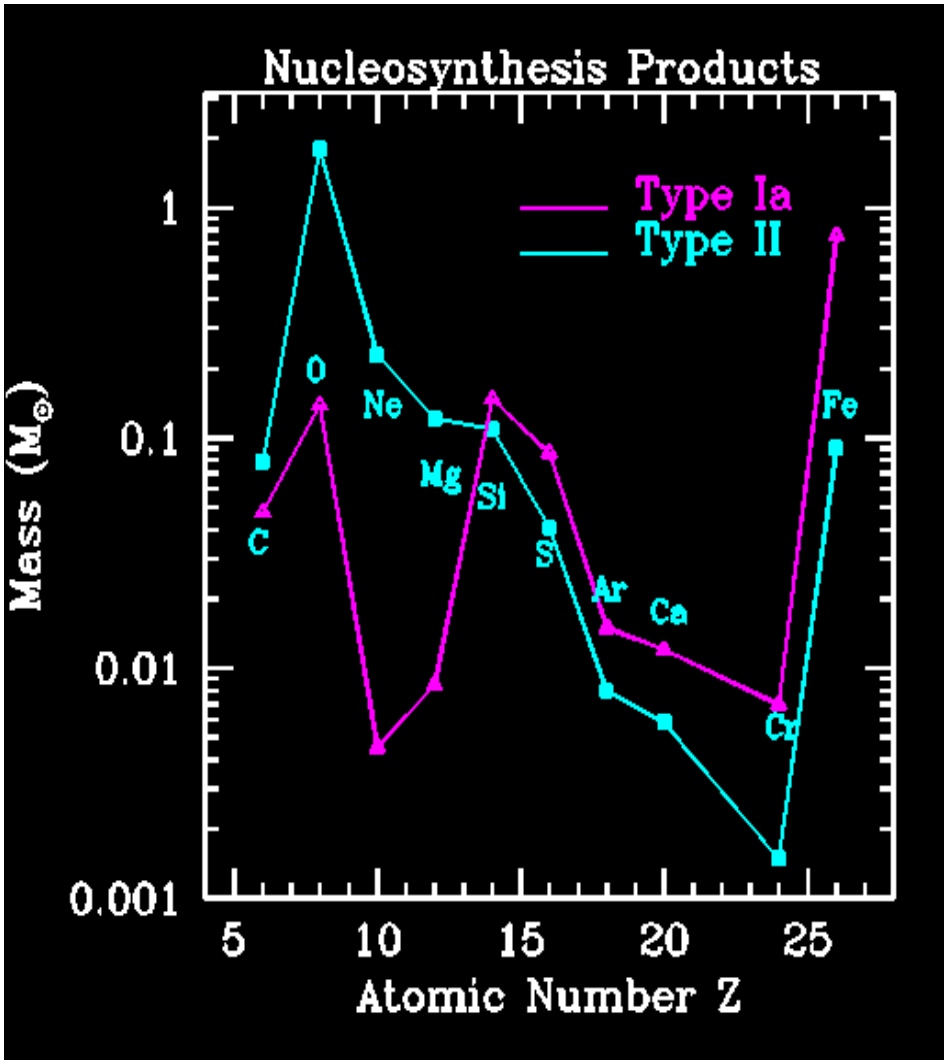

Type Ia:

Complete burning of C-O white dwarf produces mostly Fe-peak nuclei (Ni, Fe, Co) with some intermediate mass (O, Si, S, Ar…): very low O/Fe ratio

Core Collapse:

Explosive nucleosynthesis builds up light elements: very high O/Fe ratio

O, Ne, Mg, Fe very sensitive to progenitor mass

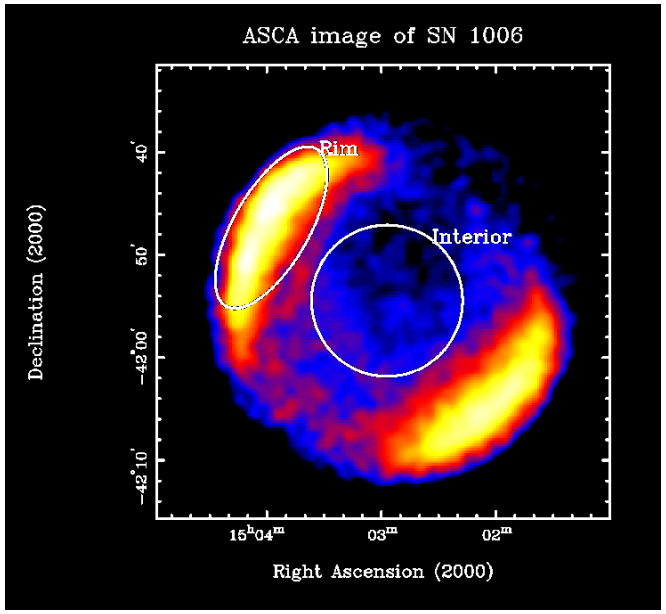

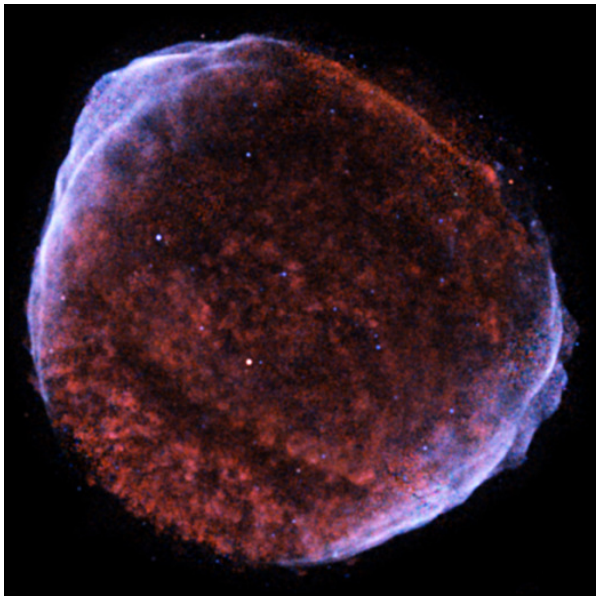

SN 1006

Type Ia

Age = 10^3 yr

Ang. Diam. 0.5°

Distance =2 kpc

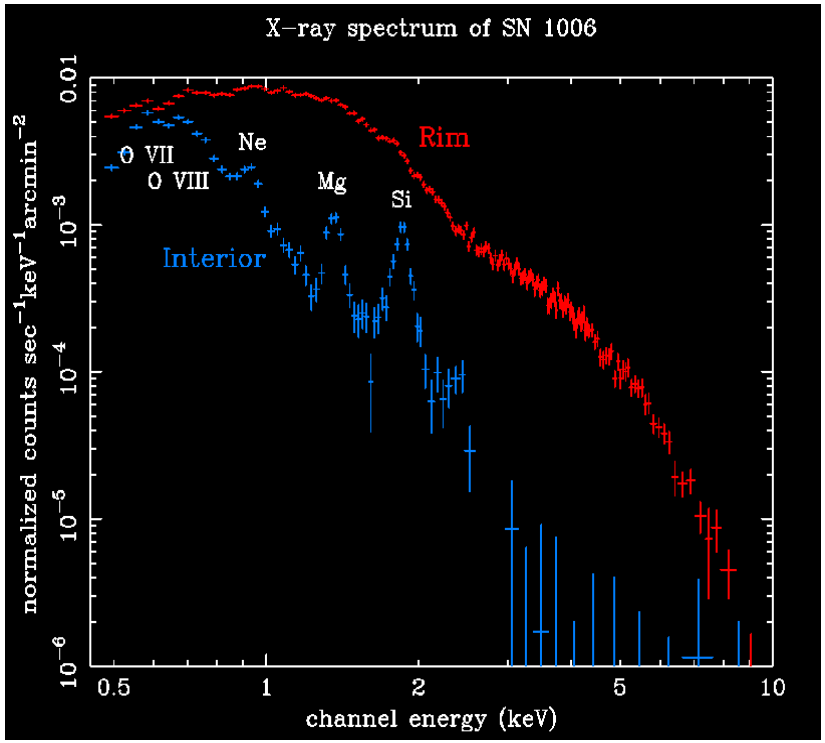

X-ray emission:
thermal in faint areas
synchrotron in bright rims

Interior shows thermal ejecta

XMM-Newton

2 – 4.5 keV
non-thermal

Oxygen band
(0.5 – 0.8 keV)
thermal

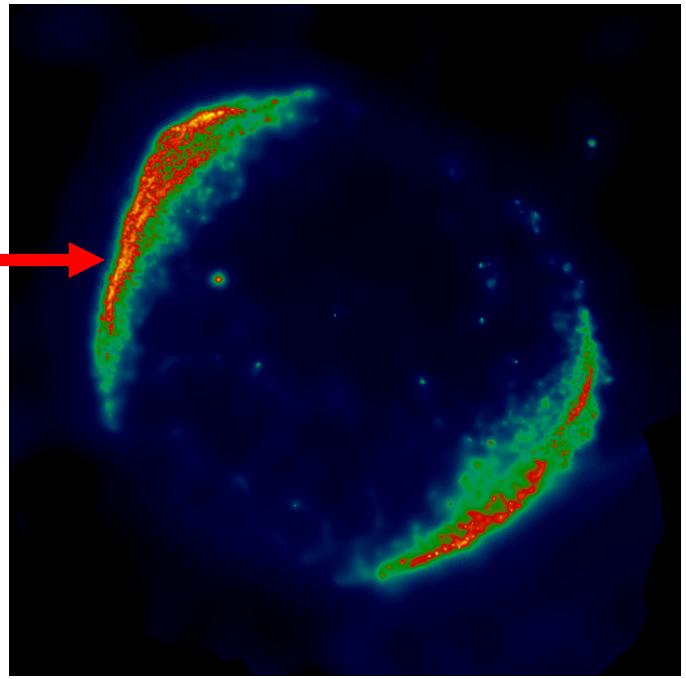

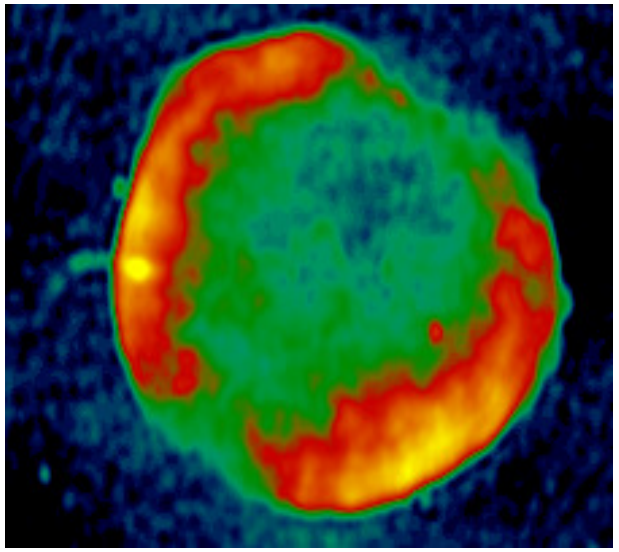

Radio

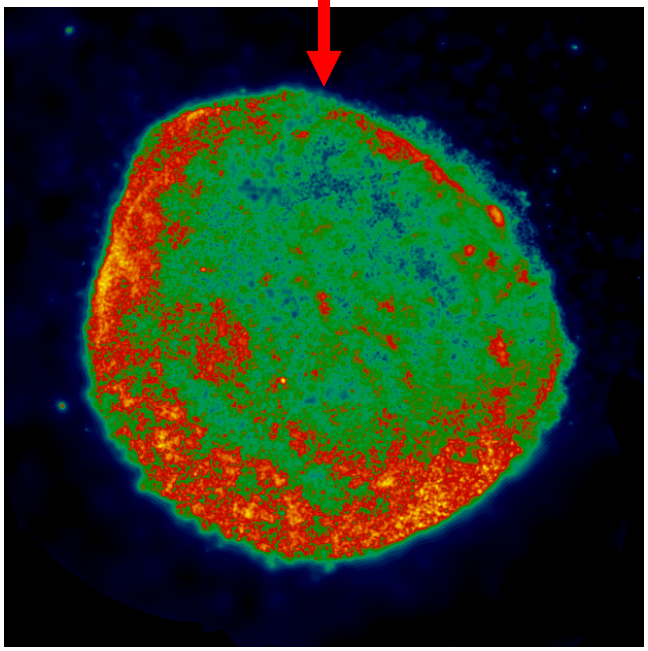

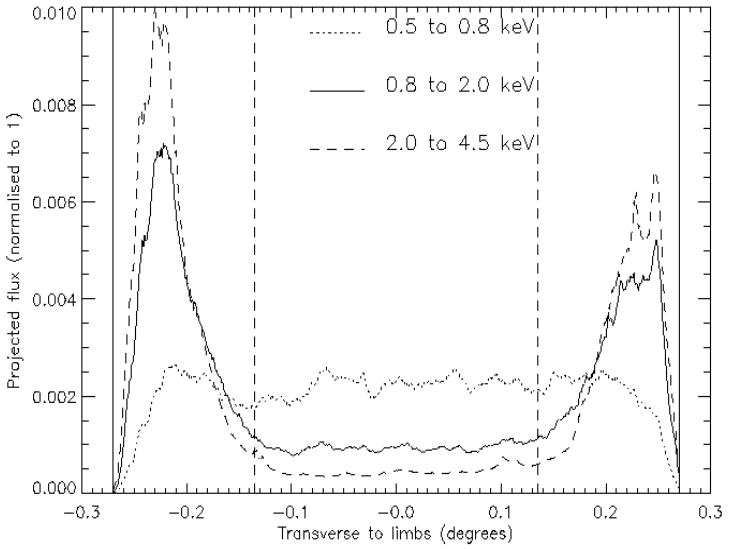

SN 1006

Profile shows magnetic field normal to bright limbs (polar caps)

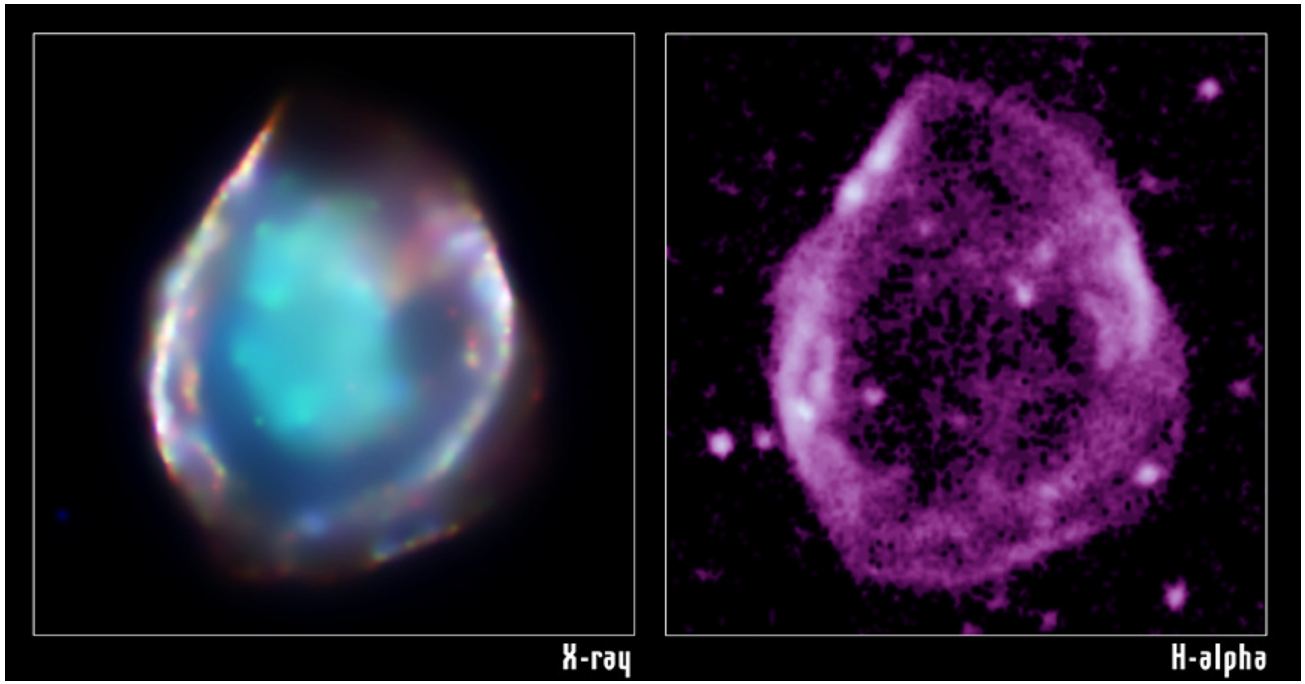

DEM L71
Type Ia
~5000 y old

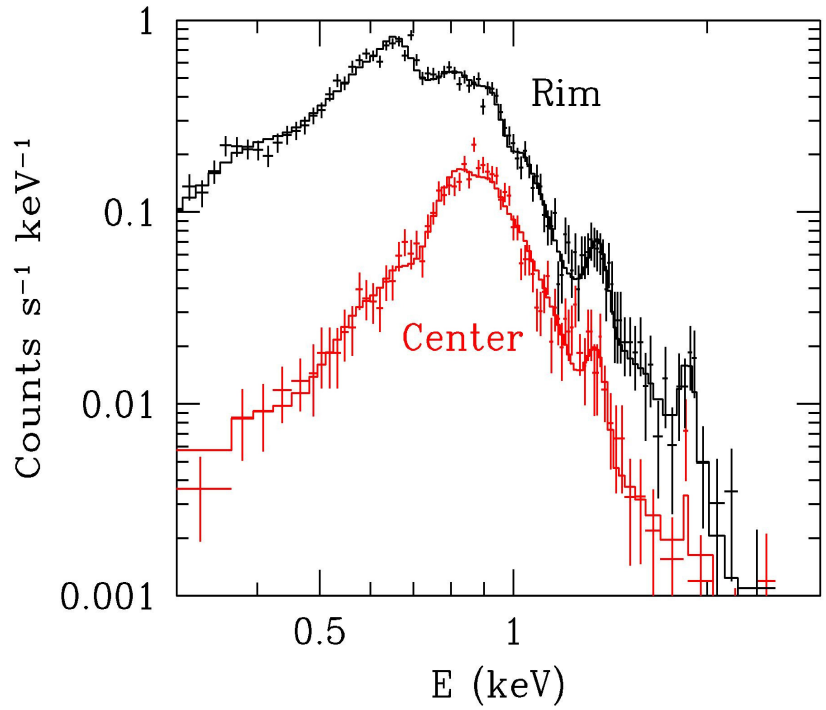

LMC SNR
LMC-like abundances
Central emission evident at E>0.7 keV
Fe/O > 5 × solar
typical of Type Ia
Reverse shock has heated all ejecta

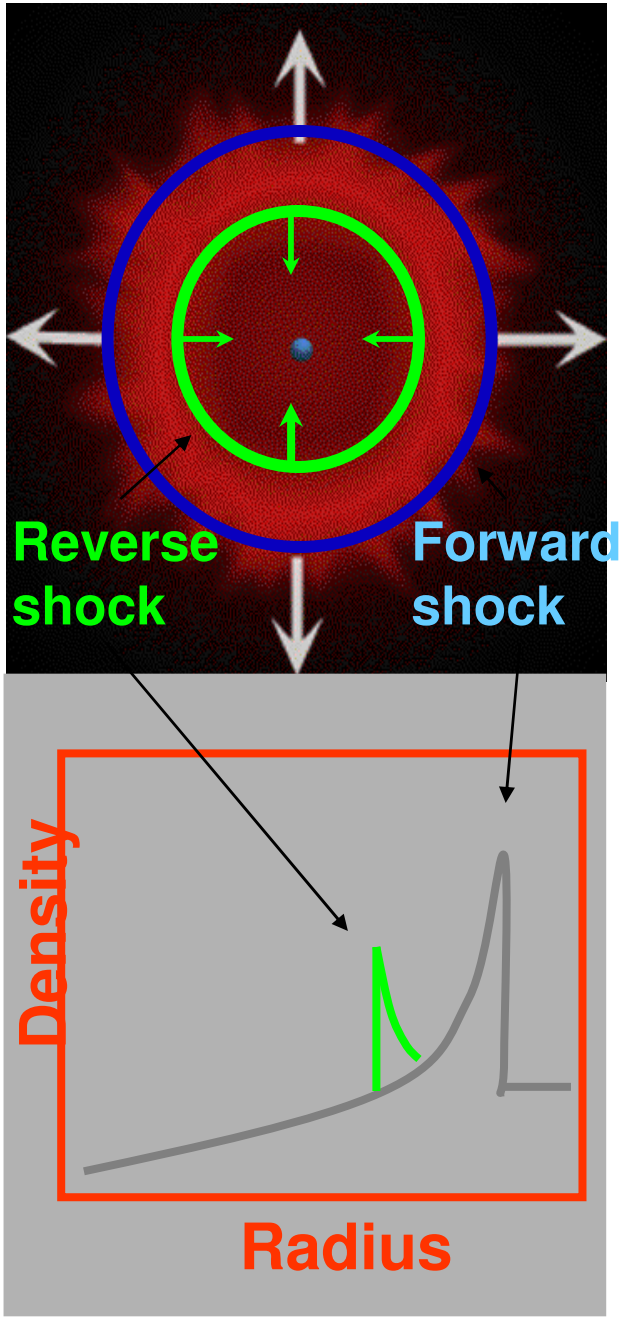

SNR shell structures

Explosion blast wave sweeps up ISM in forward shock.

As mass is swept up, forward shock decelerates and ejecta (abundances as in progenitor) catch up.

Reverse shock heats ejecta.

Nuclear reactions produce new heavy elements

Once enough mass has been swept up ($> 1\text{-}5\ M_{ej}$)

SNR enters so called Sedov phase

Particle distributions in SNRs

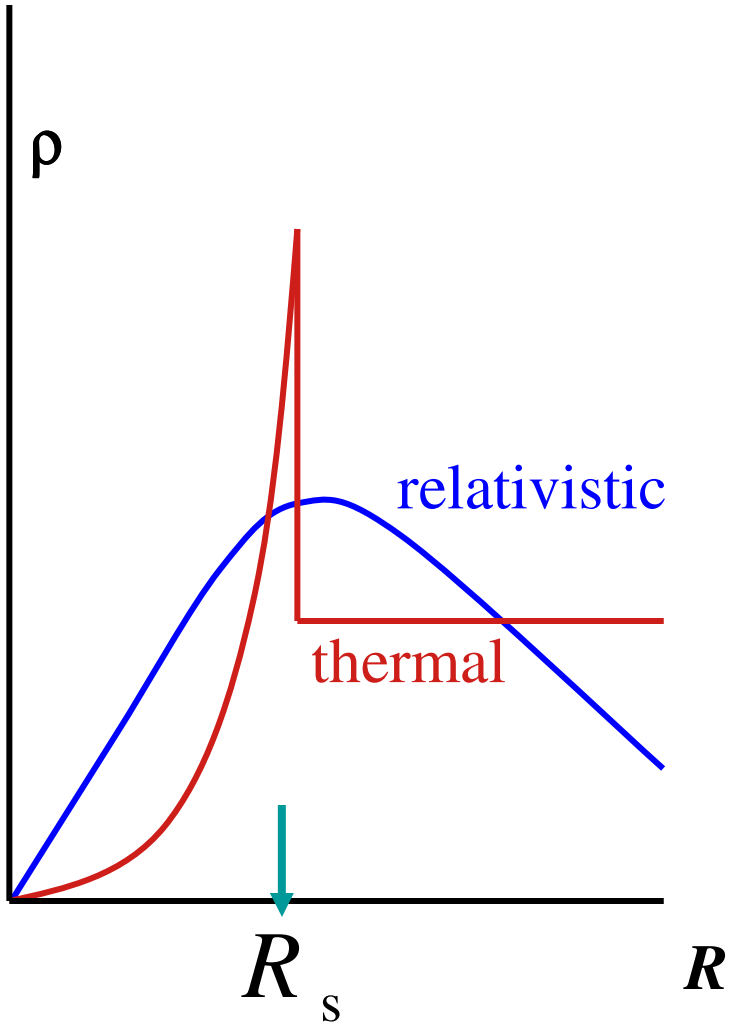

Thermal particles and magnetic field are concentrated in the shell

Relativistic particles extend to much larger distances

Synchrotron emission is confined to magnetic field region

The shock structure depends on the SNR age: distinguish between young and old SNRs

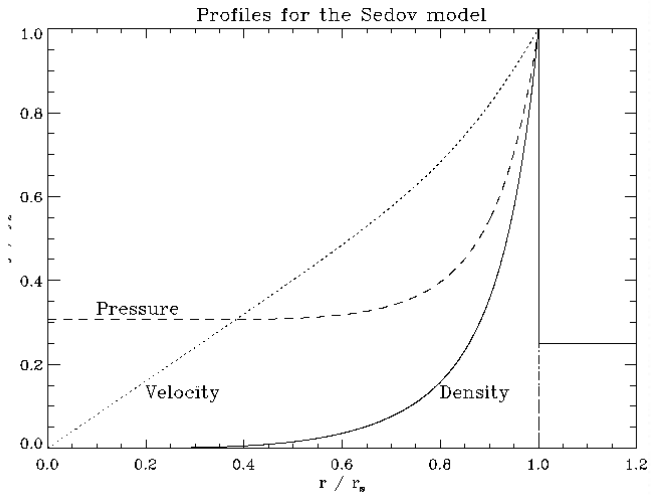

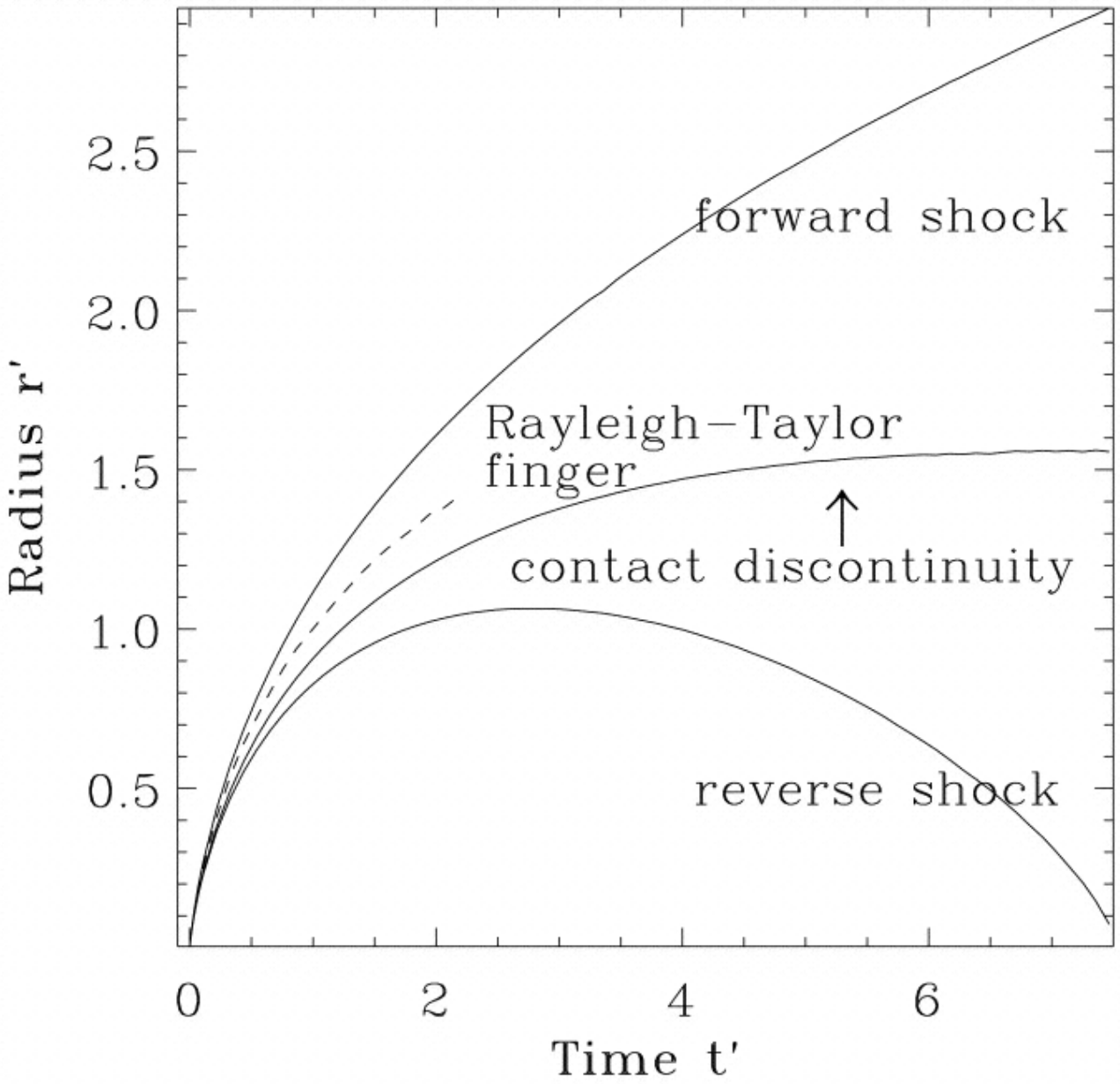

Pulsar Wind Nebula : Composite SNRs

Pulsar wind sweeps up ejecta; termination shock decelerates flow; PWN forms; Supernova Remnant sweeps up ISM; reverse shock heats ejecta; ultimately compresses PWN;

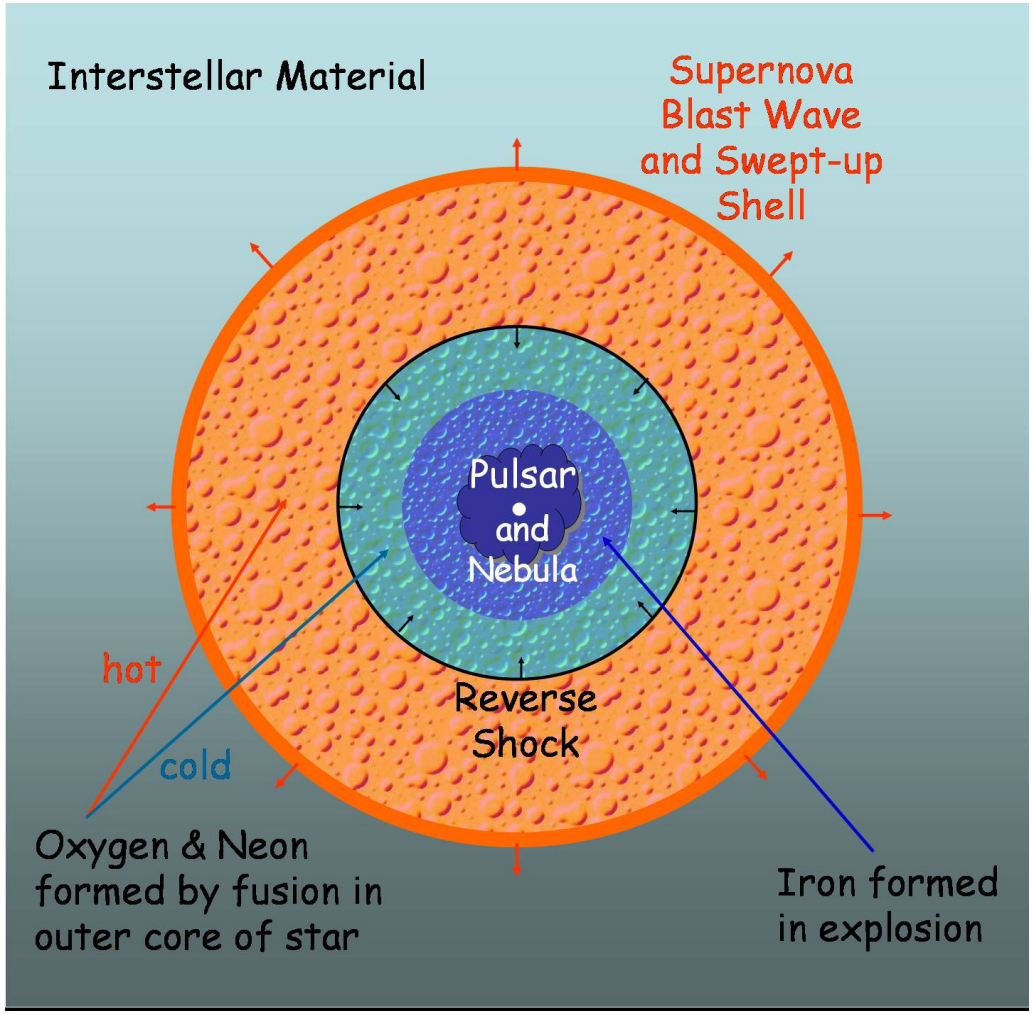

GENERALITIES ON SHOCKS

Ideal shocks (no magnetic field)

In the shock frame Mass $\rho_1 v_1 = \rho_2 v_2$

Momentum $\rho_1 v_1^2 + p_1 = \rho_2 v_2^2 + p_2$

Energy $\rho_1 v_1(\frac{1}{2} v_1^2 + \gamma p_1/\rho_1/[\gamma-1]) = \rho_2 v_2(\frac{1}{2} v_2^2 + \gamma p_2/\rho_2/[\gamma-1])$

$\gamma = C_p / C_v = (3+2n)/(1+2n)$ (n atoms/molecule)

$v_s = \sqrt{(\gamma p/\rho)}$ is the sound velocity

$M = v/v_s$ is the Mach number

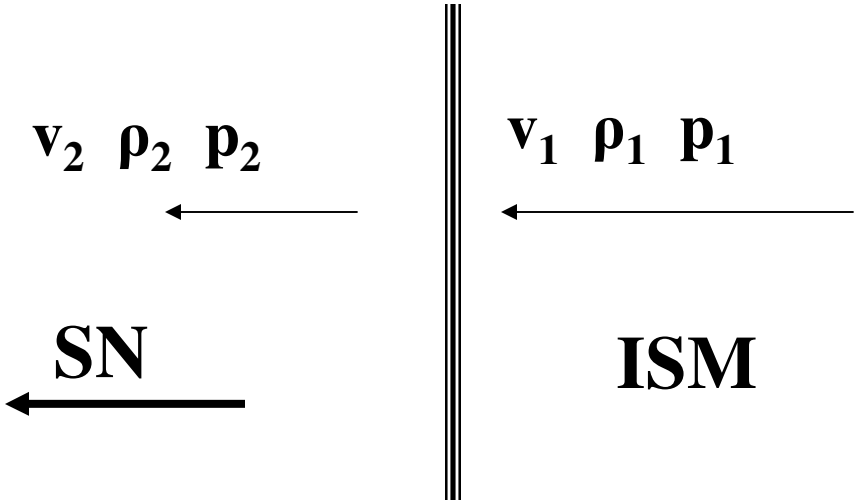

$v_1 - v_2 = 2v_1(1 - M_1^{-2})/(\gamma+1)$

$\rightarrow 2v_1/(\gamma+1) = 3v_1/4$ for large M and monoatomic gas

Compression ratio r=

$\rho_2/\rho_1 = v_1/v_2 = (\gamma+1)/(\gamma-1) = 4$

As the shock progresses into the unperturbed ISM the density increases suddenly by a typical factor of 4 and the temperature increases by a factor $\sim \frac{1}{3} M_1^2$

On either side of the shock one sees the other medium approach at a velocity $v_1 - v_2$ and a relativistic cosmic ray crossing the shock at an angle θ gets always a first order Fermi acceleration

$$\Delta E/E \sim 2(v_1 - v_2)\cos\theta$$

Writing $(v_1 - v_2) = 3v_1/4$ and $\cos\theta \sim 2/3$

$$\Delta E/E \sim V_{shock}/c$$

It is important to be conscious that there is no collision in the process, but magnetic field volumes acting as scattering centres and aiming at each other on either side of the shock at relative velocity $v_1 - v_2$. The above calculation serves only as an illustration but is not really what we need: we need a model of these scattering centres and an understanding of how they evolve on crossing the shock.

The conservation relations that have been written on either side of the shock must of course include the magnetic pressure and energy density.

But this is not enough, one needs to understand in detail the nature of the magnetic scattering centres and how they meet at the shock : this is not well understood but only crudely modelled.

Energy spectrum

The rate of acceleration is given by the ratio of the relative energy gain when crossing the shock back and forth, $\Delta E/E \sim V_{shock}$, to the time Δt it takes. In the relativistic limit and in the approximation where the distribution of the scattering centres is irrelevant, the length of the trajectories scales with energy, $\Delta t = kE$.

Once in region 1, the particle will always be caught by the shock, which is aiming toward it. However, once in region 2, it may escape the shock region for ever with a probability P_{esc}. In this region, the scattering centres move away from the shock at velocity $v_2 \sim ¼ v_{shock}$ while the particle moves at light velocity at varying angles to the shock. Integrating over these angles, $P_{esc} = \beta_{shock}$

$\Delta E/E \sim \beta_{shock}$ $\Delta t = kE$ $P_{esc} = \beta_{shock}$

After n cycles across the shock,

$$E_n = E_0(1+\beta_{shock})^n$$

At each cycle only a fraction

$(1-P_{esc}) = (1-\beta_{shock})$ survives

Hence after n cycles one has

$N = N_0(1-\beta_{shock})^n$ particles

having energy $E = E_0(1+\beta_{shock})^n$

$$\ln(N/N_0)/\ln(E/E_0) =$$

$$= \ln(1-\beta_{shock})/\ln(1+\beta_{shock}) = -1$$

$N = N_0(E/E_0)^{-1}$ and $dN/dE \approx E^{-2}$

In general, for a compression ratio r,
$dN/dE \approx E^{-\alpha}$ with $\alpha=(r+2)/(r-1)$

Diffusive shock acceleration results in a universal power law energy distribution

TURBULENCES AND MAGNETIC FIELD AMPLIFICATION

There exists copious evidence in favor of strong magnetic turbulences and magnetic field amplification in the shock region of young SNRs.

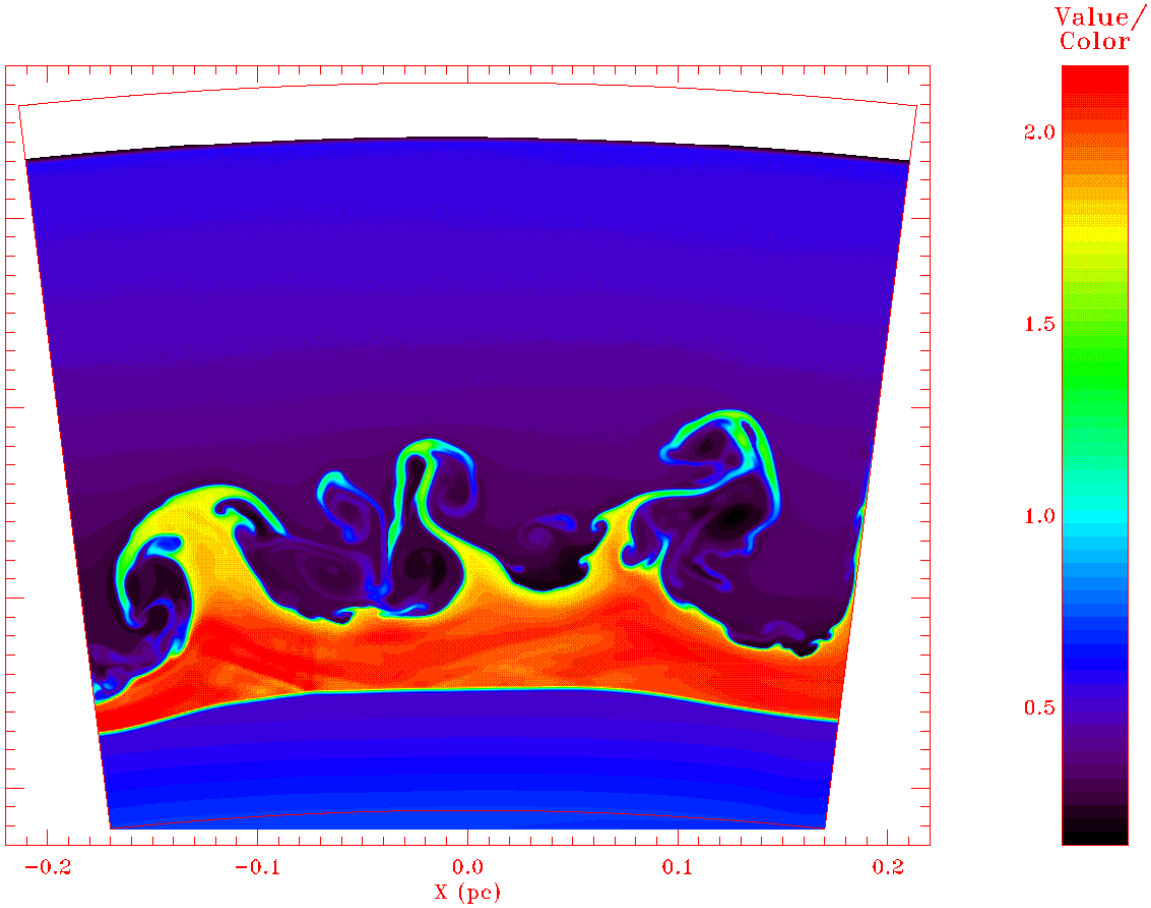

Hydrodynamic instabilities: density map

HESS/Suzaku RX J1713

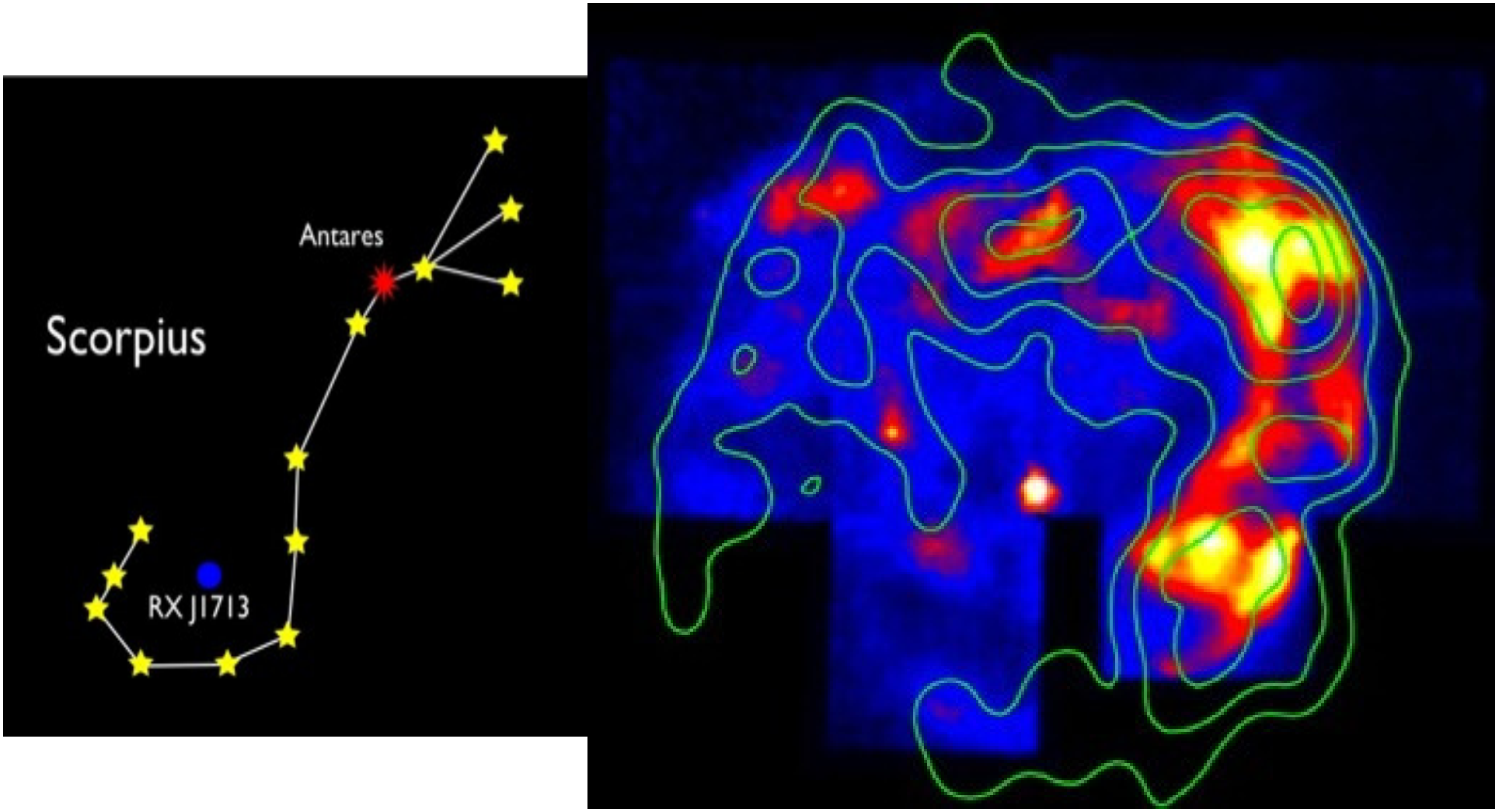

RX J1713: Chandra observes variable shock structure, suggestive of substantial magnetic field amplification

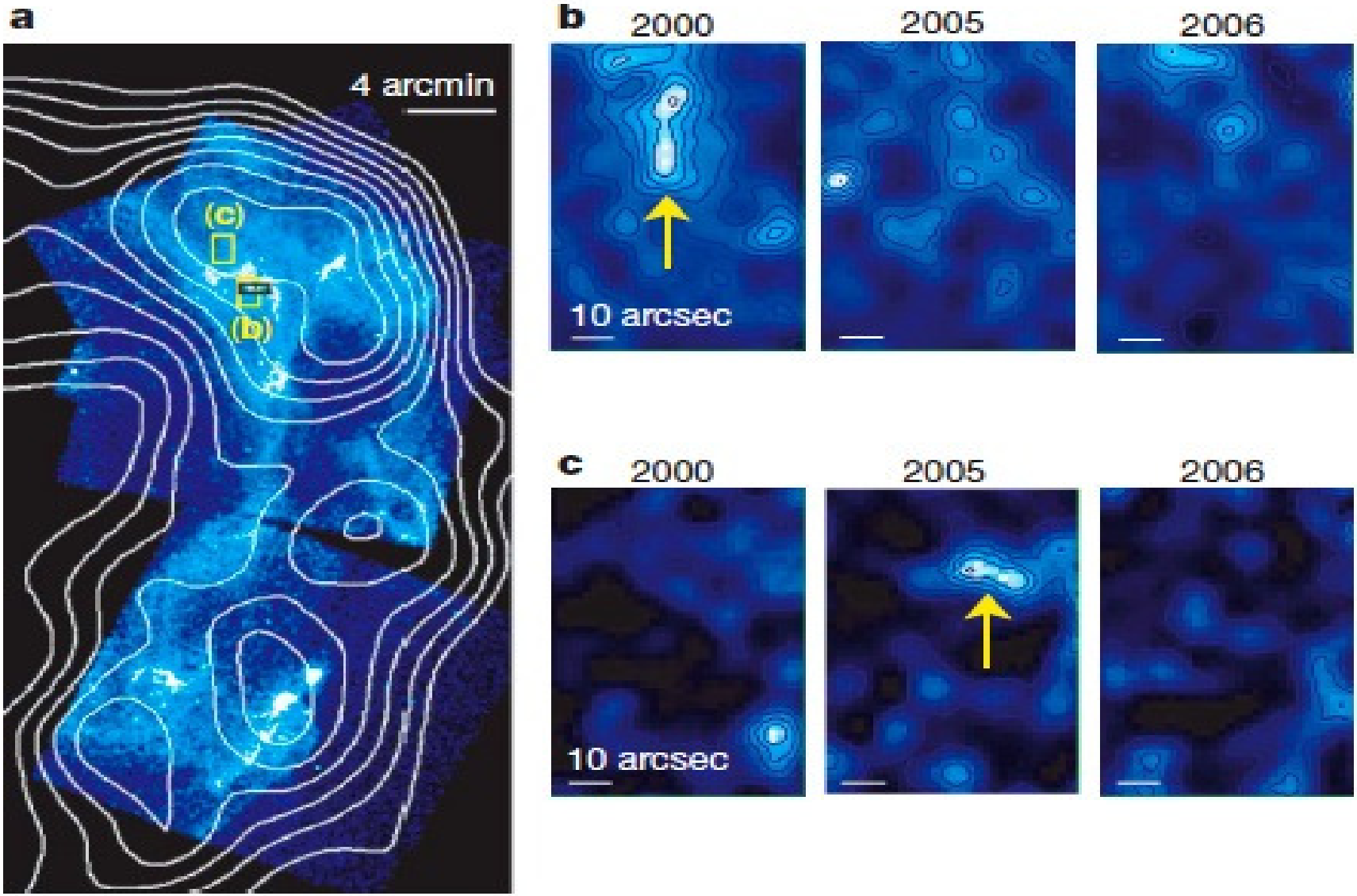

Particle Acceleration in SN 1006

Chandra observations show distinct shock structure in shell

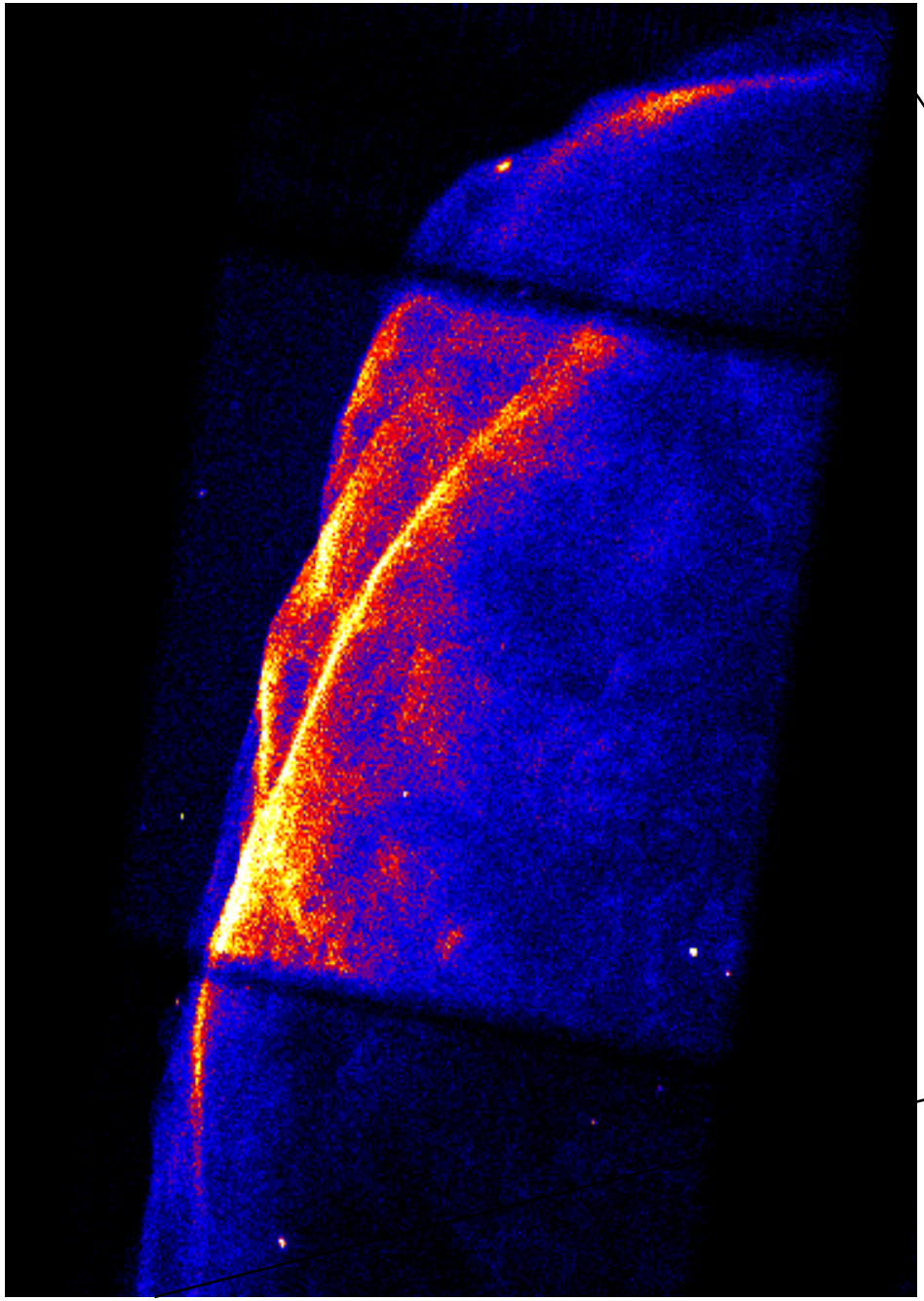

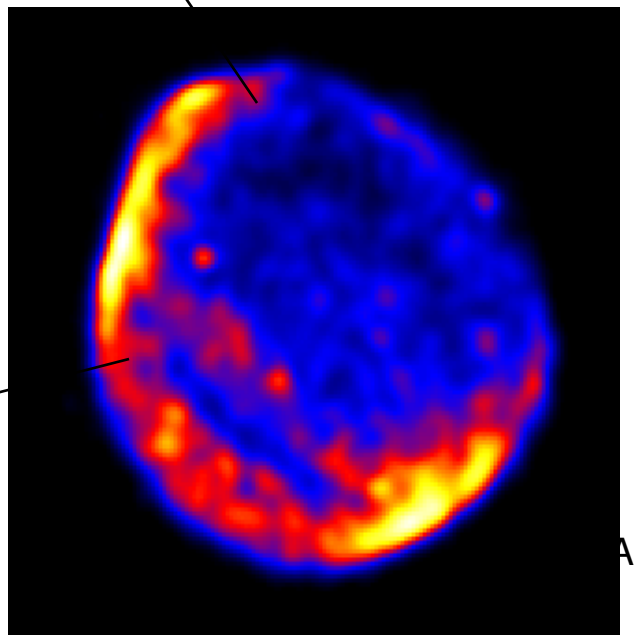

Cassiopeia A, young core-collapse SNR

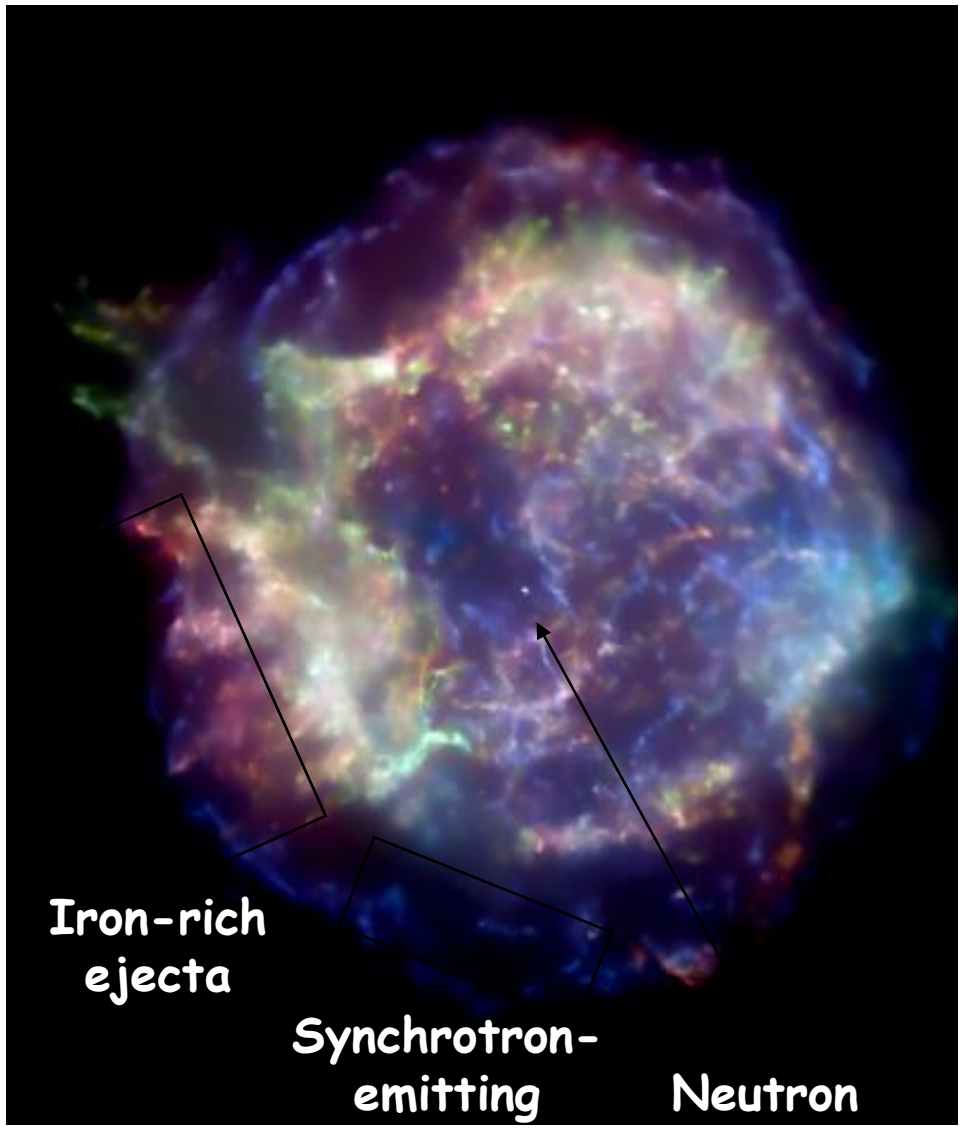

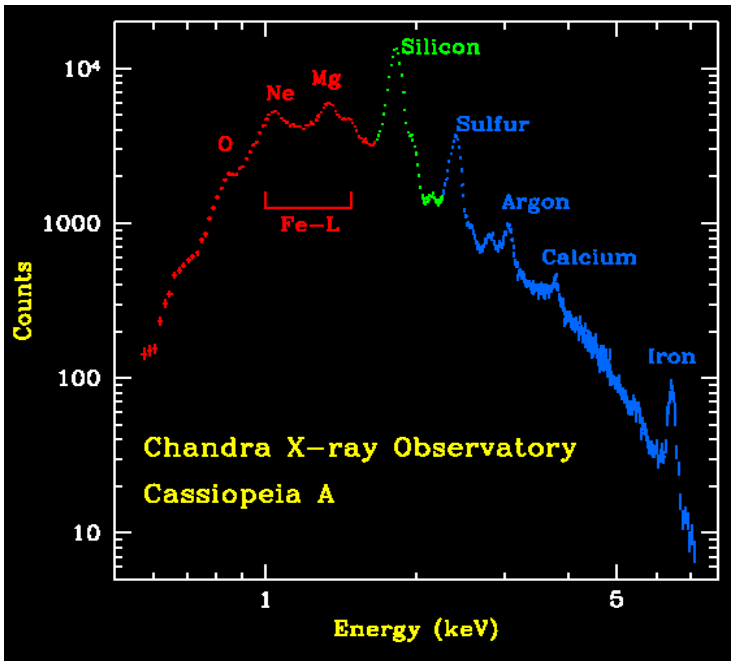

Complex ejecta distribution

Neutron star in centre

Nonthermal filaments: cosmic-ray acceleration

Cas A: X-ray imaging of the blast wave

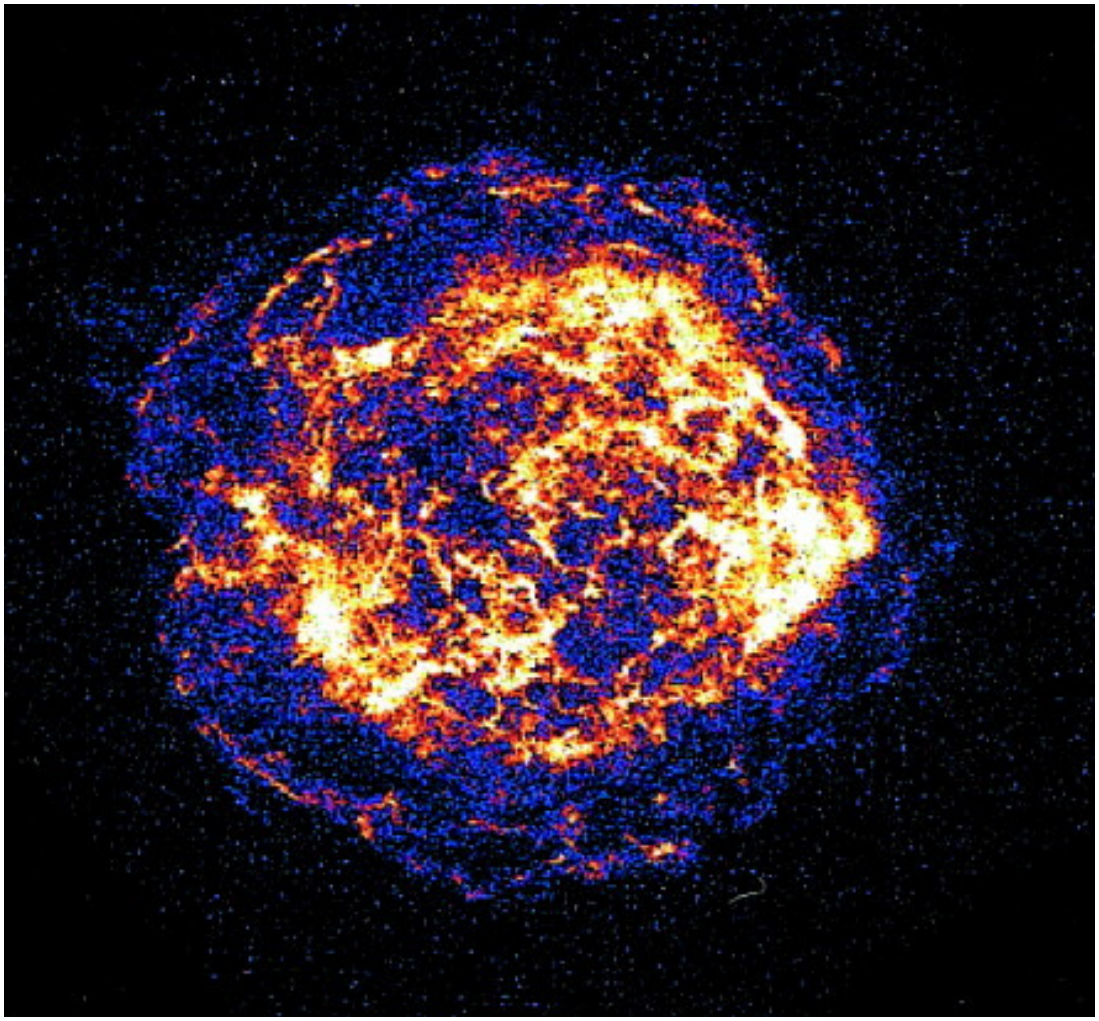

Continuum band
(4 to 6 keV)
Chandra
(resolution <1”)
resolves the blast
wave from the
reverse shock.
Sharp filaments are
apparent at the
blast wave all around

EVIDENCE FOR MAGNETIC FIELD AMPLIFICATION

From the ratio of radio to TeV emission: a same distribution of electrons produces synchrotron (radio, X-ray) and TeV (IC) but synchrotron depends directly on field while IC and pion decays do not.

From sharp outer X-ray edges seen in several young SNRs (Kepler, Cas A, Tycho, SN1006). Shock front compression is a revelator of field amplification. X-ray synchrotron emission from TeV electrons enhanced by strong field implies short electron lifetime and short diffusion lengths → narrow X-ray structures.

Magnetic fields are enhanced by factors of hundred, much more than the factor of 4 associated with the compression factor of an ideal shock

Projected X-ray brightness of Cassiopeia A

direct evidence for magnetic field amplification

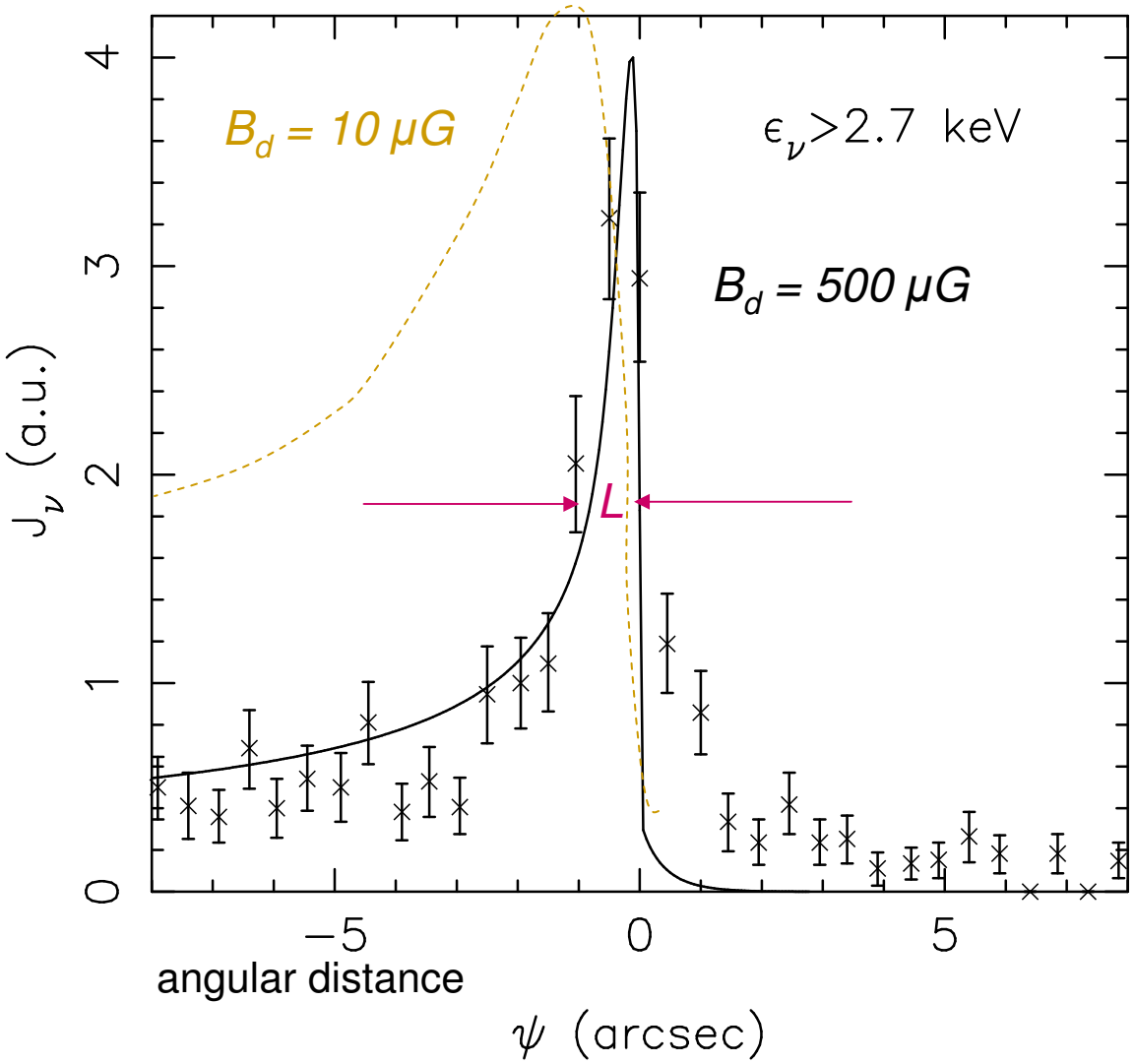

Experiment confirms high internal magnetic field extracted from the fit of volume integrated synchrotron flux

Radial X-ray profiles show
very sharp (3 - 4") outer rim
Width is only
2% of the SNR radius
Mostly in continuum emission

Hwang et al. 2002, (Tycho)

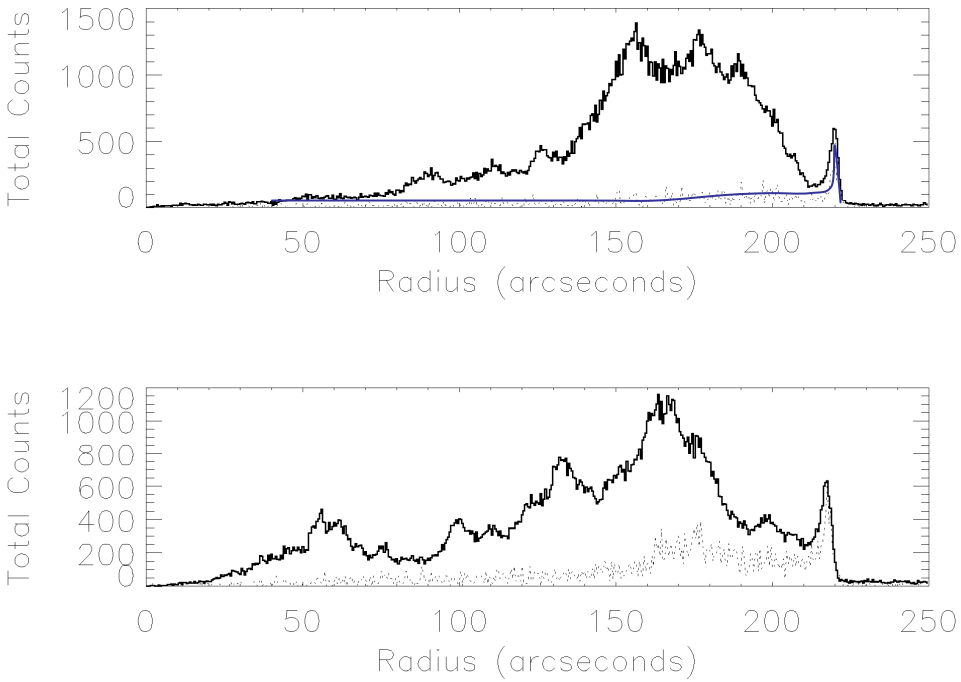

Gotthelf et al. 2001
(Cas A)

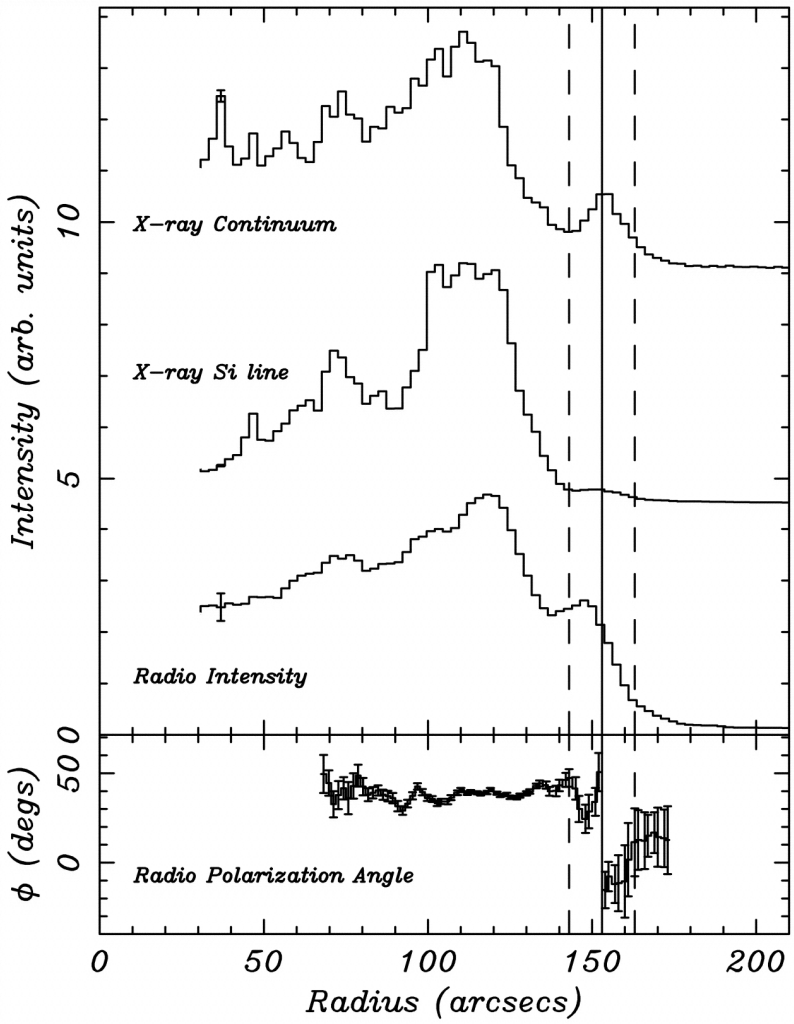

Cosmic rays and the magnetized plasma carry similar energy densities: they do interact on each other.

Accelerated particles tend to stream ahead upstream, which causes the generation of streaming instabilities and makes the evolution non linear, resulting in a strong amplification of the mean field.

The structure of the shock is modified by cosmic ray retroaction

The higher field, in turn, depresses IC wrt synchrotron emission, implying faster scattering and increased maximum momentum.

Sharply peaked X-rays at forward shock are evidence that the field is large and increases sharply at the shock, and that diffusive shock acceleration is efficient and nonlinear at SNR outer blast wave shocks.

Older remnants do not show such field amplification: The excitation of turbulences decreases with shock velocity, while damping (by non-linear wave interactions and ion-neutral collisions) does not.

TYCHO (CHANDRA, 2005)

Contact discontinuity (green line) lies close to outer blast wave determined from 4-6keV (non thermal) X-rays

2-D hydro simulation Blondin/Ellison
No acceleration Efficient acceleration

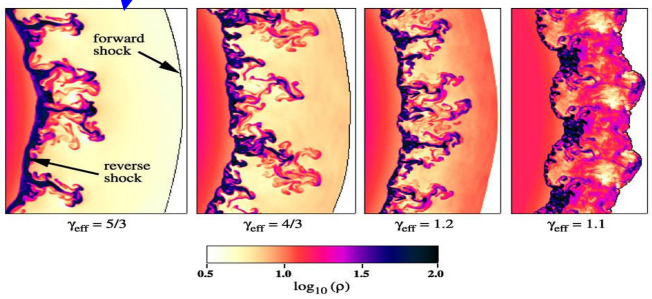

Tycho's SNR 1572

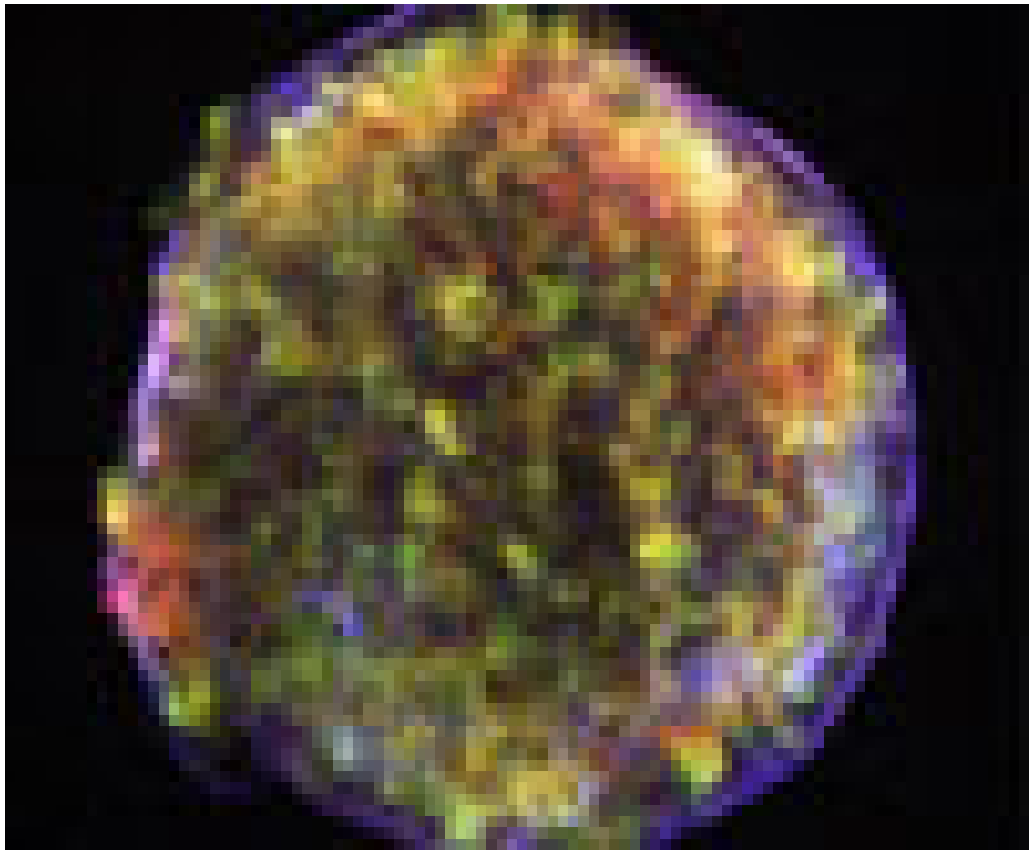

The energy contained in accelerated nuclei is about 100 times that in electrons

Chandra found that the stellar debris are only half a light-year behind the outer shock instead of two expected, suggesting that a large fraction of the energy of the outward-moving shock wave is going into the acceleration of atomic nuclei (in addition to the electrons revealed by radio and X ray observations).

Radio observations (images from interferometric arrays, global fluxes from single dish telescopes, mostly 6 to 90 cm) show limb brightening similar to X-rays, young remnants have steeper spectra than old remnants.

Observed polarization (a few %) is much smaller than for intrinsic synchrotron emission in an ordered field (~ 70%) because the field is turbulent.

In young remnants, the magnetic field direction tends to be radial (magnetic amplification at interface), in older remnants, it tends to be tangential (shock compression).

Cas A

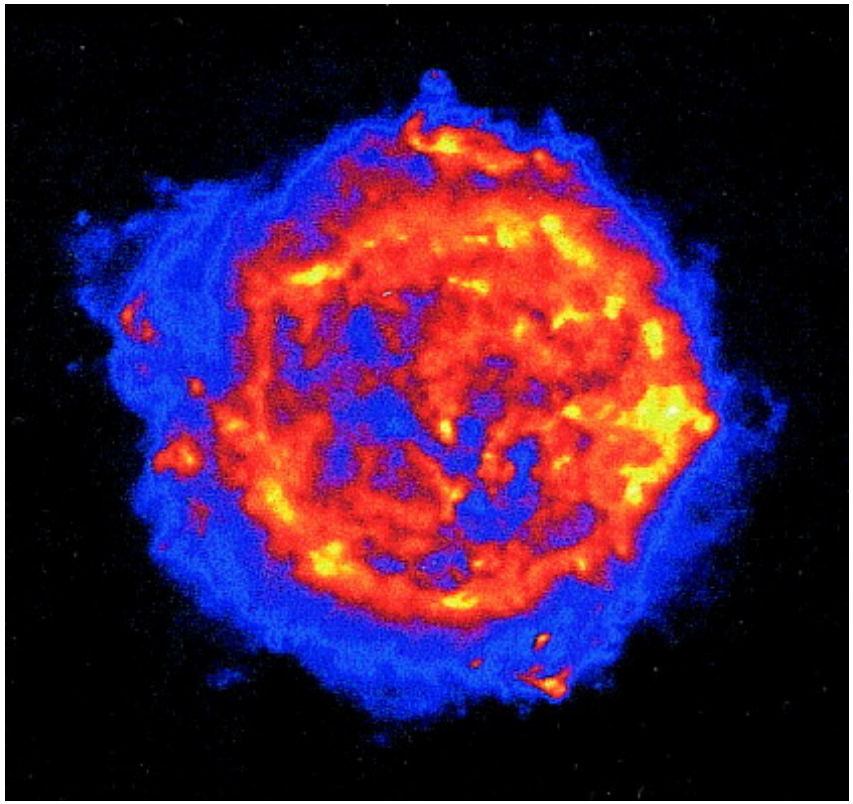

Successful modelling of emission over the whole frequency range

SN 1006

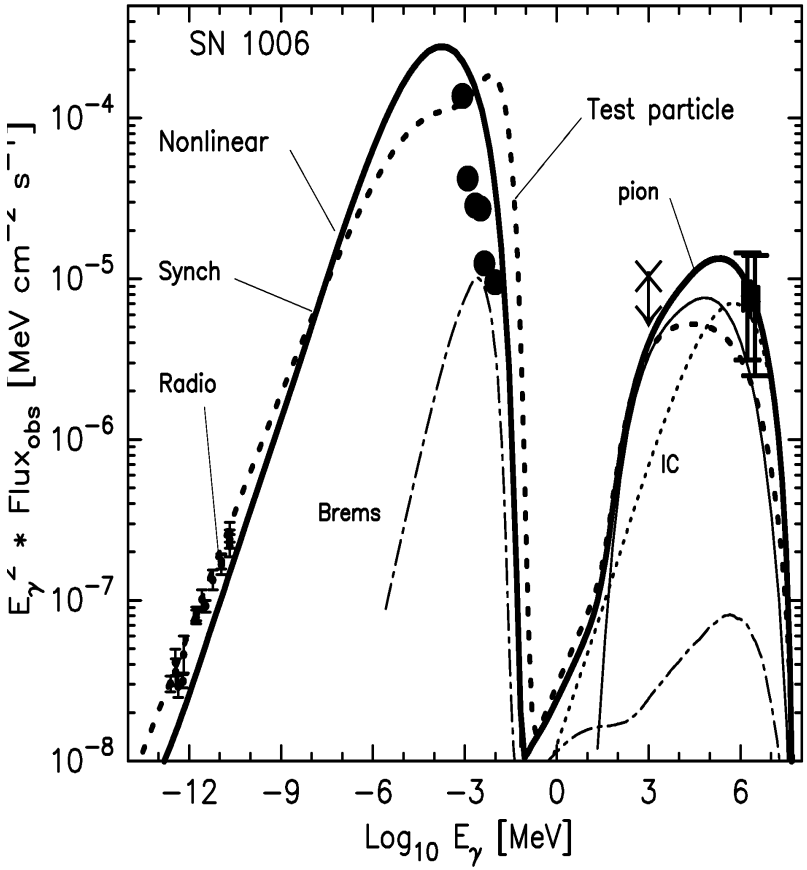

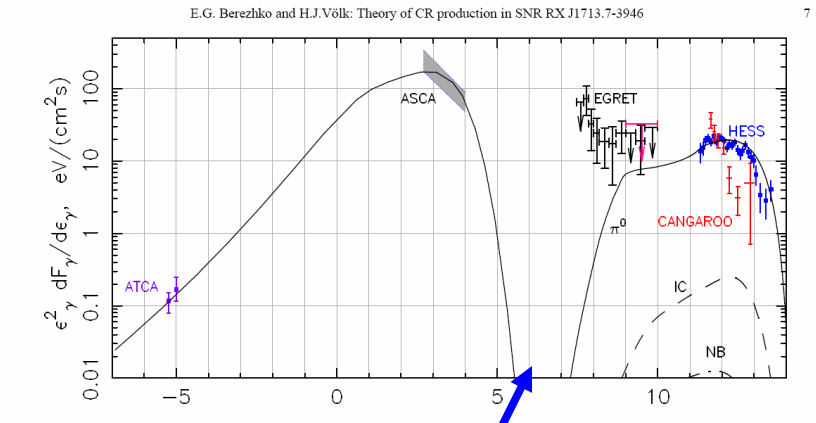

SNR J1713

Cas A

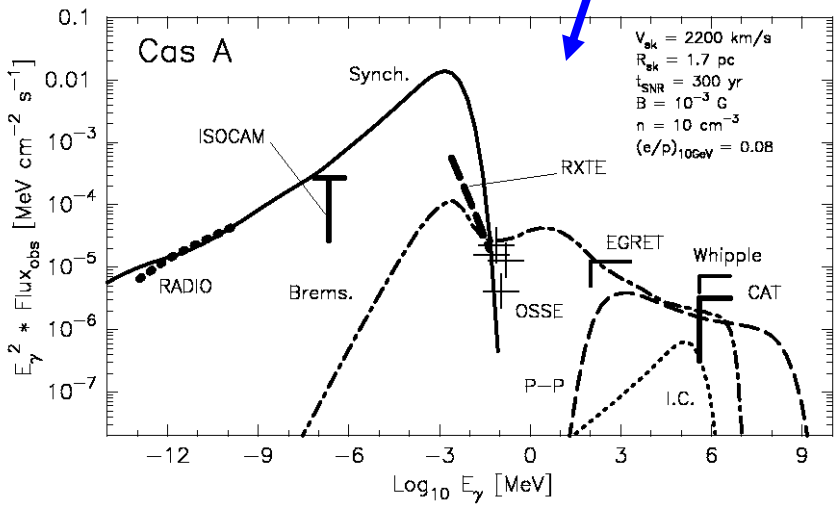

LARGE SCALE SHOCKS

Galaxy collisions

Recent observations and studies of colliding galaxies and merging galaxy clusters suggest that these were common phenomena in the early denser Universe. Such collisions are now believed to have played an important role in the process of galaxy formation. Galaxy collisions usually do not imply direct star collisions but the strongly increased gravity field enhances the collapse of hydrogen clouds and the formation of new stars, many of which very massive and therefore having a short life time.

A typical example is that of the Antennae galaxy, 20 or so Mpc away from us

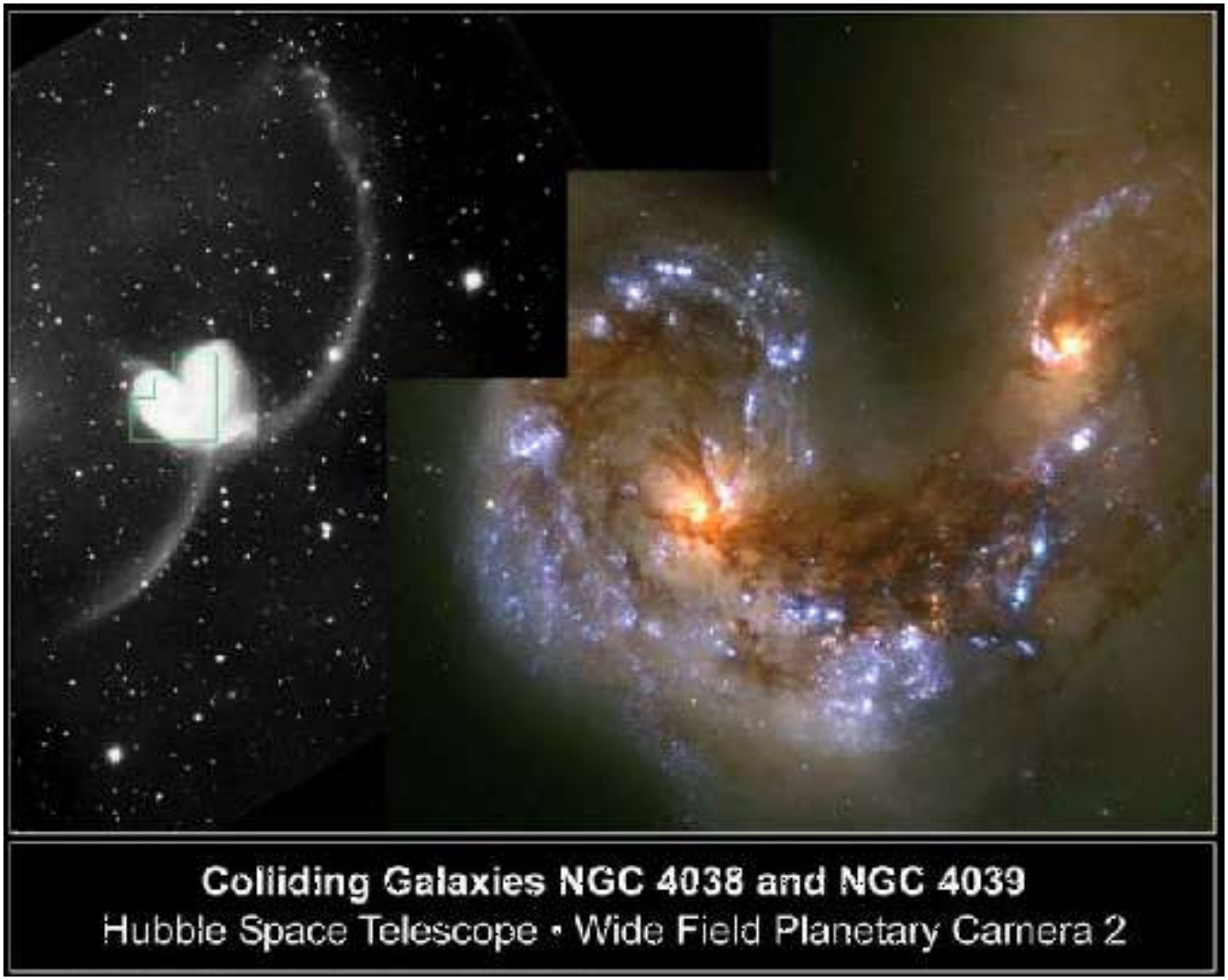

Left: ground telescope. Right: zooming with HST

Details reveal intense star formation activity

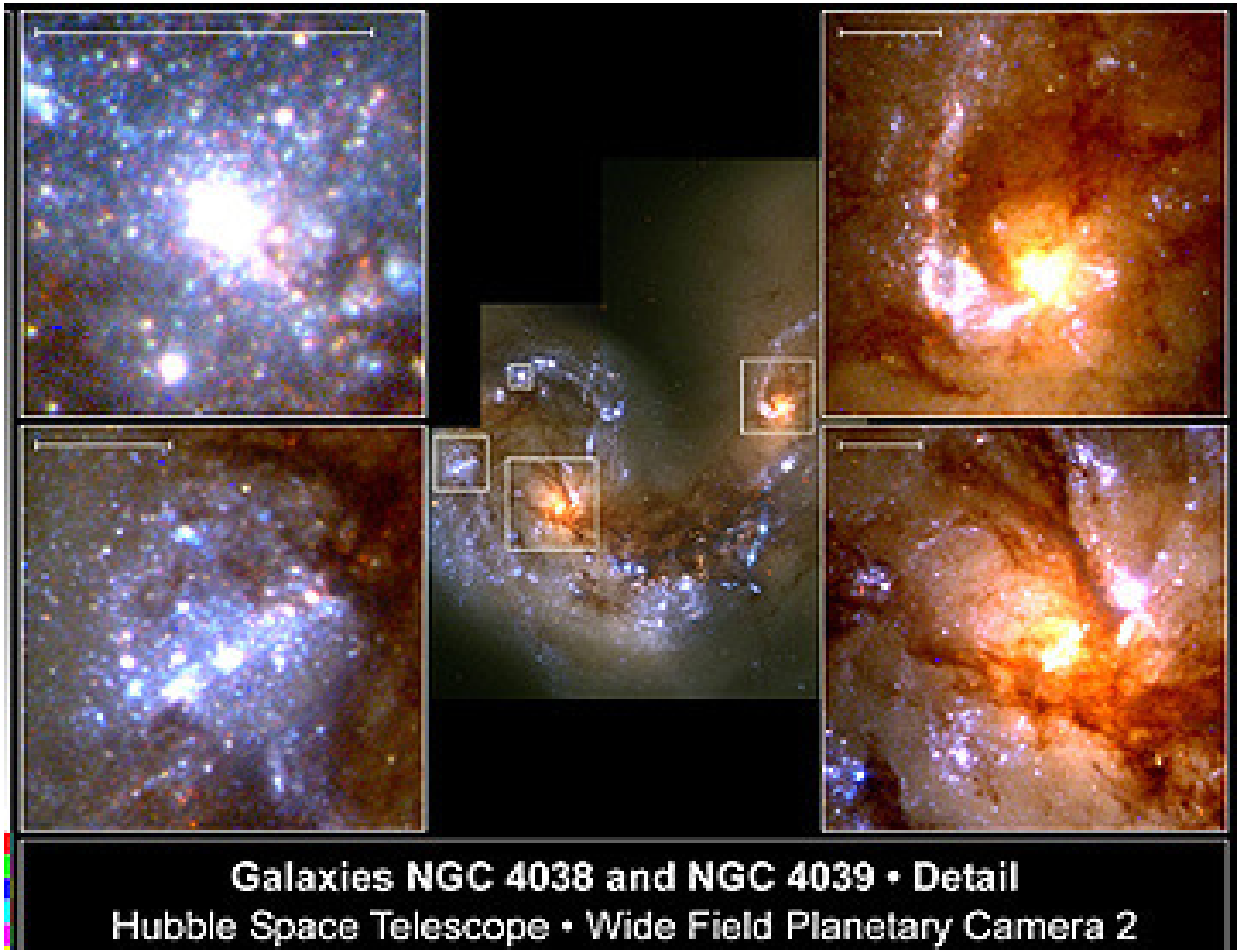

There now exist many documented examples, including collisions of >2 galaxies

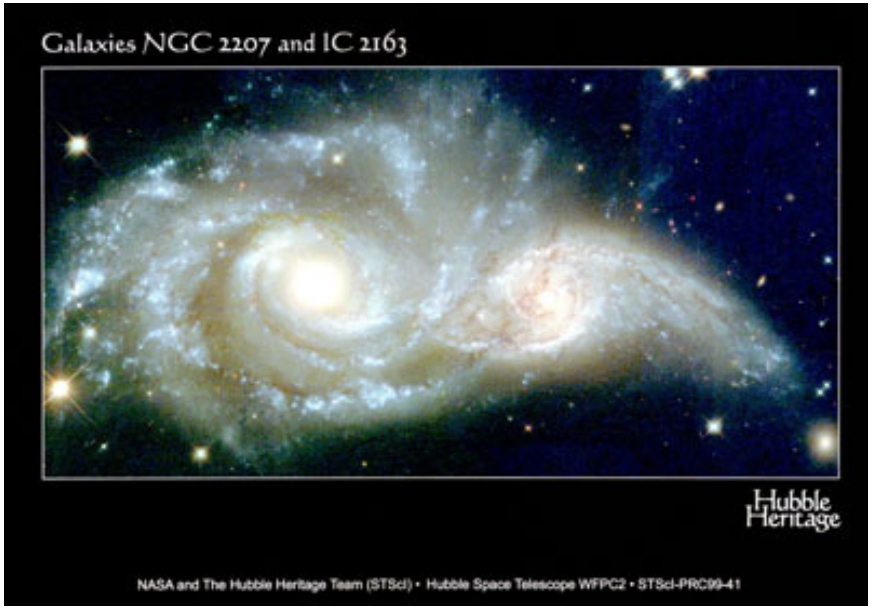

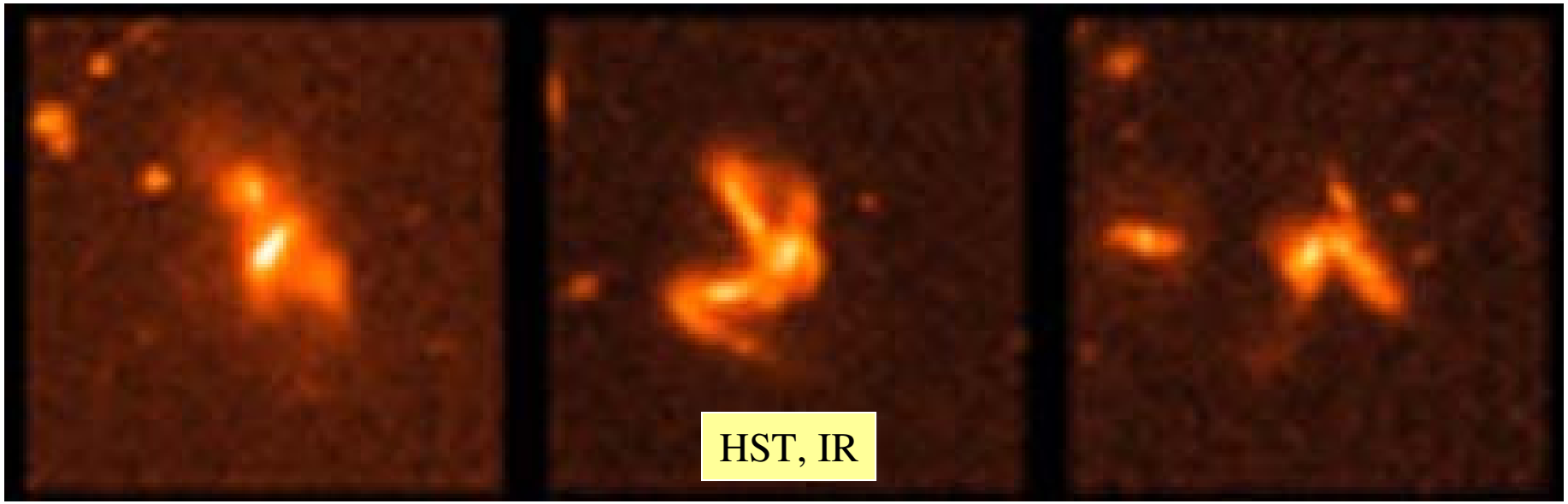

Other examples of multiple collisions

The Cartwheel Galaxy, a collision between two galaxies

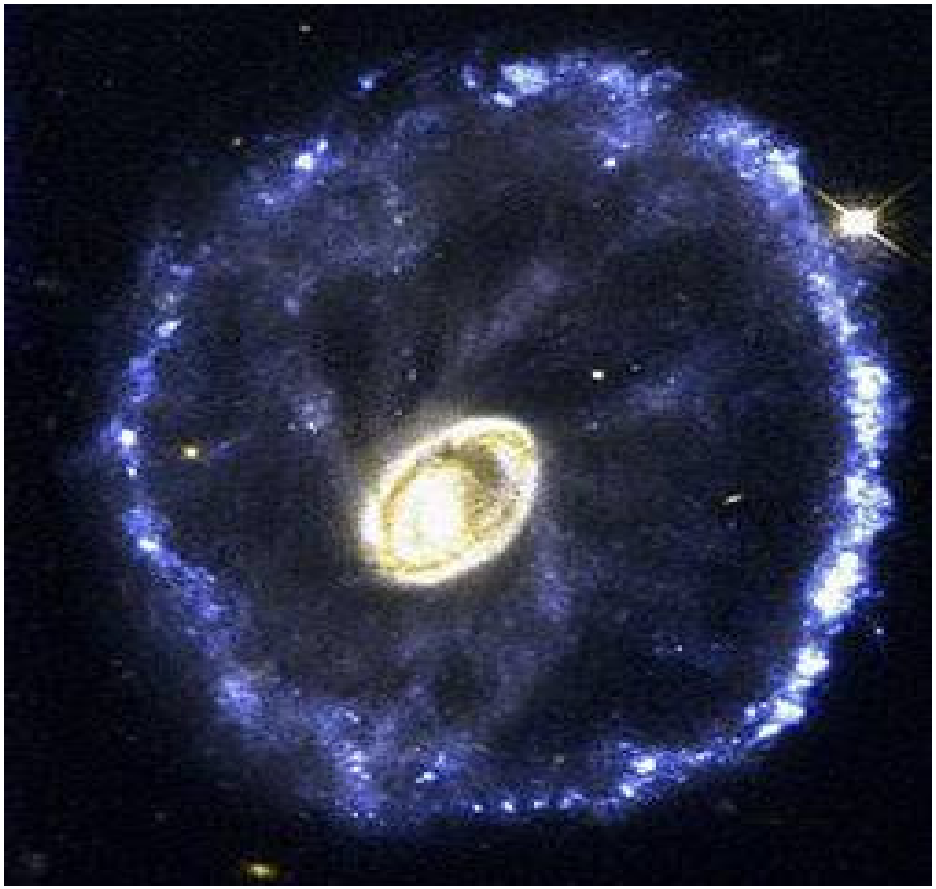

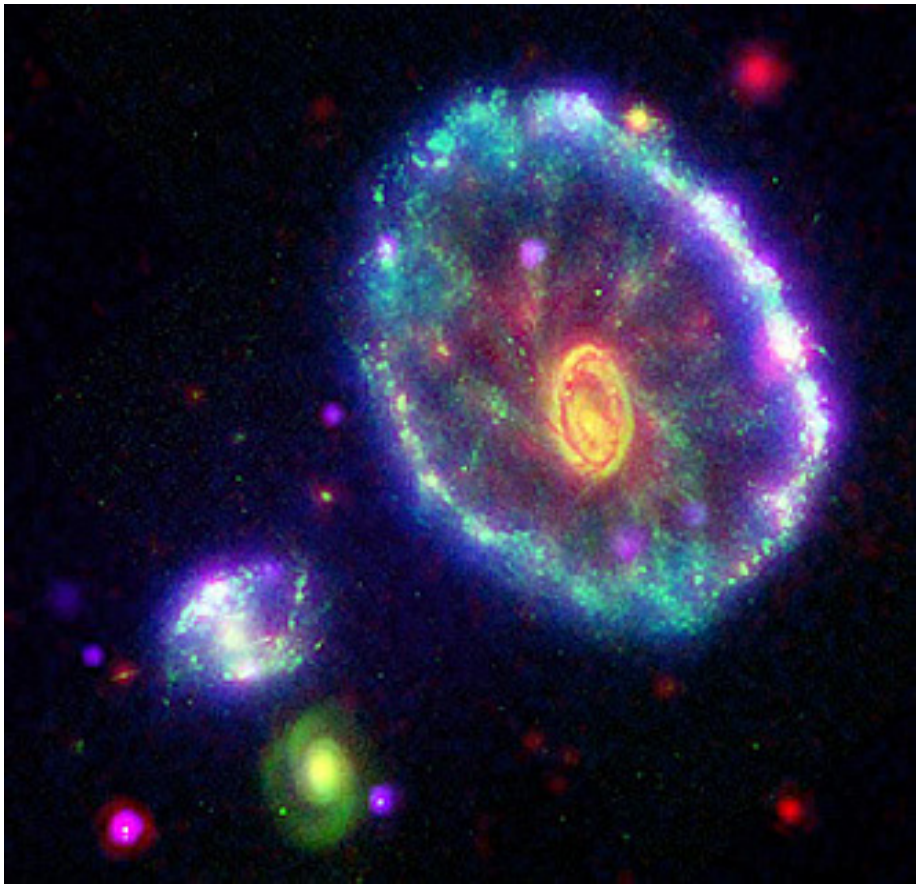

Abell 754 is made of the merging of two small clusters

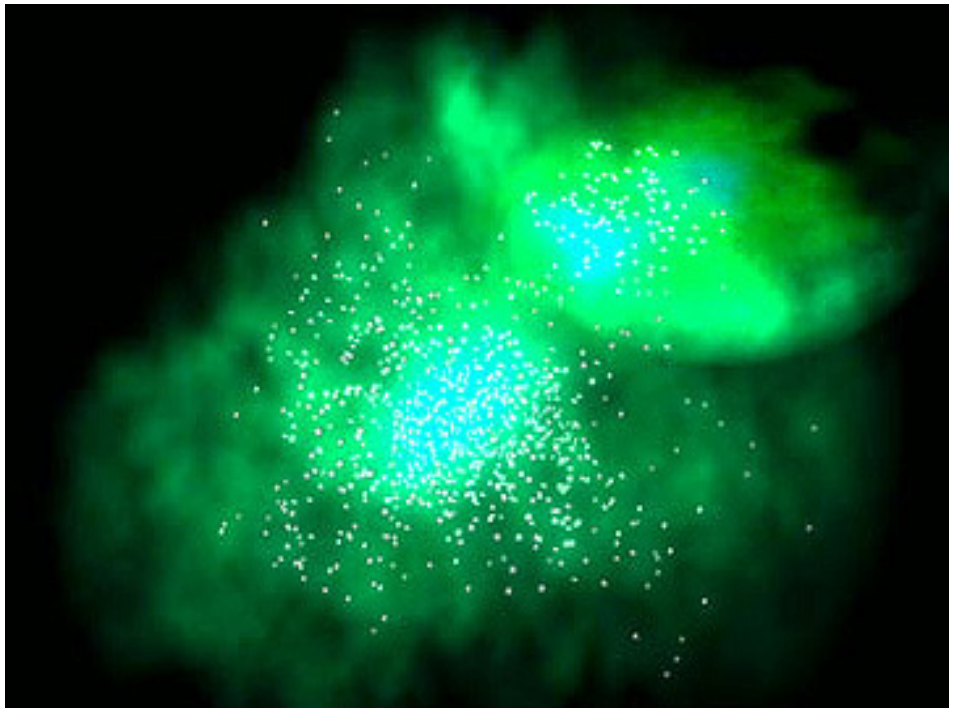

NGC1700, 30 kpc in diameter, intense X-ray source (Chandra) likely to result from a collision between an elliptical and a spiral

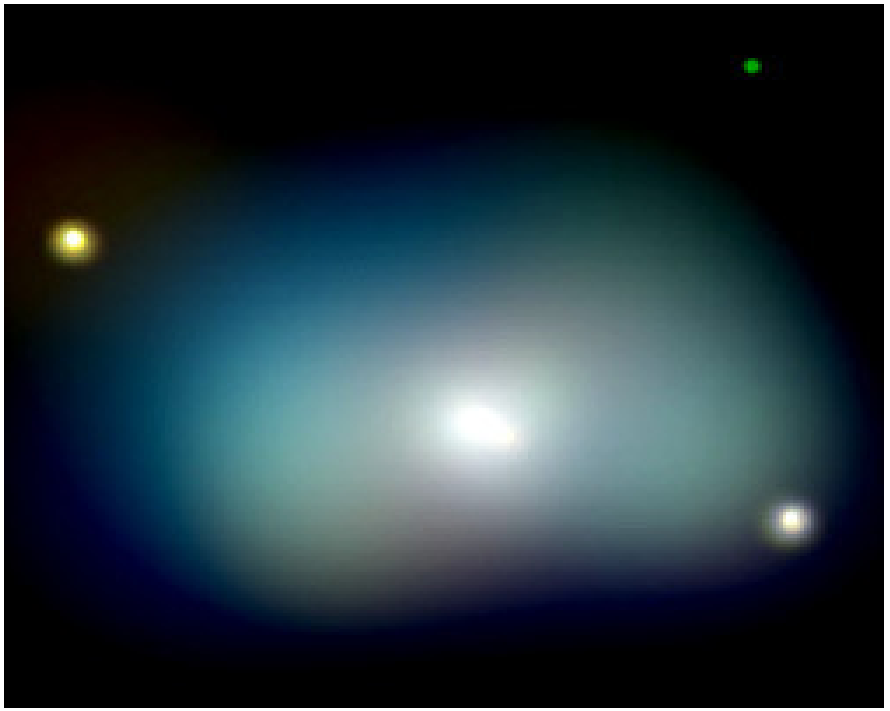

Colliding galaxies and merging galaxy clusters are sites of large scale shocks

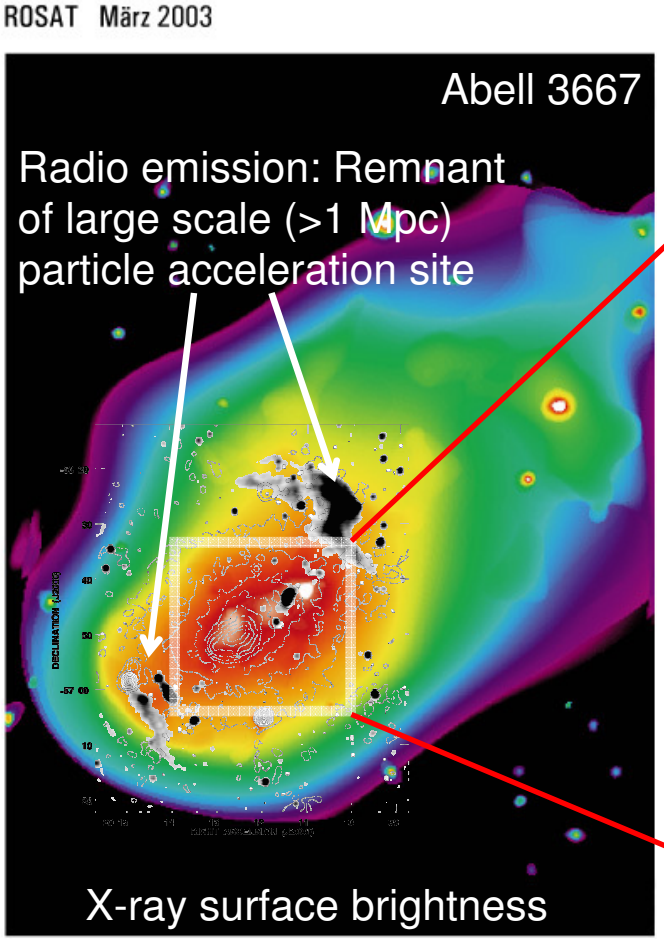

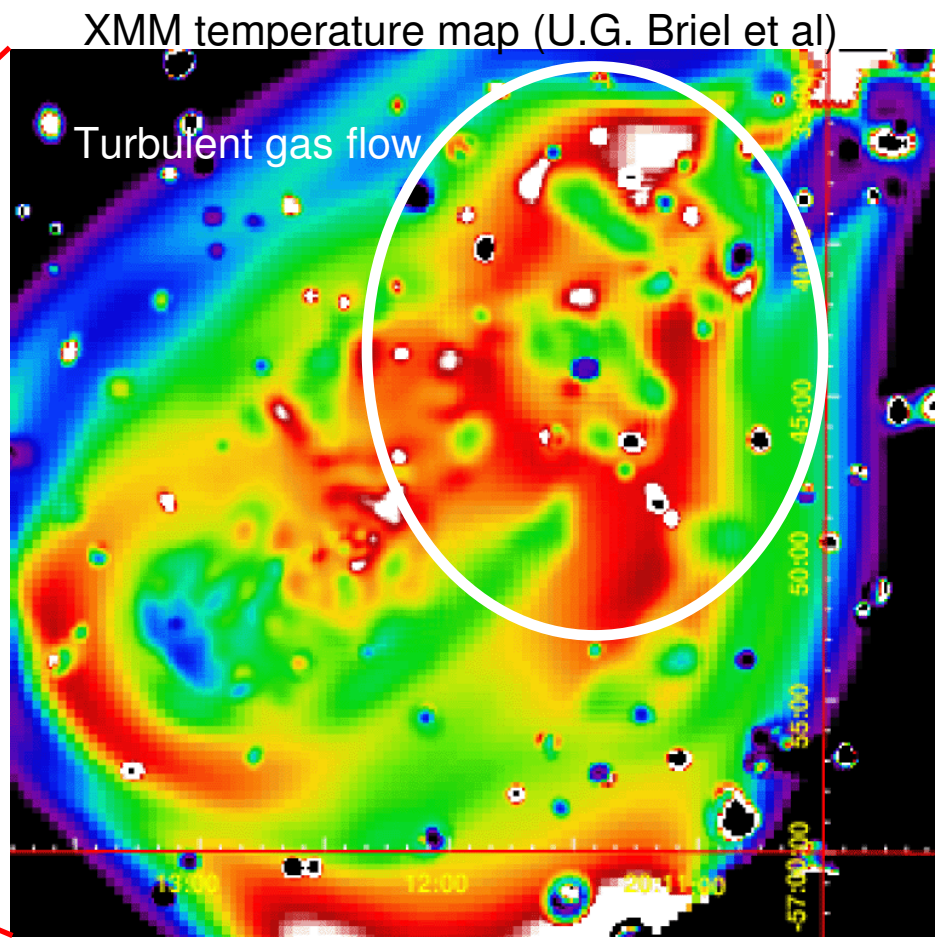

AGN's

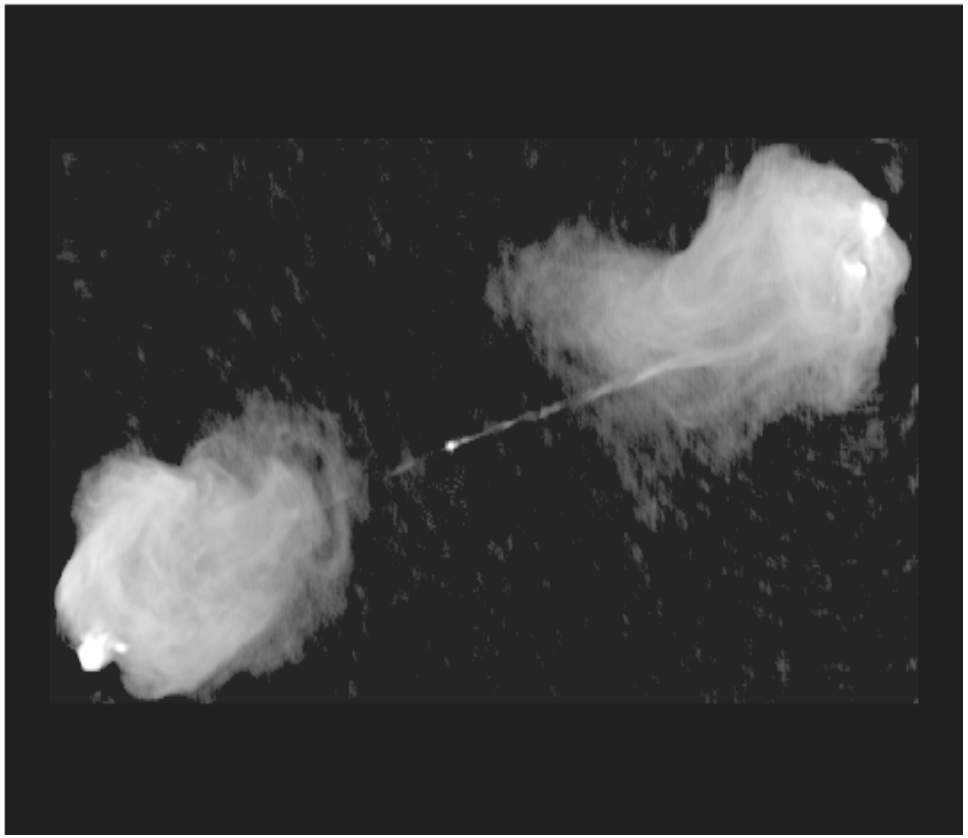

Cyg A (radio)

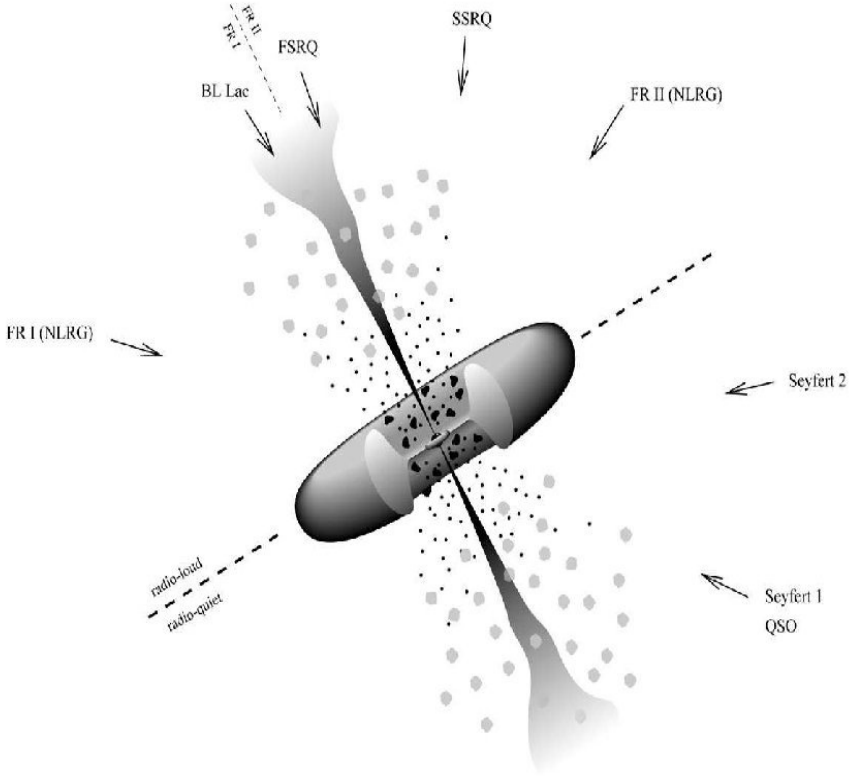

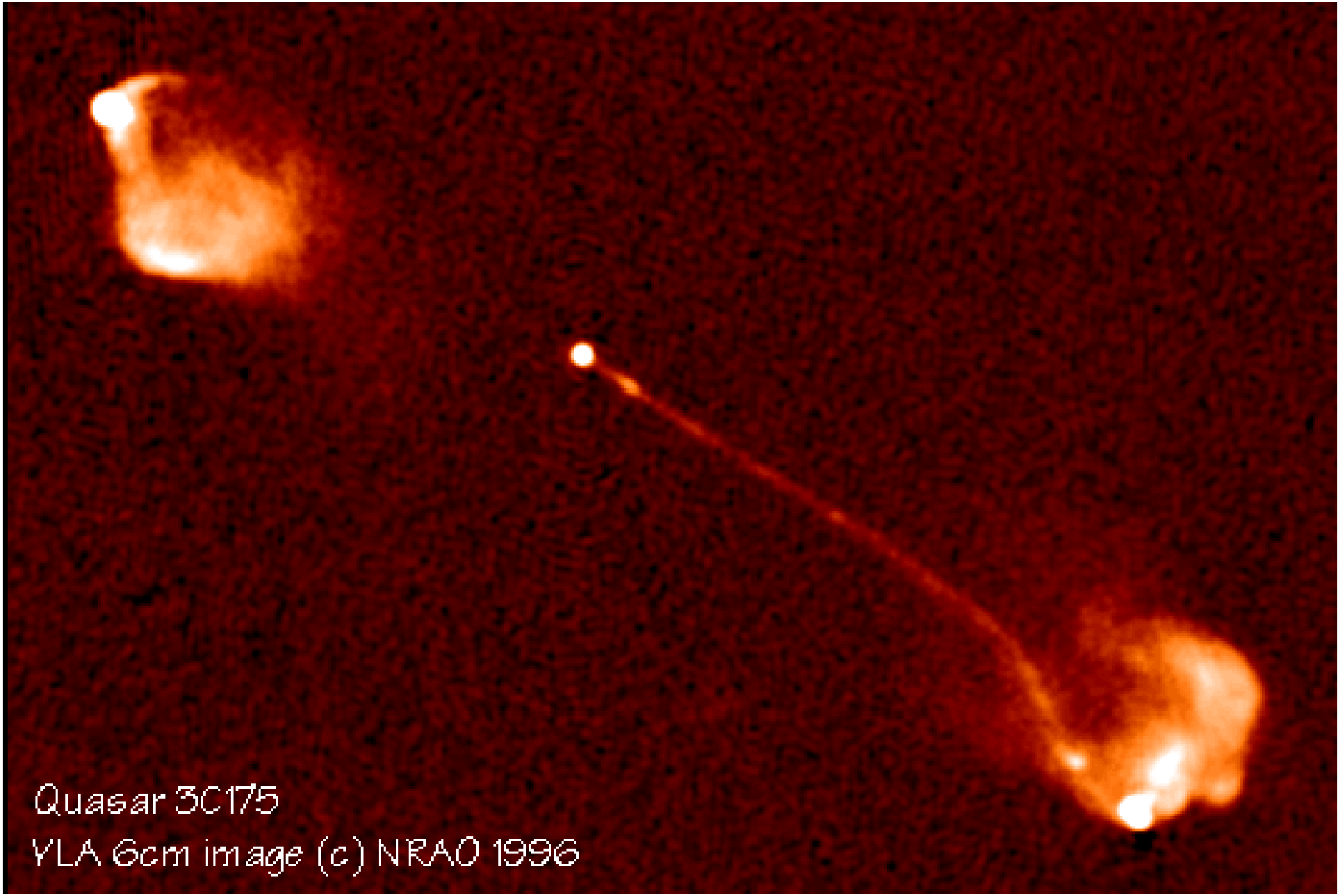

Bridle et al. (1994)

Jets of Active Galactic Nuclei provide powerful large scale shocks

Shear flow
Effective frictional acceleration

Diffusive shock acceleration

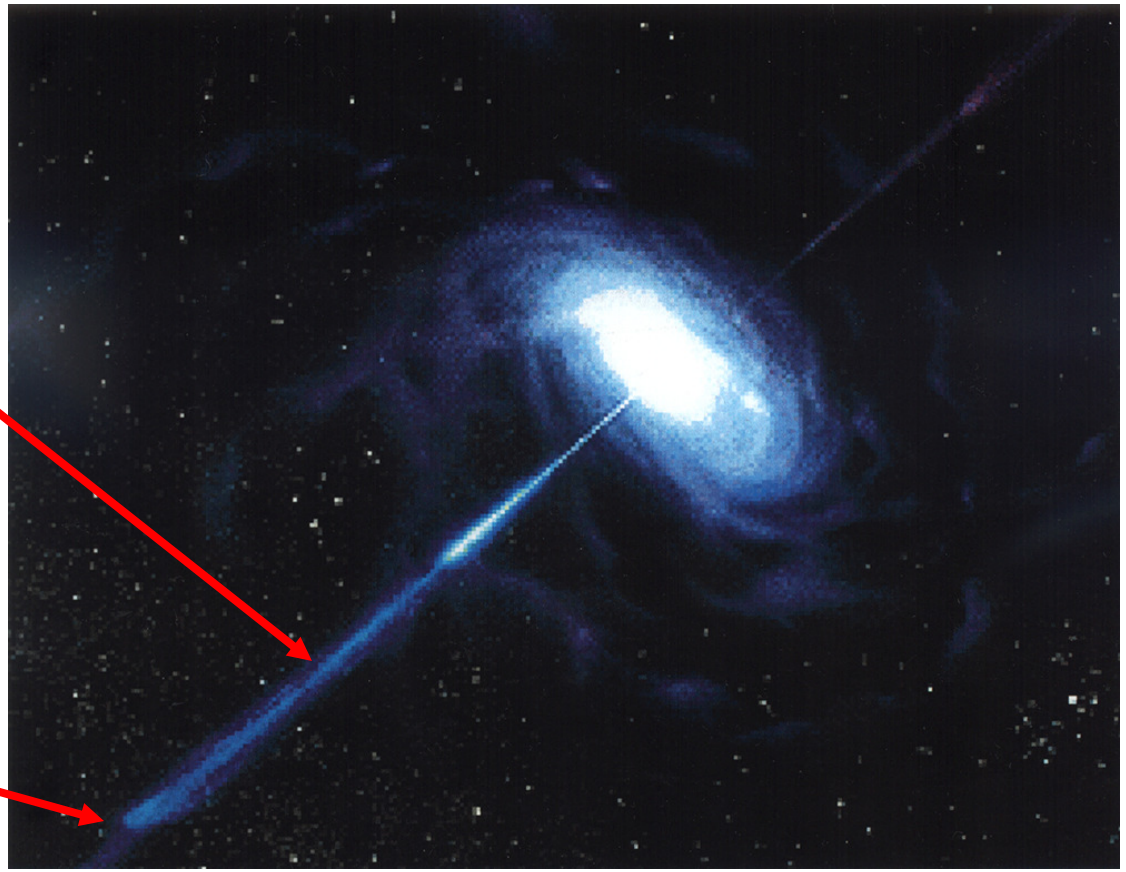

Image of the galaxy cluster Abell 400
(blue=X, pink=radio)
showing jets from two merging AGNs.

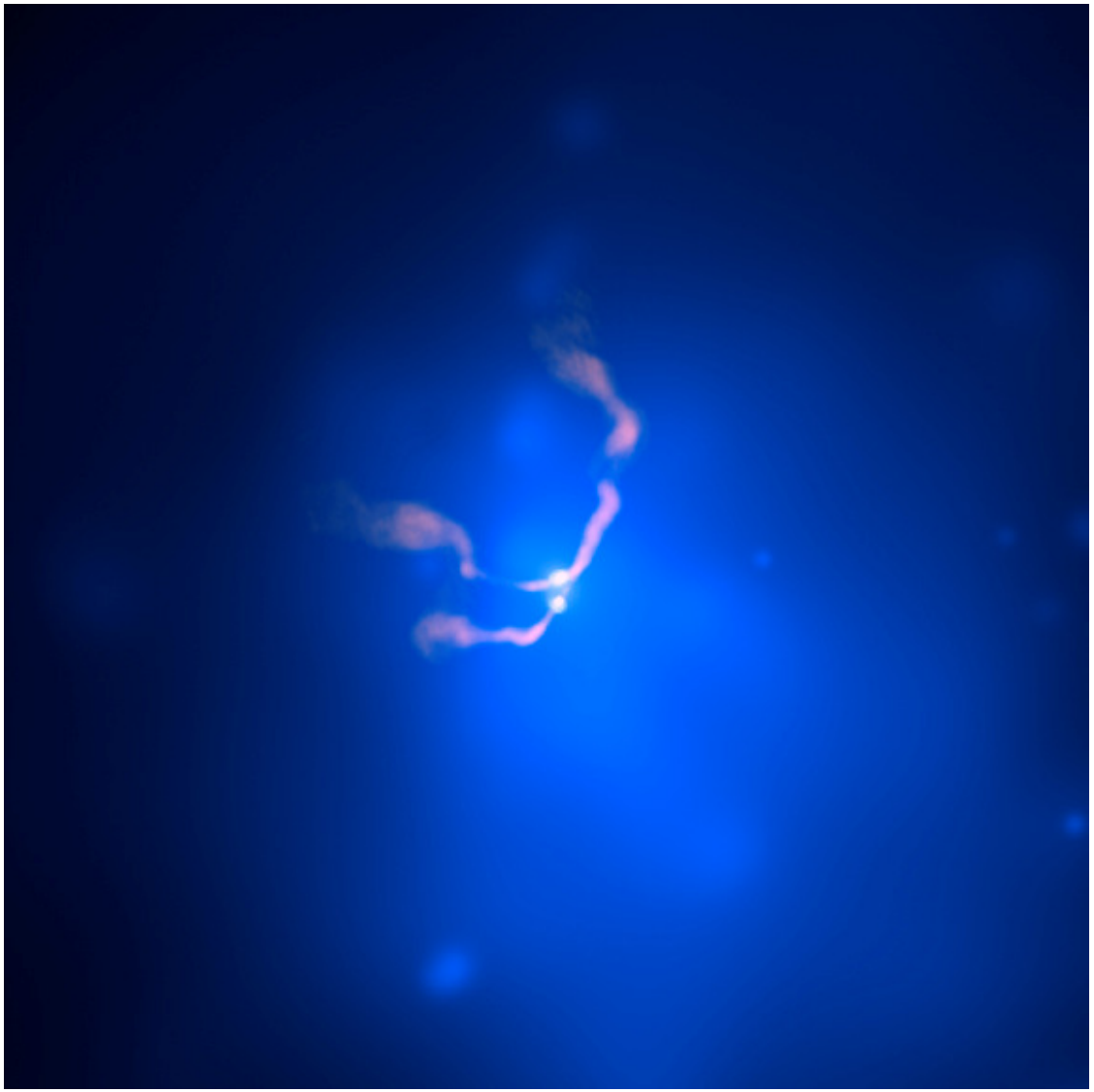

Centaurus A (NGC1528) is the closest AGN, 33 Mpc away from us, result of a collison between a spiral and an elliptical. The Black hole has a mass of some 10 billion solar masses

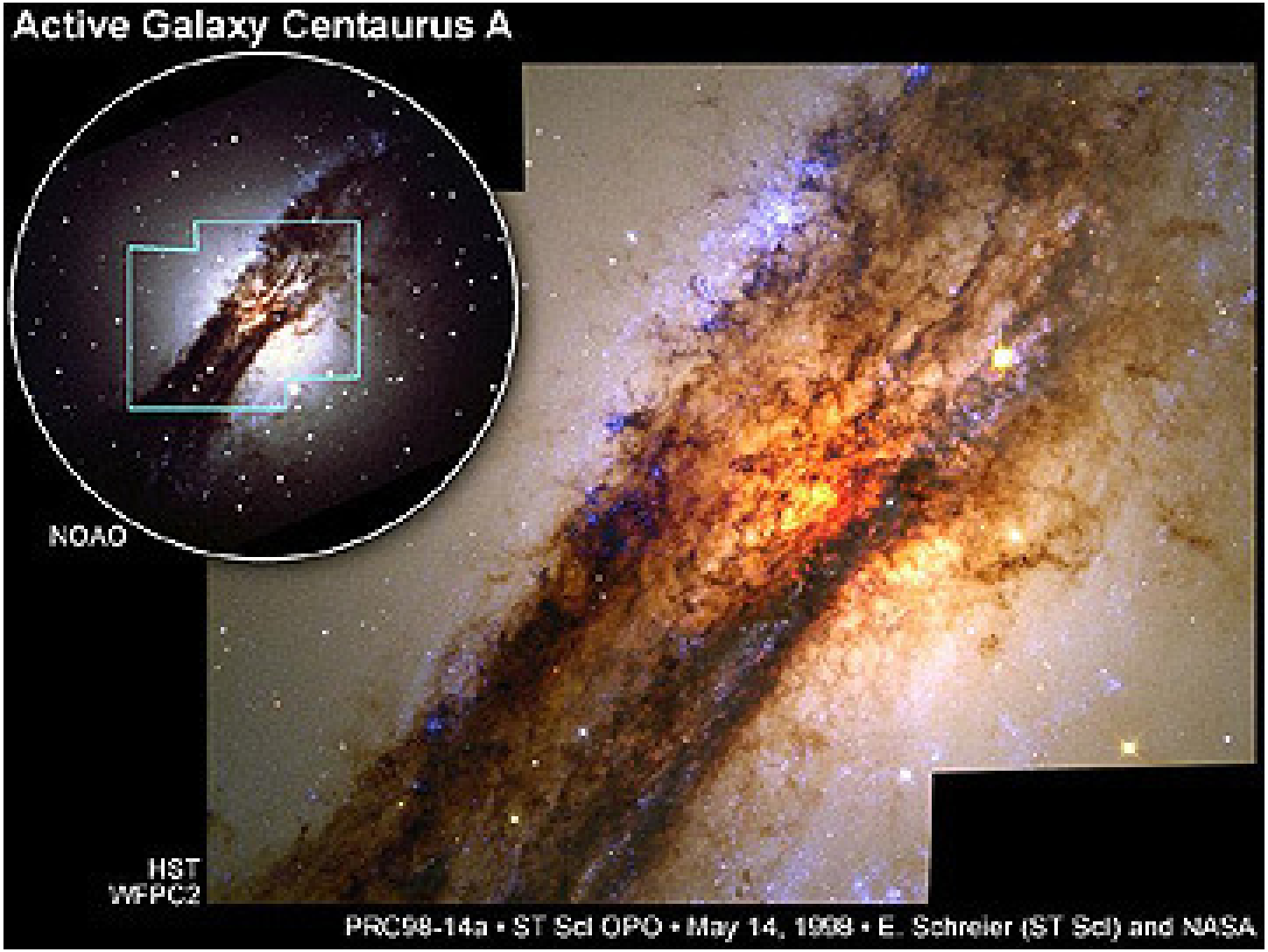


© Anglo-Australian Observatory

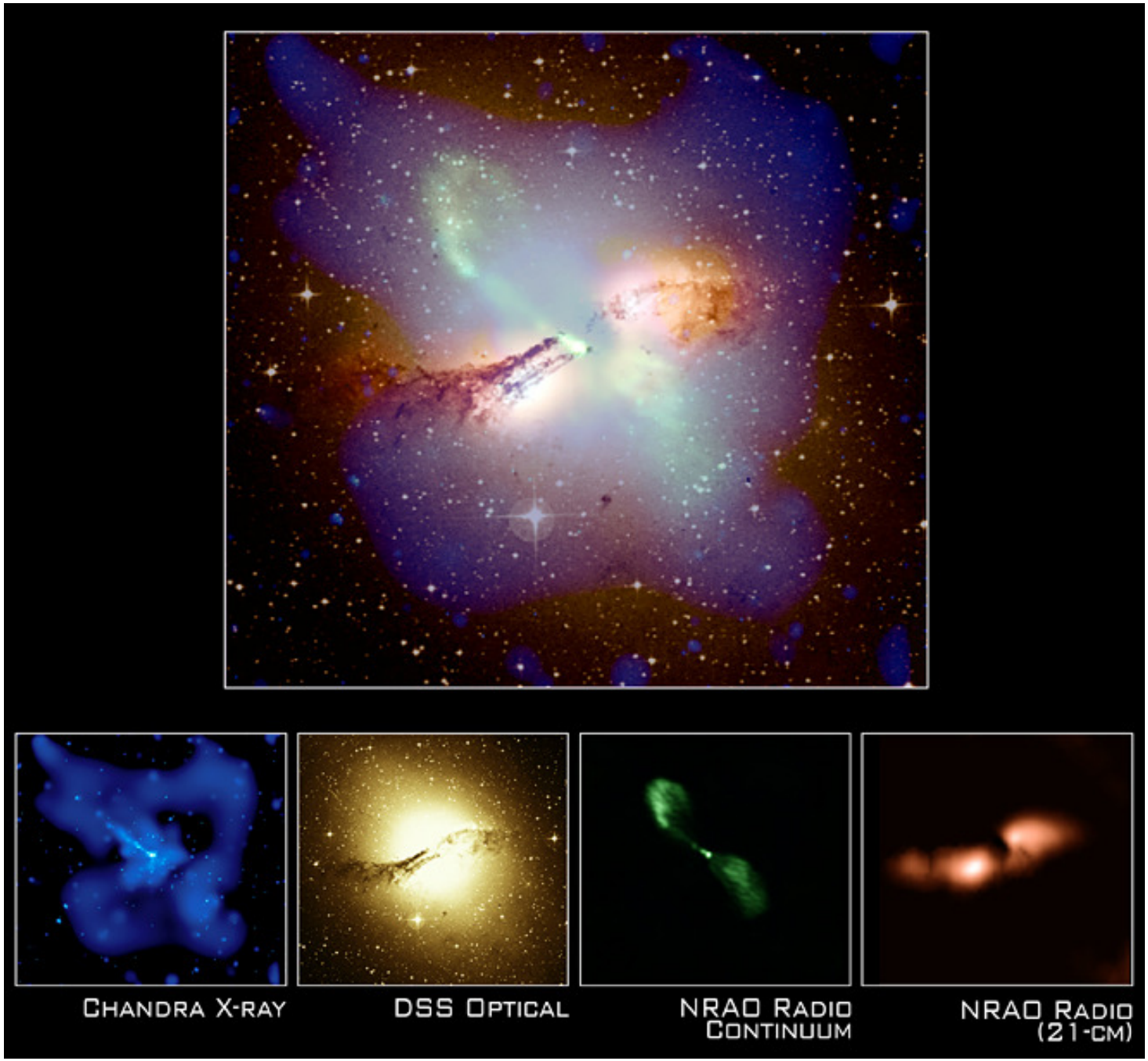
Chandra X-ray
DSS Optical
NRAO Radio Continuum
NRAO Radio (21-cm)

X-rays (Chandra) reveal two jets

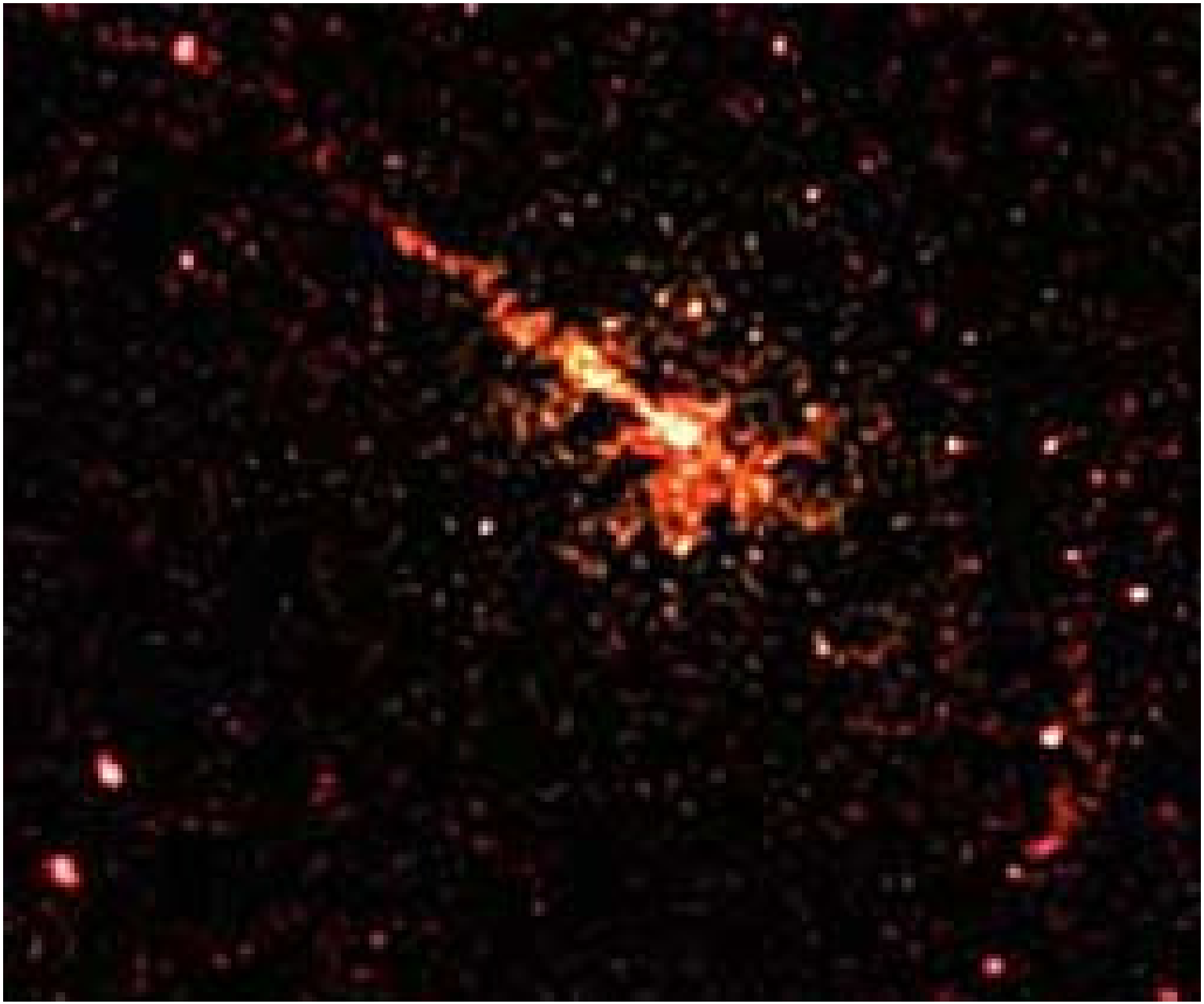

M82 may have collided with M81 and produce NGC3077. It has an AGN in its centre

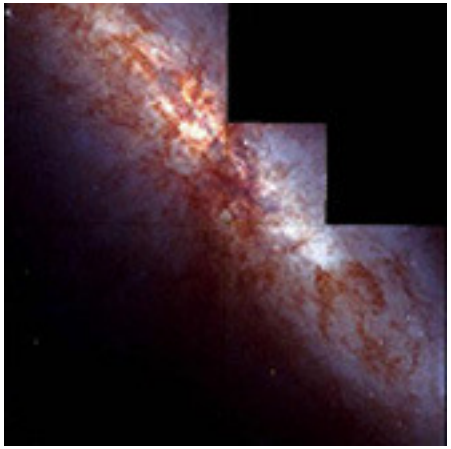

Central region (HST)

Subaru

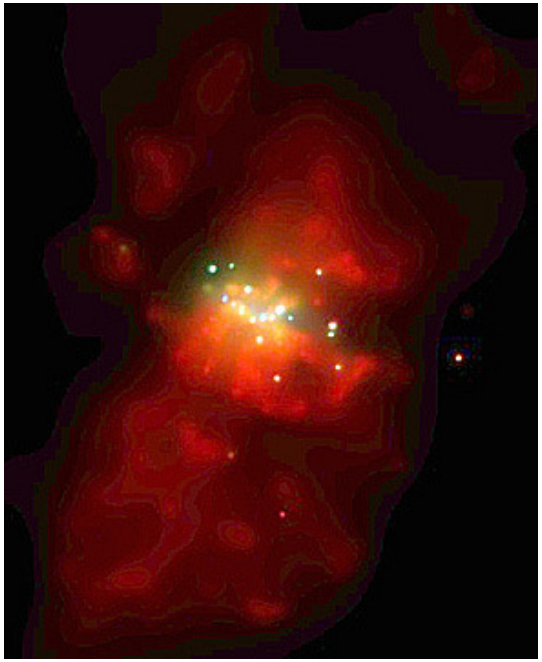

Chandra

UV

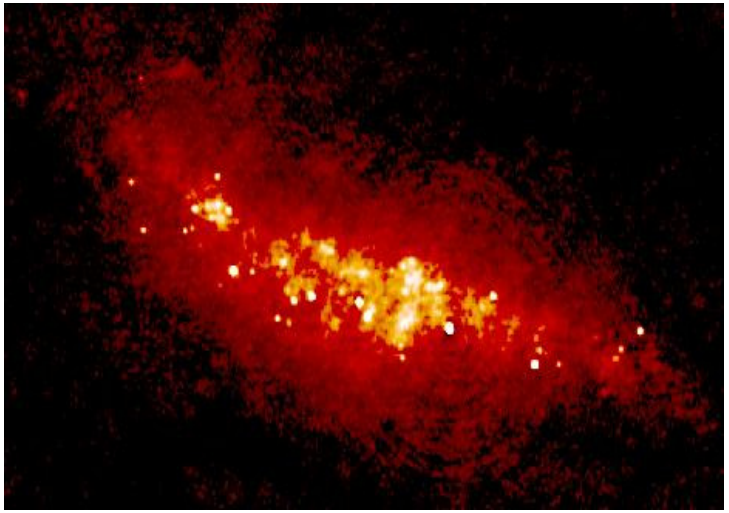

radio

Spectacular rings of stars are visible near the centres of active galaxies

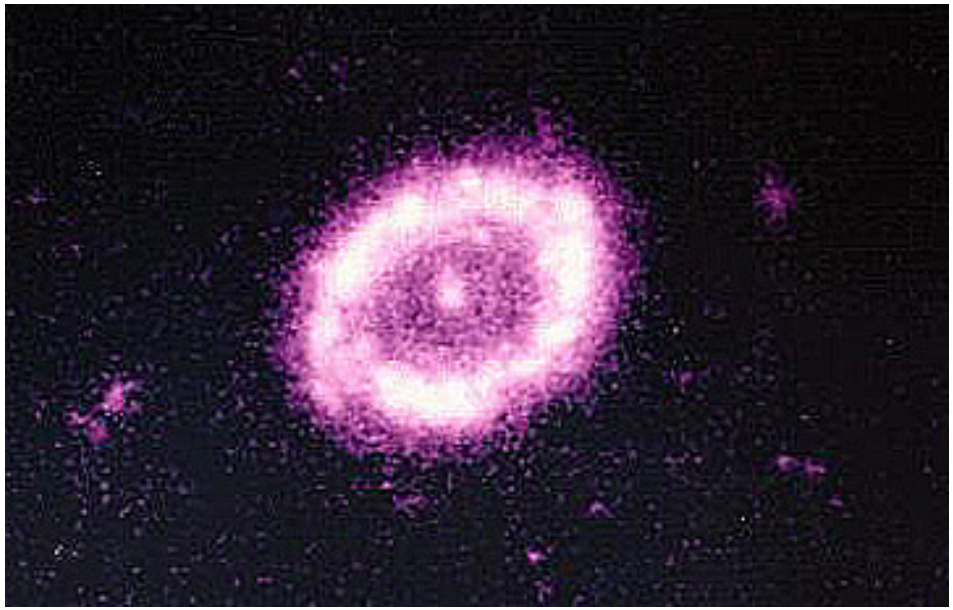

M94 (UV)

centre of NGC4314

NGC 1808

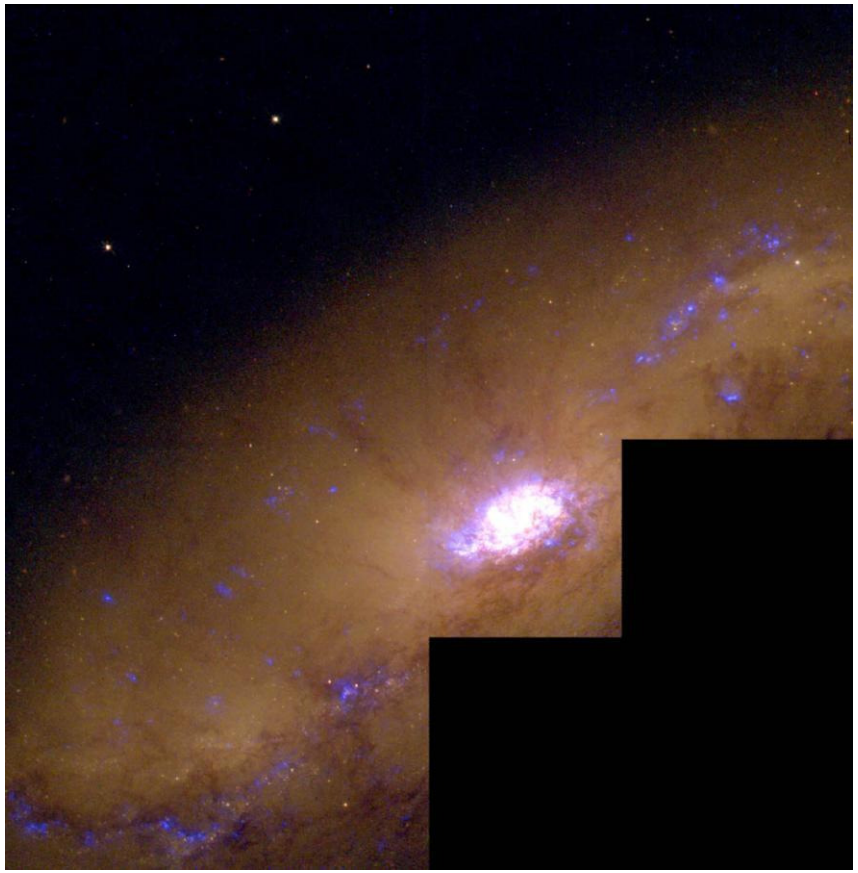

NGC 9812

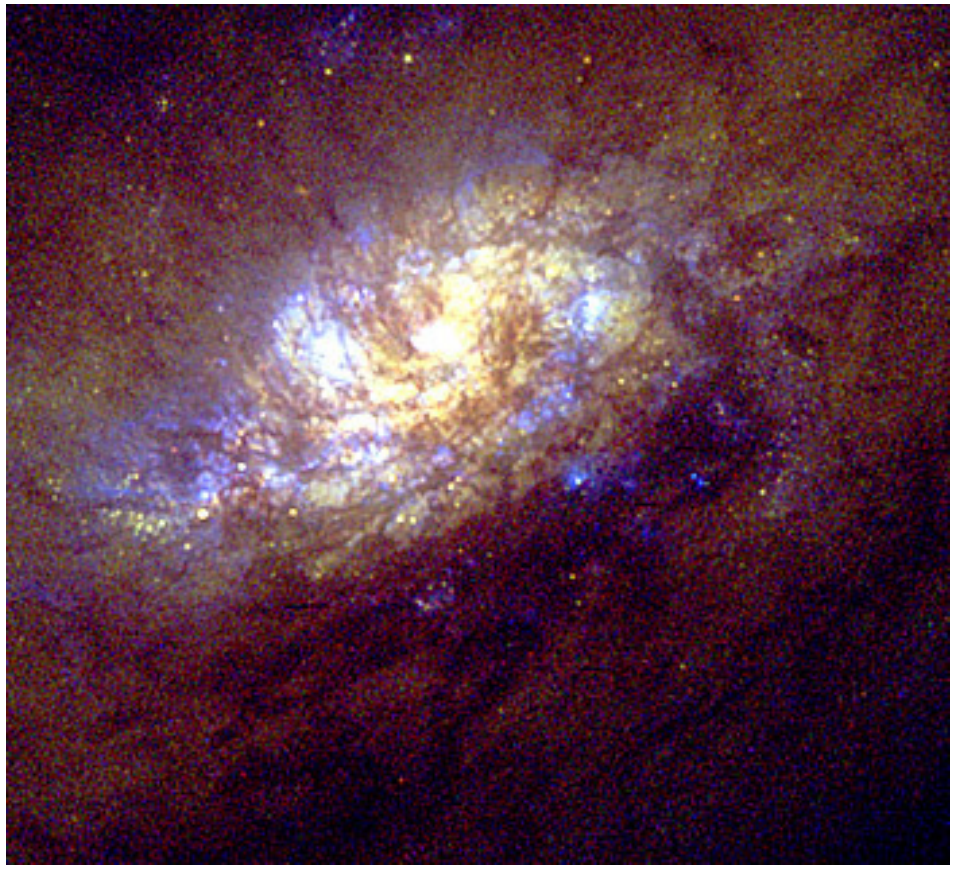

Galaxies having well defined AGNs in their centres

SUMMARY OF THE SECOND LECTURE

Spectacular progress in the understanding of the acceleration of galactic cosmic rays from SNR shocks suggest diffusive shock acceleration as a universal acceleration process. Magnetic turbulences and field amplification play an essential role.

It seems possible to accommodate UHECRs in such a scenario as evidence in favor of sufficiently large scale shocks is now growing. Such shocks may be found in colliding galaxies or galaxy clusters where active galaxies are numerous.

Yet, many unknowns subsist on the details and the relevant colisionless plasma physics which governs the shock region is still not well understood. The focus and emphasis placed in these lectures on diffusive shock acceleration should not make the student think that it *must* be *the* mechanism at play. It simply is the most likely scenario in the present state of knowledge.

The years to come, in particular with the PAO identifying numerous UHECR sources, will teach us a lot.


Thank you for your attention!

SPARES

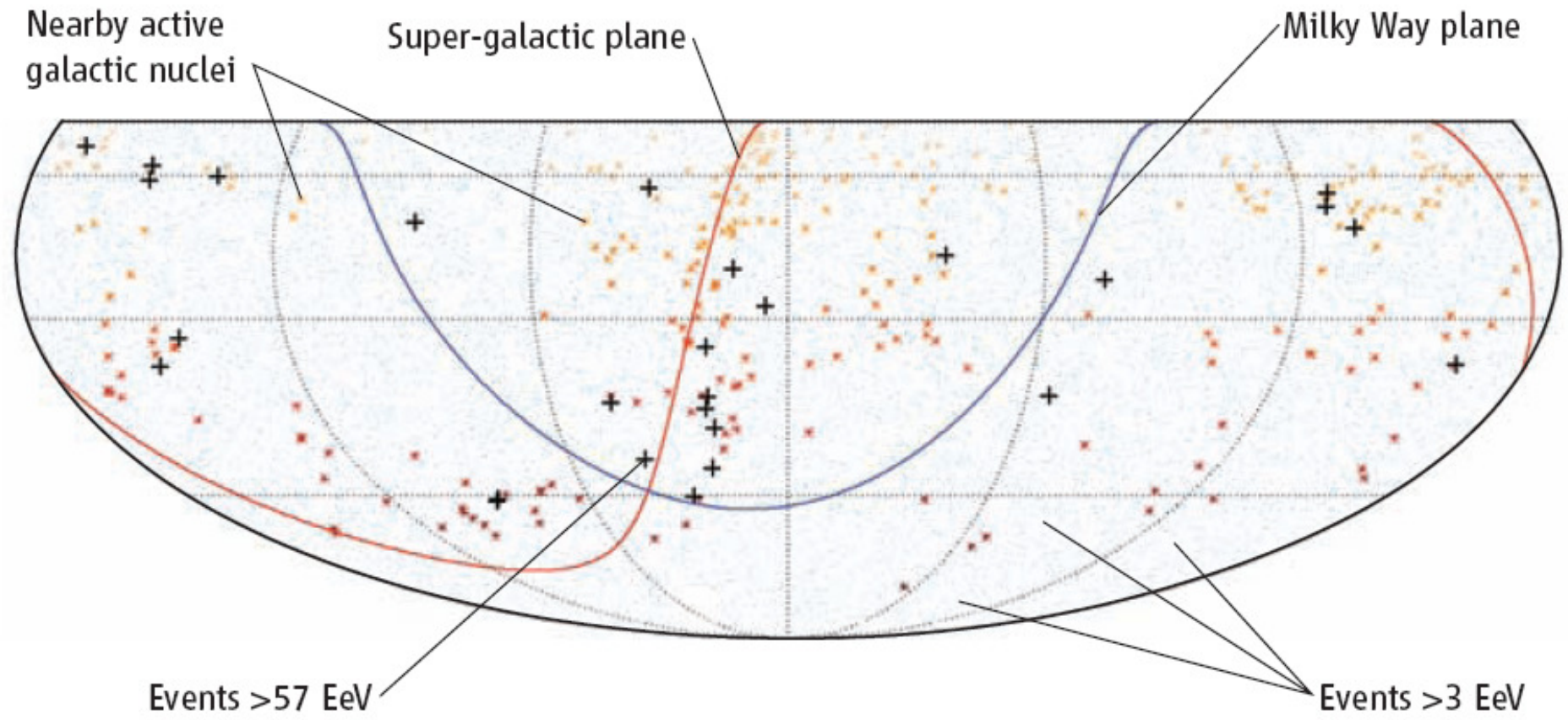

Sky map (*2*) showing cosmic rays detected by the Pierre Auger Observatory. Low-energy cosmic rays appear to originate from evenly distributed sources (blue dots), but the origins of the highest-energy events (crosses) correlate with the distribution of local matter as represented by nearby active galactic nuclei (red stars). Thus, active galactic nuclei are a likely source of these rare high-energy cosmic rays.

The preceding example corresponds to what is called
first order Fermi acceleration
Consider now a moving volume where exists a spatial distribution of magnetic fields (energy is conserved)

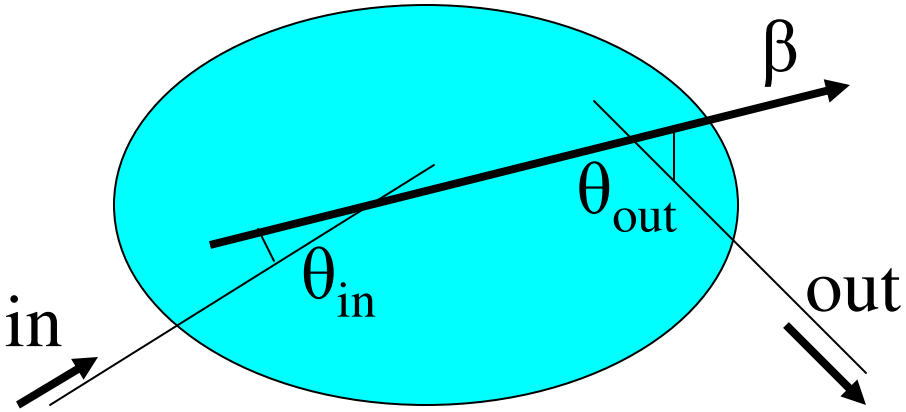

$E'_{in}=\gamma E_{in}(1-\beta\cos\theta_{in})$

$E_{out}=\gamma E'_{out}(1+\beta\cos\theta_{out})$

$E_{out}=\gamma^2 E_{in}(1-\beta\cos\theta_{in})(1+\beta\cos\theta_{out})$

For isotropic uncorrelated in and out distributions, $\langle\cos\rangle=0$

$\Delta E/E=\gamma^2-1 \sim \beta^2>0$

Assuming isotropization inside the volume but correcting for the fact that θ_{in} is not isotropic (collision frequency depends on particle velocity wrt volume) one finds

$\Delta E/E \sim (4/3)\beta^2$

This is second order Fermi acceleration

$\Delta E/E \approx \beta^2$

Its effect is negligible

maximum energy

condition of acceleration, critical Pecklet number (parameter of modulation)

$$\frac{u_{sh}R_{sh}}{D(p)} \geq 10$$

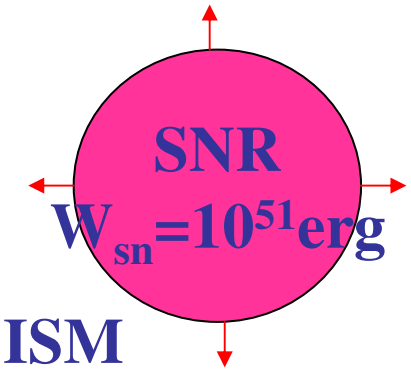

$$u_{sh}R_{sh} \approx 10^{28}\left(W_{51}/n_0\right)^{2/5} \; cm^2/s$$ **-maximum value**

$$D_{ism} \approx 6\times10^{28}\,\beta P_{GV}^{0.3} \; cm^2/s$$ **-typical in interstellar medium**

→ **diffusion should be anomalously slow near the shock (upstream and downstream)**

→ **cosmic ray streaming instability in shock precursor**

Bell 1978, Lagage & Cesarsky 1983, McKenzie & Völk 1982, Achterberg 1983, Völk et al. 1988, Fedorenko 1990, Bell & Lucek 2000, 2001

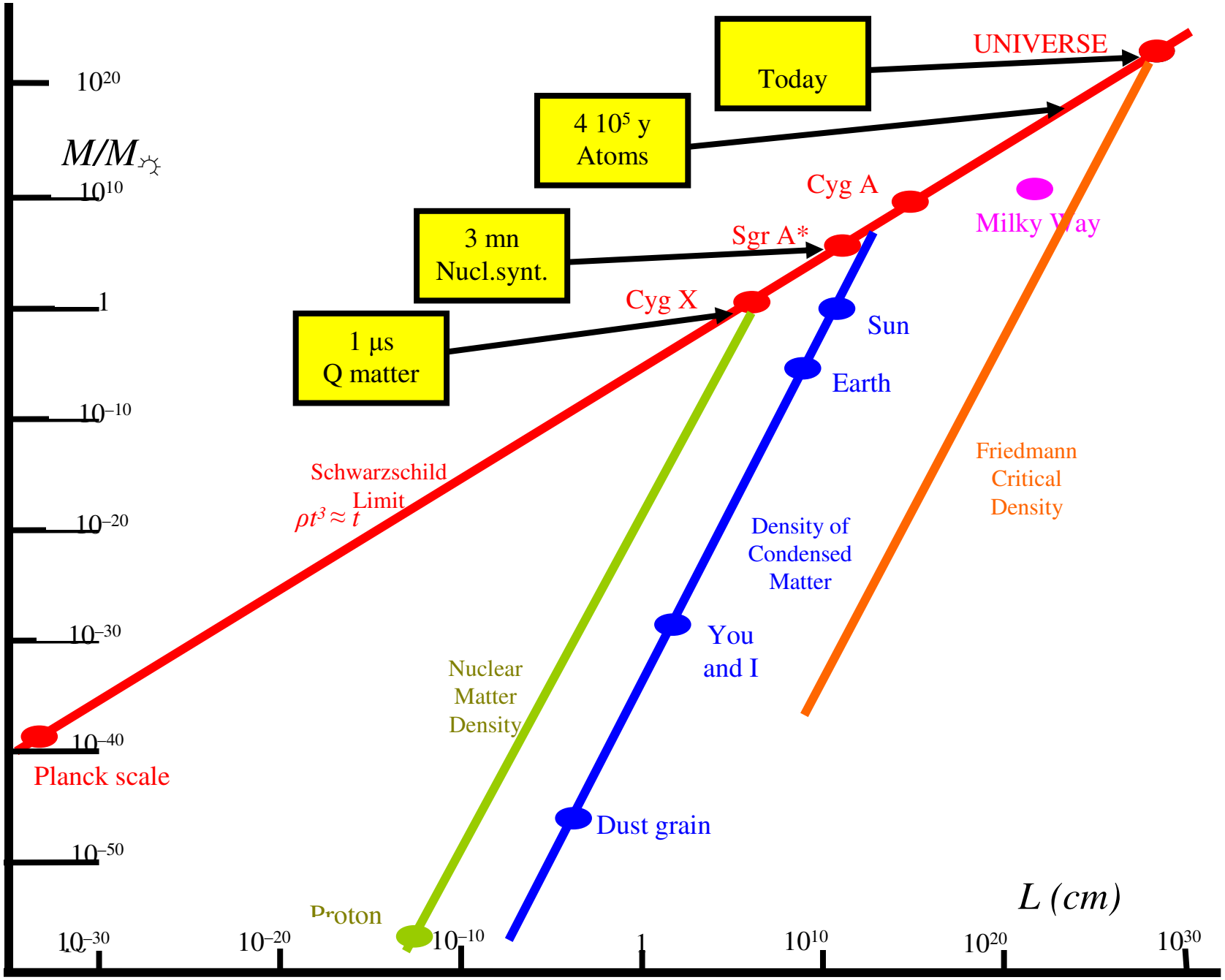
10^{20}
$M/M_{\odot}$
10^{10}
1
10^{-10}
10^{-20}
10^{-30}
10^{-40}
10^{-50}
Planck scale
Today
UNIVERSE
4 10^5 y
Atoms
Cyg A
Milky Way
3 mn
Nucl.synt.
Sgr A*
Cyg X
1 µs
Q matter
Sun
Earth
Schwarzschild
Limit
$\rho t^3 \approx t$
Friedmann
Critical
Density
Density of
Condensed
Matter
You
and I
Nuclear
Matter
Density
Dust grain
Proton
$L\ (cm)$
10^{-30}
10^{-20}
10^{-10}
1
10^{10}
10^{20}
10^{30}

Energy spectrum of CRs

Ankle scenario

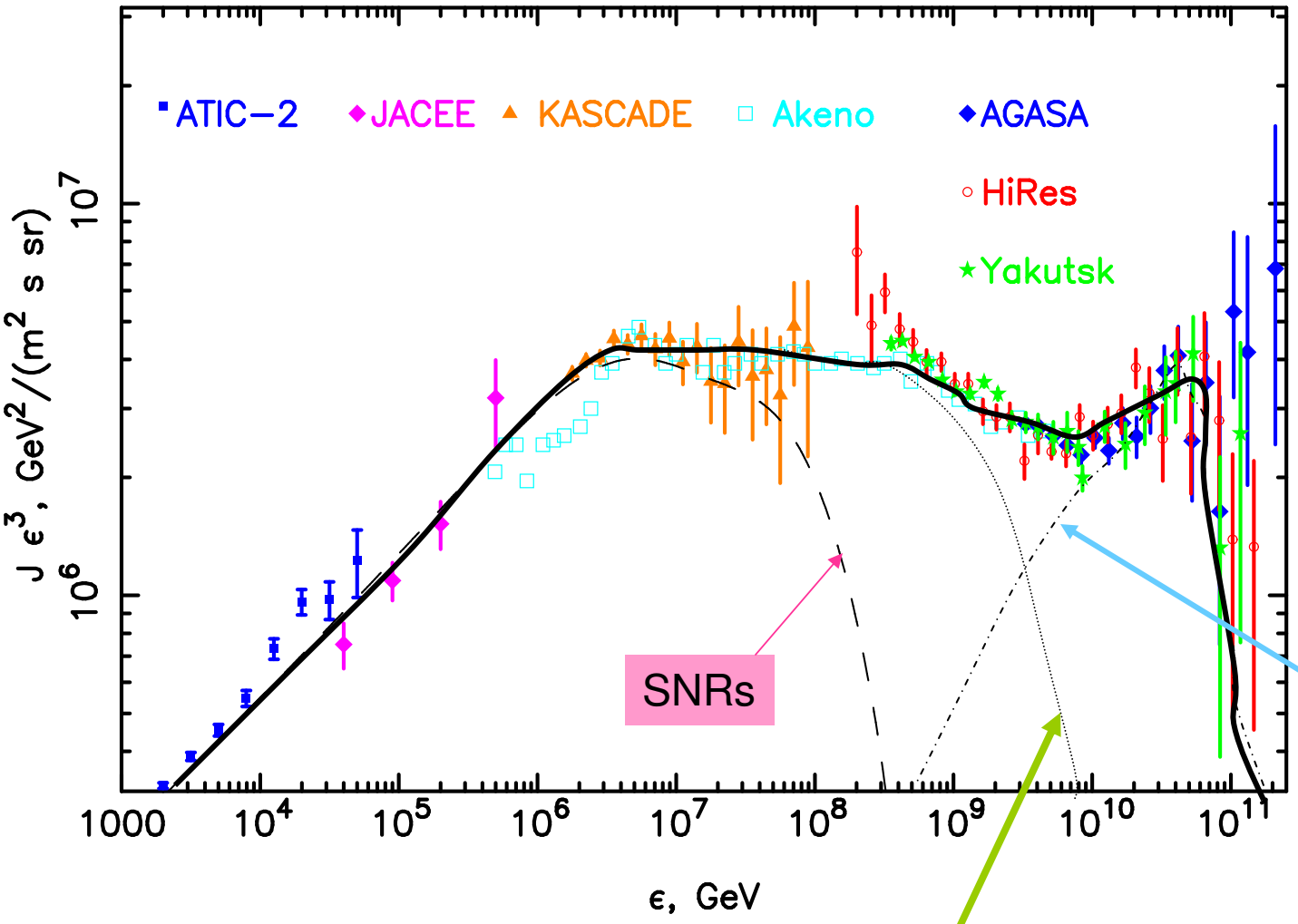

Extragalactic (AGNs, GRBs…)

$J_{EG} \sim \varepsilon^{-2}$

Berezinsky et al.(2006)

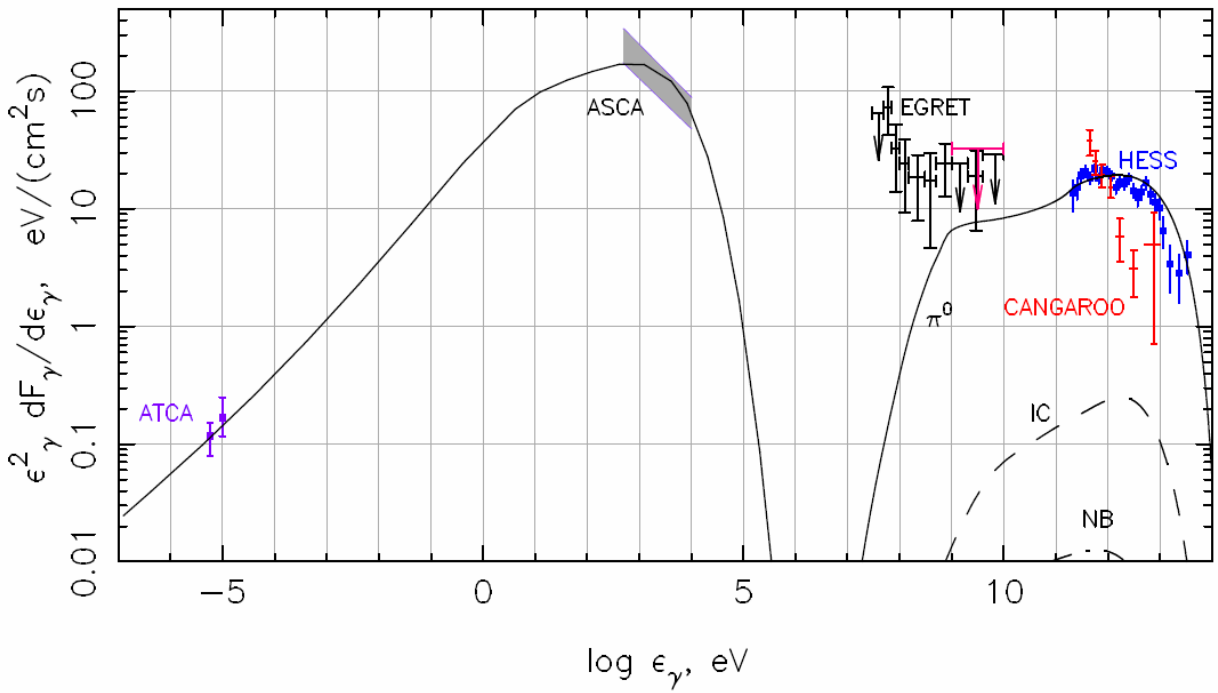

Fig. 3. Spatially integrated spectral energy distribution of RX J1713.7-3946 . The ATCA radio data (cf. Aharonian et al. 2005), ASCA X-ray data (cf. Aharonian et al. 2005), EGRET spectrum of 3EG J1714-3857 (Reimer & Pohl 2002), CANGAROO data (Enomoto et al. 2002), in red color) and H.E.S.S. data (Aharonian et al. 2005), in blue color) are shown. The EGRET upper limit for the RX J1713.7-3946 position (Aharonian et al. 2005) is shown as well (red colour). The solid curve at energies above 10^7 eV corresponds to π^0-decay γ-ray emission, whereas the dashed and dash-dotted curves indicate the inverse Compton (IC) and Nonthermal Bremsstrahlung (NB) emissions, respectively.

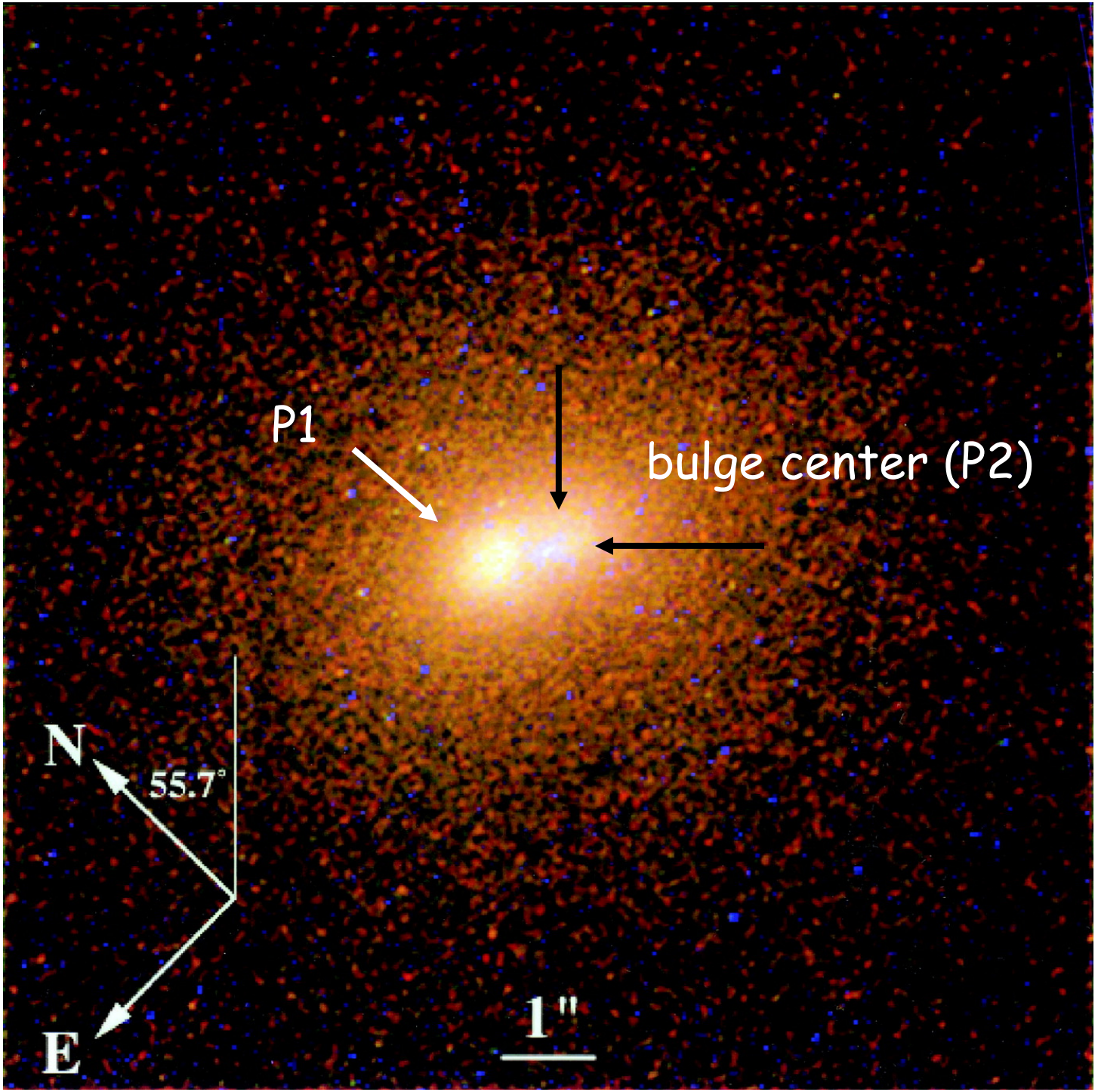

- faint component (P2) is at the bulge center
- P2 is cuspy
- P2 has a compact blue component at its center (P3)
- bright component P1 is smooth
- total luminosity 6×10^6 $L_\odot$ (r~0.5 pc) and is cuspy

Lauer et al. (1998)

M31

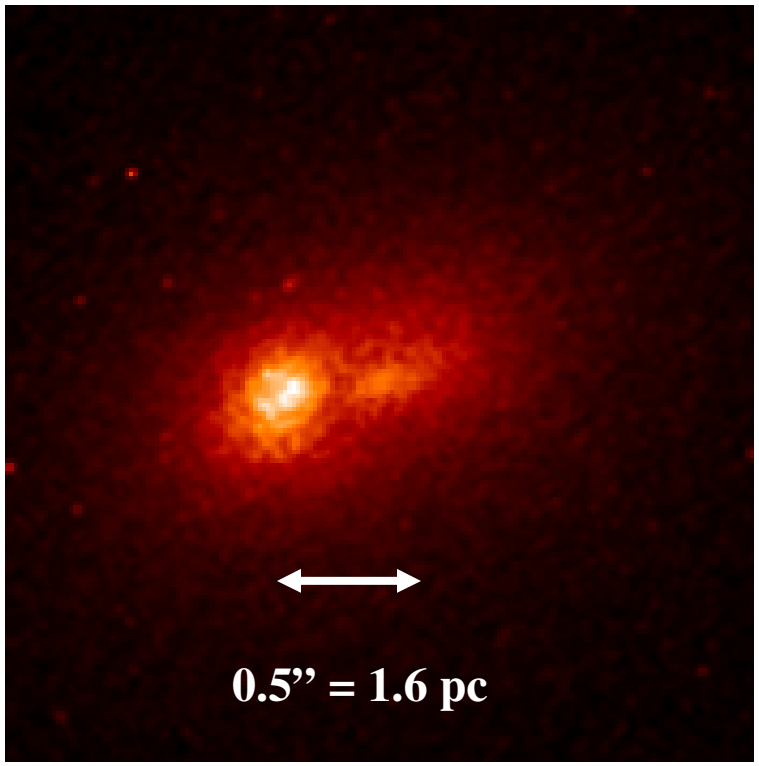

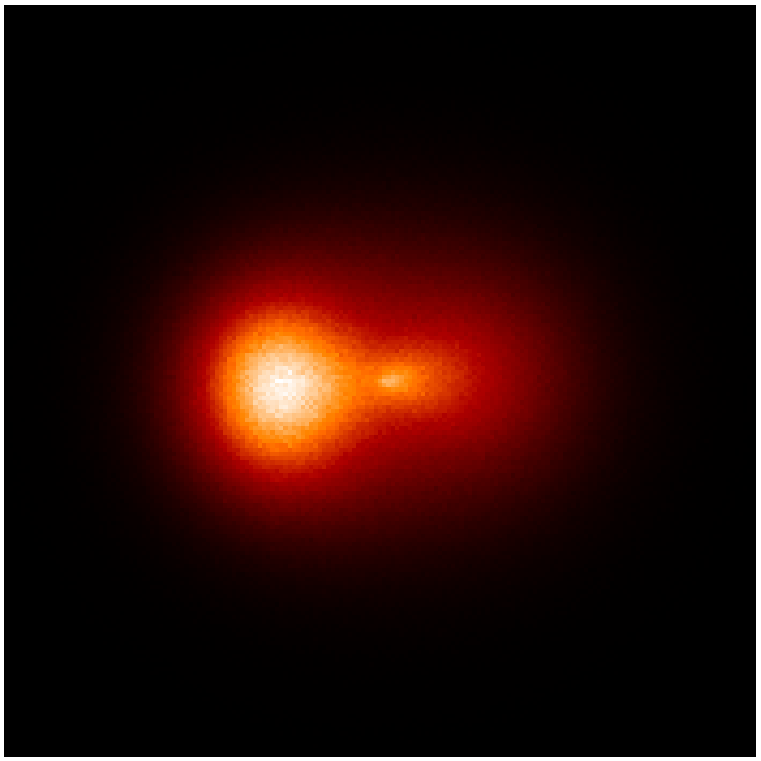

- the double nucleus is probably a thick eccentric disk of stars orbiting a black hole (Tremaine 1995)
- black hole is at P2; P1 is apocenter region of disk

Peiris & Tremaine (2003)